NASA Contractor Report 4481

BLSTA—A Boundary Layer Code for Stability Analysis

Yong-Sun Wie
High Technology Corporation
Hampton, Virginia

Prepared for
Langley Research Center
under Contract NAS1-19299

National Aeronautics and
Space Administration
Office of Management
Scientific and Technical
Information Program
1992

SUMMARY

A computer program is developed to solve the compressible, laminar boundary-layer equations for two-dimensional flow, axisymmetric flow, and quasi-three-dimensional flows including the flow along the plane of symmetry, flow along the leading-edge attachment line, and swept wing flows with a conical flow approximation. The finite-difference numerical procedure used to solve the governing equations is second-order accurate. The flow over a wide range of speed, from subsonic to hypersonic speed with perfect gas assumption, can be calculated. Various wall boundary conditions, such as wall suction or blowing and hot or cold walls, can be applied.

The results indicate that this boundary-layer code gives velocity and temperature profiles which are accurate, smooth, and continuous through the first and second normal derivatives. The code presented herein can be coupled with a stability analysis code and used to predict the onset of the boundary-layer transition which enables the assessment of the laminar flow control techniques. A user's manual is also included.

TABLE OF CONTENTS

PART I. NUMERICAL METHOD

PART II. USER'S MANUAL

NOMENCLATURE

A, B	stagnation point velocity gradients
a, b	major and minor semiaxis lengths of the ellipsoid of revolution
C	$\rho\mu/\rho_e\mu_e$
C^*	B/A
c	ρ_e/ρ or chord
C_{fx}	skin friction coefficient in the x-direction based on the edge condition, Eq. (83) or Eq. (84) or Eq. (85a)
C_{fy}	skin friction coefficient in the y-direction based on the edge condition, Eq. (85b)
C_p	Pressure coefficient
c_p	specific heat
E	H/H_e
F	u/u_e
f_ζ	F
G	v/V_{ref} or v_y/V_{ref}
g_ζ	G
H	total enthalpy
h_1, h_2	metric coefficients in the x and y coordinates, respectively.
i, j, k	indices in the x, y, and z direction, respectively
K	coefficient of thermal conductivity$(= c_p\mu/Pr)$
K_1, K_2	geodesic curvature of the curves $y = const.$ and $x = const.$, respectively, Eq. (5)
K_{12}, K_{21}	parameters defined in Eq. (6)
l	length scale (to be used by the stability analysis codes)
M	Mach number
$m_1, .., m_{13}$	coefficients, defined in Eqs. (55),(61),(63),(68),(70)

N	logarithmic disturbance amplification ratio
n_1, n_2, n_3	coefficients defined in Eqs. (55),(61),(63),(68),(70)
p	pressure
Pr	Prandtl number
r	radius measured from the center of rotation for axisymmetric body (Fig. 1)
q_w	heat transfer at the wall, Eqs. (89)-(91)
s	arc length measured along x direction (from $x = 0$).
T	temperature
u, v, w	velocity components in the x, y, and z directions
v_y	$\partial v/\partial y$
v_{ye}	$\partial v_e/\partial y$
V	total velocity
x, y, z	boundary-layer coordinates
$\overline{x}, \overline{y}, \overline{z}$	Cartesian coordinates for wing definition, Figs. 3, 4, 5.
x', y'	reference rectangular coordinates
X	distance measured along the chord line ($X/c = 1$ at the trailing edge)
α	angle of attack
γ	ratio of specific heat
$\Delta x, \Delta y, \Delta\zeta$	grid spacing in the x, y, ζ directions, respectively.
δ	boundary-layer thickness; $(z)_{V/V_e=0.995}$
δ_x^*	displacement thickness in x-direction, defined in Eq. (87) or (88a)
δ_y^*	displacement thickness in y-direction, defined in Eq. (88b)
ζ	transformed normal coordinate, Eq. (40) or Eq. (43) or Eq. (45)
θ	angle between x and y coordinates
κ	$\Delta\zeta(k+1)/\Delta\zeta(k)$, or curvature
λ	sweep angle

λ_1	leading-edge sweep angle
λ_2	trailing-edge sweep angle
μ	viscosity
ν	kinematic viscosity, μ/ρ
ρ	density
ϕ	azimuthal angle, 0 and π on the windward and leeward plane of symmetry, respectively, see Fig. 2
	or stretching variable for an airfoil, $cos^{-1}(1 - X/c)$, Fig. 6

subscript

aw	adiabatic wall
e	edge of the boundary-layer
le	leading-edge
s	stagnation point or stagnation line (leading-edge attachment line)
t	total
w	wall
x	partial differentiation with respect to x
y	partial differentiation with respect to y
ζ	partial differentiation with respect to ζ
∞	free stream

superscript

$'$	ordinary differentiation with respect to ζ

LIST OF FIGURES

PART I. NUMERICAL METHOD

1. INTRODUCTION

Over the past decade, the major emphasis in computational fluid mechanics has focused on numerically solving the Euler and Navier-Stokes equations for increasingly complex aerodynamic shapes. Navier-Stokes solutions, however, are generally much more expensive to obtain in terms of computer resources than the boundary-layer solutions, and while capable of simulating the physics of complex flows, they are often of low resolution due to grid point restrictions. Therefore, Navier-Stokes solution may not be adequate for the stability analysis which requires accurate solution inside the boundary layer. Furthermore, Navier-Stokes solutions are not essential for many design and analysis procedures.

Renewed emphasis on drag reduction [1], laminar flow control [2], and transition prediction [1] has indicated the need to develop boundary-layer software that can be routinely applied to aerospace vehicles at a fraction of the cost associated with solutions obtained from the thin-layer Navier-Stokes equations. Research at the NASA Langley Research Center has resulted in the development and verification of three-dimensional boundary-layer procedures [3] [4] for application to aerospace configurations.

In preliminary design, especially for the design of the laminar flow control wing, empenage, nacelle, or fuselage, it is convenient to use simplified two-dimensional or axisymmetric or quasi-three-dimensional flow calculations to limit computation expense. A boundary-layer code for the application to swept-back and tapered wings developed by Kaups-Cebeci [5] has been used for the design of a laminar flow control wing. This boundary-layer code, however, can only solve subsonic and swept-back wing flow with a spanwise conical flow approximation. Also, this code yields discontinuous first and second normal derivatives of the velocity along with an oscillatory skin friction coefficient for some flow cases, especially when suction is applied.

In this report, an efficient, second-order accurate, finite-difference method is used to solve the two-dimensional or axisymmetric or quasi-three-dimensional, compressible, laminar boundary-layer equations. The quasi-three-dimensional flows considered in the present report include flow along the plane of symmetry, flow along the leading-edge attachment line, and swept wing flows with conical flow approximations. The swept wing case includes swept-back tapered wings and swept-forward tapered wing with a spanwise conical flow assumption, and swept-back delta (low aspect ratio) wings with a streamwise conical flow assumption which is more appropriate for the flow over a low aspect-ratio wing.

Results are presented for several test cases. This method was used for the boundary-layer stability analysis of axisymmetric laminar-flow-control nacelles [6] and of the flow along the leading-edge attachment line [7]. The method is valid for perfect gas flows from subsonic to hypersonic Mach numbers. Interaction between the inviscid and viscous flow is not included. A user's manual with a detailed description of the computer program for the boundary-layer analysis is presented in PART. II.

2. BOUNDARY-LAYER EQUATIONS

Three-dimensional, compressible, laminar boundary-layer equations (in dimensional form) for the general nonorthogonal body-oriented coordinate system, from which the governing equations for two-dimensional, axisymmetric, and quasi-three-dimensional flows are derived, are as follows [3], [8], [9]:

continuity equation

$$\frac{\partial}{\partial x}(\rho u h_2 \sin\theta) + \frac{\partial}{\partial y}(\rho v h_1 \ sin\theta) + \frac{\partial}{\partial z}(\rho w h_1 h_2 \sin\theta) = 0 \tag{1}$$

x-momentum equation

$$\begin{aligned}&\frac{\rho u}{h_1}\frac{\partial u}{\partial x} + \frac{\rho v}{h_2}\frac{\partial u}{\partial y} + \rho w\frac{\partial u}{\partial z} - \rho u^2 K_1 \cot\theta + \rho v^2 K_2 \csc\theta + \rho u v K_{12} \\ &= -\frac{\csc^2\theta}{h_1}\frac{\partial p}{\partial x} + \frac{\cot\theta \csc\theta}{h_2}\frac{\partial p}{\partial y} + \frac{\partial}{\partial z}(\mu\frac{\partial u}{\partial z})\end{aligned} \tag{2}$$

y-momentum equation

$$\begin{aligned}&\frac{\rho u}{h_1}\frac{\partial v}{\partial x} + \frac{\rho v}{h_2}\frac{\partial v}{\partial y} + \rho w\frac{\partial v}{\partial z} - \rho v^2 K_2 \cot\theta + \rho u^2 K_1 \csc\theta + \rho u v K_{21} \\ &= \frac{\cot\theta \csc\theta}{h_1}\frac{\partial p}{\partial x} - \frac{\csc^2\theta}{h_2}\frac{\partial p}{\partial y} + \frac{\partial}{\partial z}(\mu\frac{\partial v}{\partial z})\end{aligned} \tag{3}$$

energy equation

$$\frac{\rho u}{h_1}\frac{\partial H}{\partial x} + \frac{\rho v}{h_2}\frac{\partial H}{\partial y} + \rho w\frac{\partial H}{\partial z} = \frac{\partial}{\partial z}\left\{\frac{\mu}{Pr}\frac{\partial H}{\partial z} + \mu(1 - \frac{1}{Pr})\frac{\partial}{\partial z}(\frac{V^2}{2})\right\} \tag{4}$$

The metric coefficients h_1 and h_2 are functions of x and y. Theta, θ, is the angle between the x and y coordinates. The parameters K_1 and K_2 are the geodesic curvatures of the curves $y = const$ and $x = const$ respectively, where

$$K_1 = \frac{1}{h_1 h_2 \sin\theta}\left\{\frac{\partial}{\partial x}(h_2 \cos\theta) - \frac{\partial h_1}{\partial y}\right\}, \qquad K_2 = \frac{1}{h_1 h_2 \sin\theta}\left\{\frac{\partial}{\partial y}(h_1 \cos\theta) - \frac{\partial h_2}{\partial x}\right\} \tag{5}$$

and

$$\begin{aligned}K_{12} &= \frac{1}{h_1 h_2 \sin^2\theta}\left\{(1 + \cos^2\theta)\frac{\partial h_1}{\partial y} - 2\cos\theta\frac{\partial h_2}{\partial x}\right\} \\ K_{21} &= \frac{1}{h_1 h_2 \sin^2\theta}\left\{(1 + \cos^2\theta)\frac{\partial h_2}{\partial x} - 2\cos\theta\frac{\partial h_1}{\partial y}\right\}\end{aligned} \tag{6}$$

V is the total velocity and is given by

$$V = (u^2 + v^2 + 2uv\cos\theta)^{1/2} \tag{7}$$

The boundary conditions are

$$z = \delta, \qquad u = u_e(x,y), \quad v = v_e(x,y), \quad H = H_e \tag{8.a}$$

$$z = 0, \qquad u = v = 0, \quad w = w_w, \quad H = H_w \quad or \quad (\frac{\partial H}{\partial z})_w = 0 \tag{8.b}$$

The pressure gradients are related to the inviscid velocities by the following equations at the edge of the boundary-layer:

$$\rho_e \left\{ \frac{u_e}{h_1}\frac{\partial u_e}{\partial x} + \frac{v_e}{h_2}\frac{\partial u_e}{\partial y} - u_e^2 K_1 \cot\theta + v_e^2 K_2 \csc\theta + u_e v_e K_{12} \right\}$$
$$= -\frac{\csc\theta}{h_1}\frac{\partial p}{\partial x} + \frac{\cot\theta\csc\theta}{h_2}\frac{\partial p}{\partial y} \tag{9.a}$$

$$\rho_e \left\{ \frac{u_e}{h_1}\frac{\partial v_e}{\partial x} + \frac{v_e}{h_2}\frac{\partial v_e}{\partial y} - v_e^2 K_2 \cot\theta + u_e^2 K_1 \csc\theta + u_e v_e K_{21} \right\}$$
$$= \frac{\cot\theta\csc\theta}{h_1}\frac{\partial p}{\partial x} - \frac{\csc^2\theta}{h_2}\frac{\partial p}{\partial y} \tag{9.b}$$

The perfect gas equation of state and Sutherland's viscosity are used to close the equation set.

2.1 Stagnation Point

To obtain the boundary-layer solutions at the three-dimensional stagnation point, the governing equations for three-dimensional laminar compressible flows in Cartesian coordinates are required and can be obtained by setting $h_1 = 1$, $h_2 = 1$, and $\theta = \pi/2$ in Eqs. (1)-(4).

continuity equation

$$\frac{\partial}{\partial x}(\rho u) + \frac{\partial}{\partial y}(\rho v) + \frac{\partial}{\partial z}(\rho w) = 0 \tag{10}$$

x-momentum equation

$$\rho u\frac{\partial u}{\partial x} + \rho v\frac{\partial u}{\partial y} + \rho w\frac{\partial u}{\partial z} = -\frac{\partial p}{\partial x} + \frac{\partial}{\partial z}(\mu\frac{\partial u}{\partial z}) \tag{11}$$

y-momentum equation

$$\rho u\frac{\partial v}{\partial x}+\rho v\frac{\partial v}{\partial y}+\rho w\frac{\partial v}{\partial z}=-\frac{\partial p}{\partial y}+\frac{\partial}{\partial z}(\mu\frac{\partial v}{\partial z}) \tag{12}$$

energy equation

$$\rho u\frac{\partial H}{\partial x}+\rho v\frac{\partial H}{\partial y}+\rho w\frac{\partial H}{\partial z}=\frac{\partial}{\partial z}\left\{\frac{\mu}{Pr}\frac{\partial H}{\partial z}+\mu(1-\frac{1}{Pr})\frac{\partial}{\partial z}(\frac{V^2}{2})\right\} \tag{13}$$

where

$$V=(u+v)^{1/2} \tag{14}$$

The boundary conditions are

$$z=\delta, \qquad u=u_e(x,y), \quad v=v_e(x,y), \quad H=H_e \tag{15.a}$$

$$z=0, \qquad u=v=0, \quad w=w_w, \quad H=H_w \quad or \quad (\frac{\partial H}{\partial z})_w=0 \tag{15.b}$$

2.2 Two-dimensional and Axisymmetric Flow

The boundary-layer equations for two-dimensional and axisymmetric flow can be obtained from Eqs. (1)-(4) by substituting $\theta=\pi/2$, $v=0$, $h_1=1$, $h_2=r^j$ ($j=0$ for 2-D flow; $j=1$ for axisymmetric flow). See Figure 1 for the coordinate system for 2-D and axisymmetric flow.

continuity equation

$$\frac{\partial}{\partial x}(\rho u r^j)+\frac{\partial}{\partial z}(\rho w r^j)=0 \tag{16}$$

x-momentum equation

$$\rho u\frac{\partial u}{\partial x}+\rho w\frac{\partial u}{\partial z}=-\frac{\partial p}{\partial x}+\frac{\partial}{\partial z}(\mu\frac{\partial u}{\partial z}) \tag{17}$$

energy equation

$$\rho u\frac{\partial H}{\partial x}+\rho w\frac{\partial H}{\partial z}=\frac{\partial}{\partial z}\left\{\frac{\mu}{Pr}\frac{\partial H}{\partial z}+\mu(1-\frac{1}{Pr})\frac{\partial}{\partial z}(\frac{V^2}{2})\right\} \tag{18}$$

where

$$V=u \tag{19}$$

The boundary conditions are

$$z = \delta, \qquad u = u_e(x), \quad H = H_e \tag{20.a}$$

$$z = 0, \qquad u = 0, \quad w = w_w, \quad H = H_w \quad or \quad (\frac{\partial H}{\partial z})_w = 0 \tag{20.b}$$

The pressure gradients are related to the inviscid velocity by the following equation at the edge of the boundary-layer:

$$\rho_e u_e \frac{d\,u_e}{d\,x} = -\frac{d\,p}{d\,x} \tag{21}$$

2.3 Flow along Plane of Symmetry and Along Leading-Edge Attachment Line

Along the windward and leeward plane of symmetry and along the leading-edge attachment line, v and $K_1 \csc\theta$ are zero and θ is generally $\pi/2$.(θ is retained for the general system) Consequently, each term in the y-momentum equation(Eq.(3)) vanishes. However, partial differentiation of Eq. (3) with respect to y yields an equation for $\partial v/\partial y$. After differentiation and using the appropriate symmetry conditions ($\partial u/\partial y = \partial w/\partial y = \partial^2 v/\partial y^2 = \partial H/\partial y = \partial h_1/\partial y = \partial h_2/\partial y = 0$) along with Eq. (9), the governing equations for the flow along these lines become (See Figure 2 for the coordinate system.):

continuity equation

$$\frac{\partial}{\partial x}(\rho u h_2 \sin\theta) + \rho v_y h_1 \sin\theta + \frac{\partial}{\partial z}(\rho w h_1 h_2 \sin\theta) = 0 \tag{22}$$

x-momentum equation

$$\frac{\rho u}{h_1}\frac{\partial u}{\partial x} + \rho w \frac{\partial u}{\partial z} - \rho u^2 K_1 \cot\theta = \rho_e(\frac{u_e}{h_1}\frac{\partial u_e}{\partial x} - u_e^2 K_1 \cot\theta) + \frac{\partial}{\partial z}(\mu\frac{\partial u}{\partial z}) \tag{23}$$

y-momentum equation

$$\begin{aligned}&\frac{\rho u}{h_1}\frac{\partial v_y}{\partial x} + \rho w \frac{\partial v_y}{\partial z} + \frac{\rho}{h_2}v_y^2 + \rho u v_y K_{21} + \rho u^2 \frac{\partial(K_1 \csc\theta)}{\partial y} \\ &= \rho_e(\frac{u_e}{h_1}\frac{\partial v_{ye}}{\partial x} + \frac{v_{ye}^2}{h_2} + u_e v_{ye} K_{21}) + \rho_e u_e^2 \frac{\partial(K_1 \csc\theta)}{\partial y} + \frac{\partial}{\partial z}(\mu\frac{\partial v_y}{\partial z})\end{aligned} \tag{24}$$

energy equation

$$\frac{\rho u}{h_1}\frac{\partial H}{\partial x} + \rho w \frac{\partial H}{\partial z} = \frac{\partial}{\partial z}\left\{\frac{\mu}{Pr}\frac{\partial H}{\partial z} + \mu(1 - \frac{1}{Pr})\frac{\partial}{\partial z}(\frac{V^2}{2})\right\} \tag{25}$$

where $v_y = \partial v/\partial y$, $v_{ye} = \partial v_e/\partial y$ and $V = u$ along these lines.

The boundary conditions for the plane of symmetry are

$$z = \delta, \qquad u = u_e(x), \quad v_y = v_{ye}, \quad H = H_e \tag{26.a}$$

$$z = 0, \qquad u = v = v_y = 0, \quad w = w_w, \quad H = H_w \quad or \quad (\frac{\partial H}{\partial y})_w = 0 \tag{26.b}$$

2.4 Swept Wing Flow

The governing equation for a three-dimensional compressible laminar flow in a polar coordinate system with conical flow assumption ($\partial p/\partial x = 0$) can be obtained by substituting $h_1 = 1$, $h_2 = x$, $\theta = \pi/2$ from the equations (1)-(4). Figures 3, 4, and 5 show the coordinate systems used for the swept-back wing with the spanwise conical flow assumption, the swept-forward wing with the spanwise conical flow assumption, and the swept-back delta (low aspect ratio) wing with the streamwise conical flow assumption, respectively. Fig. 6 shows the airfoil definition used for the swept wing cases.

continuity equation

$$\frac{\partial}{\partial x}(\rho u x) + \frac{\partial}{\partial y}(\rho v) + \frac{\partial}{\partial z}(\rho w x) = 0 \tag{27}$$

x-momentum equation

$$\rho u\frac{\partial u}{\partial x} + \frac{\rho v}{x}\frac{\partial u}{\partial y} + \rho w\frac{\partial u}{\partial z} - \frac{\rho v^2}{x} = \frac{\partial}{\partial z}(\mu\frac{\partial u}{\partial z}) \tag{28}$$

y-momentum equation

$$\rho u\frac{\partial v}{\partial x} + \frac{\rho v}{x}\frac{\partial v}{\partial y} + \rho w\frac{\partial v}{\partial z} + \frac{\rho u v}{x} = -\frac{1}{x}\frac{\partial p}{\partial y} + \frac{\partial}{\partial z}(\mu\frac{\partial v}{\partial z}) \tag{29}$$

energy equation

$$\rho u\frac{\partial H}{\partial x} + \frac{\rho v}{x}\frac{\partial H}{\partial y} + \rho w\frac{\partial H}{\partial z} = \frac{\partial}{\partial z}\left\{\frac{\mu}{Pr}\frac{\partial H}{\partial z} + \mu(1 - \frac{1}{Pr})\frac{\partial}{\partial z}(\frac{V^2}{2})\right\} \tag{30}$$

where

$$V = (u + v)^{1/2} \tag{31}$$

The boundary conditions are

$$z = \delta, \qquad u = u_e(y), \quad v = v_e(y), \quad H = H_e \tag{32.a}$$

$$z = 0, \qquad u = v = 0, \quad w = w_w, \quad H = H_w \quad or \quad (\frac{\partial H}{\partial z})_w = 0 \tag{32.b}$$

The pressure gradients are related to the inviscid velocities at the edge of the boundary-layer by the following equations:

$$\frac{d\,u_e}{d\,y} = v_e \tag{33.a}$$

$$\frac{d\,v_e^2}{d\,y} = -2\,u_e v_e - \frac{2}{\rho_e}\frac{d\,p}{d\,y} \tag{33.b}$$

Along the stagnation line, $v = 0$. Partial differentiation of Eq. (29) with respect to y yields an equation for $\partial v/\partial y$. After differentiation and substituting $v = 0$, the governing equations for the stagnation line become:

continuity equation

$$\frac{\partial}{\partial x}(\rho u x) + \rho v_y + \frac{\partial}{\partial z}(\rho w x) = 0 \tag{34}$$

x-momentum equation

$$\rho u\frac{\partial u}{\partial x} + \rho w\frac{\partial u}{\partial z} = \frac{\partial}{\partial z}(\mu\frac{\partial u}{\partial z}) \tag{35}$$

y-momentum equation

$$\rho u\frac{\partial v_y}{\partial x} + \frac{\rho}{x}v_y^2 + \rho w\frac{\partial v_y}{\partial z} + \frac{\rho u v_y}{x} = -\frac{1}{x}\frac{\partial^2 p}{\partial y^2} + \frac{\partial}{\partial z}(\mu\frac{\partial v_y}{\partial z}) \tag{36}$$

energy equation

$$\rho u\frac{\partial H}{\partial x} + \rho w\frac{\partial H}{\partial z} = \frac{\partial}{\partial z}\left\{\frac{\mu}{Pr}\frac{\partial H}{\partial z} + \mu(1 - \frac{1}{Pr})\frac{\partial}{\partial z}(\frac{V^2}{2})\right\} \tag{37}$$

where

$$V = u \tag{38}$$

The boundary conditions are

$$z = \delta, \qquad u = u_e, \quad v_y = v_{ye}, \quad H = H_e \tag{39.a}$$

$$z = 0, \qquad u = v_y = 0, \quad w = w_w, \quad H = H_w \quad or \quad (\frac{\partial H}{\partial z})_w = 0 \tag{39.b}$$

3. TRANSFORMED EQUATIONS

The boundary-layer equations are transformed to a coordinate system which allows a coupled solution of the continuity and momentum equations. In this report, three different transformations are used.

(A) The following transformation is used for stagnation point, 2-D flow, axisymmetric flow, and flow along the plane of symmetry.

$$x = x, \qquad y = y, \qquad \zeta = \sqrt{\frac{\rho_e u_e}{\mu_e s}} \int_0^z \frac{\rho}{\rho_e} dz \tag{40}$$

where

$$s = \int_0^x h_1 dx \tag{41}$$

together with the following definitions

$$F = f_\zeta = u/u_e, \quad G = g_\zeta = v/V_{ref}, \quad E = H/H_e \tag{42}$$

For the stagnation point, $V_{ref} = v_e$; for 2-D and axisymmetric flow, $G = g_\zeta = 0$; for the plane of symmetry, $V_{ref} = V_\infty$, and $G = g_\zeta = v_y/V_\infty$. This transformation removes the singularity at $x = 0$.

(B) The following transformation is used for the flow along the leading-edge attachment line.

$$x = x, \qquad y = y, \qquad \zeta = \sqrt{\frac{\rho_e u_e}{\mu_e}} \int_0^z \frac{\rho}{\rho_e} dz \tag{43}$$

and the definitions

$$F = f_\zeta = u/u_e, \quad G = g_\zeta = v_y/V_\infty, \quad E = H/H_e \tag{44}$$

This transformation is used to avoid an infinite transformed normal coordinate (ζ_e) near $x = 0$; such an occurrence is possible when using the transformation given in Eq.(40).

(C) The following transformation is used for the swept wing flow with conical flow assumption.

$$x = x, \qquad y = y, \qquad \zeta = \sqrt{\frac{\rho_e \mid u_e \mid}{\mu_e x}} \int_0^z \frac{\rho}{\rho_e} dz \tag{45}$$

and the definitions

$$F = f_\zeta = u/u_e, \quad G = g_\zeta = v/v_e, \quad E = H/H_e \quad \text{(off the stagnation line)} \quad (46.a)$$

$$F = f_\zeta = u/u_e, \quad G = g_\zeta = v_y/v_{ye}, \quad E = H/H_e \quad \text{(on the stagnation line)} \quad (46.b)$$

This transformation is used to handle cases when u_e is positive or negative.

3.1 Three-Dimensional Stagnation Point

The governing equations for three-dimensional laminar compressible flows in rectangular coordinates, Eqs. (10)-(13), are transformed using Eq. (40) and Howarth's [10] inviscid velocity components near the stagnation point. For s approaching zero, the following ordinary differential equations are obtained.

x-momentum equation

$$(Cf'')' + ff'' - (f')^2 + \frac{B}{A}f''g + \frac{\rho_e}{\rho} = 0 \quad (47)$$

y-momentum equation

$$(Cg'')' + fg'' - \frac{B}{A}(g')^2 + \frac{B}{A}g''g + \frac{B}{A}\frac{\rho_e}{\rho} = 0 \quad (48)$$

energy equation

$$(\frac{C}{Pr}E')' + (f + \frac{B}{A}g)E' = 0 \quad (49)$$

The equations above are based on the assumptions that the outer flow is irrotational and that the inviscid velocity components near the stagnation point can be approximated by

$$u_e = Ax, \qquad v_e = By \quad (50)$$

The primes denote ordinary differentiation with respect to ζ, i.e.,

$$f' = \frac{df}{d\zeta} = \frac{u}{u_e}, \qquad g' = \frac{dg}{d\zeta} = \frac{v}{v_e}, \qquad and \quad E = \frac{H}{H_e} \quad (51)$$

The boundary conditions are

$$\zeta = 0: \qquad f = f' = g = g' = 0, \quad E' = 0 \quad or \quad E = E_w \tag{52.a}$$

$$\zeta = \zeta_e: \qquad f' = 1, \quad g' = 1, \quad E = 1 \tag{52.b}$$

Two-dimensional and axisymmetric stagnation point equations can be obtained by substituting $C^* = B/A = 0$ (for a 2-D stagnation point) or $C^* = B/A = 1$ (for an axisymmetric stagnation point).

3.2 Two-Dimensional and Axisymmetric Flow

Using the transformation given in Eq. (40) and the relations given by Eq. (21), the governing Eqs. (16)-(18) are transformed to the following form:

x-momentum equation

$$F = f_\zeta \tag{53.a}$$

$$(CF_\zeta)_\zeta + m_1 f F_\zeta - m_2 F^2 + m_{11} c - m_{13} F_\zeta = m_{10}(FF_x - F_\zeta f_x) \tag{53.b}$$

energy equation

$$(n_1 E_\zeta)_\zeta + n_2 E_\zeta + (n_3)_\zeta - m_{13} E_\zeta = m_{10}(FE_x - E_\zeta f_x) \tag{54}$$

The coefficients m_1 to m_{13} and n_1 to n_3 are as follows:

$$m_1 = \frac{1}{2}\left\{1 + \frac{s}{h_1 u_e}\frac{\partial u_e}{\partial x}\right\} + \frac{s}{h_1 h_2 \sqrt{\rho_e \mu_e}}\frac{\partial}{\partial x}\left\{h_2\sqrt{\rho_e \mu_e}\right\} \tag{55.a}$$

$$m_2 = \frac{s}{h_1 u_e}\frac{\partial u_e}{\partial x} \tag{55.b}$$

$$m_{10} = \frac{s}{h_1} \tag{55.c}$$

$$m_{11} = m_2 \tag{55.d}$$

$$m_{13} = \frac{(\rho w)_w}{\rho_e u_e}\sqrt{\frac{\rho_e u_e s}{\mu_e}} \tag{55.e}$$

$$n_1 = \frac{C}{Pr} \tag{55.f}$$

$$n_2 = m_1 f \tag{55.g}$$

$$n_3 = \frac{Cu_e^2}{H_e}(1 - \frac{1}{Pr})FF_\zeta \tag{55.h}$$

Note that $h_1 = 1$ and $h_2 = r^j$, where $j = 0$ for 2-D flow or $j = 1$ for axisymmetric flow. The boundary conditions are

$$\zeta = 0: \qquad f = F = 0, \quad E' = 0 \quad or \quad E = E_w \tag{56.a}$$

$$\zeta = \zeta_e: \qquad F = 1, \quad E = 1 \tag{56.b}$$

3.3 Flow Along Plane of Symmetry

The governing equations for the plane of symmetry are transformed using the transformation given in Eq. (40) and by defining

$$F = f_\zeta = u/u_e, \quad G = g_\zeta = v_y/V_\infty, \quad E = H/H_e \tag{57}$$

x-momentum equation

$$F = f_\zeta \tag{58.a}$$

$$(CF_\zeta)_\zeta + m_1 f F_\zeta - m_2 F^2 + m_6 F_\zeta g + m_{11} c - m_{13} F_\zeta = m_{10}(FF_x - F_\zeta f_x) \tag{58.b}$$

y-momentum equation

$$G = g_\zeta \tag{59.a}$$

$$(CG_\zeta)_\zeta + m_1 f G_\zeta - m_3 G^2 - m_4 FG + m_6 G_\zeta g - m_9 F^2 + m_{12} c - m_{13} G_\zeta$$
$$= m_{10}(FG_x - G_\zeta f_x) \tag{59.b}$$

energy equation

$$(n_1 E_\zeta)_\zeta + n_2 E_\zeta + (n_3)_\zeta - m_{13} E_\zeta = m_{10}(FE_x - E_\zeta f_x) \tag{60}$$

The coefficients m_1-m_{13}, n_1-n_3 are defined as follows:

$$m_1 = \frac{1}{2}\left\{1 + \frac{s}{h_1 u_e}\frac{\partial u_e}{\partial x}\right\} + \frac{s}{h_1 h_2 \sin\theta\sqrt{\rho_e \mu_e}}\frac{\partial}{\partial x}\left\{h_2 \sin\theta\sqrt{\rho_e \mu_e}\right\} \tag{61.a}$$

$$m_2 = \frac{s}{h_1 u_e}\frac{\partial u_e}{\partial x} - sK_1 \cot\theta \tag{61.b}$$

$$m_3 = \frac{sV_\infty}{h_2 u_e} \tag{61.c}$$

$$m_4 = sK_{21} + \frac{s}{h_1 V_\infty}\frac{\partial V_\infty}{\partial x} \tag{61.d}$$

$$m_6 = m_3 \tag{61.e}$$

$$m_9 = \frac{su_e}{V_\infty}\frac{\partial(K_1 \csc\theta)}{\partial y} \tag{61.f}$$

$$m_{10} = \frac{s}{h_1} \tag{61.g}$$

$$m_{11} = \frac{s}{h_1 u_e}\frac{\partial u_e}{\partial x} - s\cot\theta K_1 \tag{61.h}$$

$$m_{12} = \frac{su_e}{V_\infty}\frac{\partial(K_1 \csc\theta)}{\partial y} + \frac{s}{V_\infty}\left(\frac{1}{h_1}\frac{\partial v_{ye}}{\partial x} + \frac{v_{ye}^2}{u_e h_2} + K_{21} v_{ye}\right) \tag{61.i}$$

$$m_{13} = \frac{(\rho w)_w}{\rho_e u_e}\sqrt{\frac{\rho_e u_e s}{\mu_e}} \tag{61.j}$$

$$n_1 = \frac{C}{Pr} \tag{61.k}$$

$$n_2 = m_1 f + m_6 g \tag{61.l}$$

$$n_3 = \frac{Cu_e^2}{H_e}\left(1 - \frac{1}{Pr}\right)FF_\zeta \tag{61.m}$$

The boundary conditions are

$$\zeta = 0: \qquad f = F = g = G = 0, \quad E' = 0 \quad or \quad E = E_w \tag{62.a}$$

$$\zeta = \zeta_e: \qquad F = 1, \quad G = \frac{v_{ye}}{V_\infty}, \quad E = 1 \tag{62.b}$$

where $v_{ye} = \partial v_e/\partial y$.

3.4 Flow Along A Leading-Edge Attachment Line

The governing equations for the flow along the leading-edge attachment line are transformed using the transformation given in Eq. (43) to the same equations as for the flow

along the plane of symmetry (Eqs.(58)-(60)). However, because of the difference in the transformation, the coefficients m_1 to m_{13} and n_1 to n_3 are defined now as follows:

$$m_1 = \frac{1}{2\,h_1\,u_e}\frac{\partial u_e}{\partial x} + \frac{1}{h_1 h_2 \sin\theta\sqrt{\rho_e\mu_e}}\frac{\partial}{\partial x}\{h_2 \sin\theta\sqrt{\rho_e\mu_e}\} \tag{63.a}$$

$$m_2 = \frac{1}{h_1 u_e}\frac{\partial u_e}{\partial x} - K_1 \cot\theta \tag{63.b}$$

$$m_3 = \frac{V_\infty}{h_2 u_e} \tag{63.c}$$

$$m_4 = K_{21} \tag{63.d}$$

$$m_6 = m_3 \tag{63.e}$$

$$m_9 = \frac{u_e}{V_\infty}\frac{\partial(K_1 \csc\theta)}{\partial y} \tag{63.f}$$

$$m_{10} = \frac{1}{h_1} \tag{63.g}$$

$$m_{11} = \frac{1}{h_1 u_e}\frac{\partial u_e}{\partial x} - \cot\theta K_1 \tag{63.h}$$

$$m_{12} = \frac{u_e}{V_\infty}\frac{\partial(K_1 \csc\theta)}{\partial y} + \frac{1}{V_\infty}(\frac{1}{h_1}\frac{\partial v_{ye}}{\partial x} + \frac{v_{ye}^2}{u_e h_2} + K_{21} v_{ye}) \tag{63.i}$$

$$m_{13} = \frac{(\rho w)_w}{\rho_e u_e}\sqrt{\frac{\rho_e u_e}{\mu_e}} \tag{63.j}$$

$$n_1 = \frac{C}{Pr} \tag{63.k}$$

$$n_2 = m_1 f + m_6 g \tag{63.l}$$

$$n_3 = \frac{C u_e^2}{H_e}(1 - \frac{1}{Pr})FF_\zeta \tag{63.m}$$

The boundary conditions are the same as for the flow along the plane of symmetry and are repeated here for completeness:

$$\zeta = 0: \qquad f = F = g = G = 0, \quad E' = 0 \quad or \quad E = E_w \tag{64.a}$$

$$\zeta = \zeta_e: \qquad F = 1, \quad G = \frac{v_{ye}}{V_\infty}, \quad E = 1 \tag{64.b}$$

3.5 Swept Wing Flow

The governing equations for the swept wing flow (off the stagnation line) are transformed using the transformation given in Eq. (45) to the following equations.

x-momentum equation

$$F = f_\zeta \tag{65.a}$$

$$(CF_\zeta)_\zeta + m_1 f F_\zeta - m_2 F^2 + m_6 F_\zeta g + m_{11} c - m_{13} F_\zeta = m_7 (G F_y - F_\zeta g_y) \tag{65.b}$$

y-momentum equation

$$G = g_\zeta \tag{66.a}$$

$$(CG_\zeta)_\zeta + m_1 f G_\zeta - m_3 G^2 - m_4 F G + m_6 G_\zeta g - m_9 F^2 + m_{12} c - m_{13} G_\zeta$$

$$= m_7 (G G_y - G_\zeta g_y) \tag{66.b}$$

energy equation

$$(n_1 E_\zeta)_\zeta + n_2 E_\zeta + (n_3)_\zeta - m_{13} E_\zeta = m_7 (G E_y - E_\zeta g_y) \tag{67}$$

The coefficients m_1 to m_{13} and n_1 to n_3 are defined as follows:

$$m_1 = -1.5 \tag{68.a}$$

$$m_2 = 0 \tag{68.b}$$

$$m_3 = \frac{1}{\mid u_e \mid} \frac{d v_e}{d y} \tag{68.c}$$

$$m_4 = \frac{u_e}{\mid u_e \mid} \tag{68.d}$$

$$m_5 = \frac{v_e^2}{u_e \mid u_e \mid} \tag{68.e}$$

$$m_6 = \frac{1}{\mid u_e \mid} \frac{d v_e}{d y} + \frac{1}{2} (\frac{v_e}{u_e})^2 + \frac{v_e}{2 \rho_e \mu_e \mid u_e \mid} \frac{d(\rho_e \mu_e)}{d y} \tag{68.f}$$

$$m_7 = \frac{v_e}{\mid u_e \mid} \tag{68.g}$$

$$m_8 = -\frac{v_e^2}{u_e \mid u_e \mid} \tag{68.h}$$

$$m_9 = 0 \tag{68.i}$$

$$m_{11} = 0 \tag{68.j}$$

$$m_{12} = \frac{1}{\mid u_e \mid}\frac{d\,v_e}{dy} + \frac{u_e}{\mid u_e \mid} \tag{68.k}$$

$$m_{13} = \frac{(\rho w)_w}{\rho_e \mid u_e \mid}\sqrt{\frac{\rho_e \mid u_e \mid x}{\mu_e}} \tag{68.l}$$

$$n_1 = \frac{C}{Pr} \tag{68.m}$$

$$n_2 = m_1 f + m_6 g \tag{68.n}$$

$$n_3 = \frac{C u_e^2}{H_e}(1 - \frac{1}{Pr})\left\{F F_\zeta + G G_\zeta (\frac{v_e}{u_e})^2)\right\} \tag{68.o}$$

The boundary conditions are

$$\zeta = 0: \qquad f = F = g = G = 0, \quad E' = 0 \quad or \quad E = E_w \tag{69.a}$$

$$\zeta = \zeta_e: \qquad F = 1, \quad G = 1, \quad E = 1 \tag{69.b}$$

The governing equations on the stagnation line (leading-edge attachment line) for the swept wing flow are transformed to the following equations:

x-momentum equation

$$F = f_\zeta \tag{70.a}$$

$$(C F_\zeta)_\zeta + m_1 f F_\zeta - m_2 F^2 + m_6 F_\zeta g + m_{11} c - m_{13} F_\zeta = 0. \tag{70.b}$$

y-momentum equation

$$G = g_\zeta \tag{71.a}$$

$$(C G_\zeta)_\zeta + m_1 f G_\zeta - m_3 G^2 - m_4 F G + m_6 G_\zeta g - m_9 F^2 + m_{12} c - m_{13} G_\zeta = 0 \tag{71.b}$$

energy equation

$$(n_1 E_\zeta)_\zeta + n_2 E_\zeta + (n_3)_\zeta - m_{13} E_\zeta = 0 \tag{72}$$

The coefficients m_1, m_2, m_3, m_4, m_5, m_9, m_{11}, m_{12}, m_{13}, n_1, n_2 are the same as in Eq. (68). The remaining coefficients are defined as follows:

$$m_6 = \frac{1}{\mid u_e \mid}\frac{d\,v_e}{dy} \tag{73.a}$$

$$m_7 = 0 \tag{73.b}$$

$$m_8 = 0 \tag{73.c}$$

$$n_3 = \frac{Cu_e^2}{H_e}(1 - \frac{1}{Pr})FF_\zeta \tag{73.d}$$

4. NUMERICAL METHOD

All the equations listed in the previous section can be expressed in the following form:

x-momentum equation

$$F = f_\zeta \tag{74.a}$$

$$(CF_\zeta)_\zeta + m_1 f F_\zeta - m_2 F^2 - m_5 FG + m_6 F_\zeta g - m_8 G^2 + m_{11} c - m_{13} F_\zeta$$
$$= m_{10}(FF_x - F_\zeta f_x) + m_7(GF_y - F_\zeta g_y) \tag{74.b}$$

y-momentum equation

$$G = g_\zeta \tag{75.a}$$

$$(CG_\zeta)_\zeta + m_1 f G_\zeta - m_3 G^2 - m_4 FG + m_6 G_\zeta g - m_9 F^2 + m_{12} c - m_{13} G_\zeta$$
$$= m_{10}(FG_x - G_\zeta f_x) + m_7(GG_y - G_\zeta g_y) \tag{75.b}$$

$$\tag{75.c}$$

energy equation

$$(n_1 E_\zeta)_\zeta + n_2 E_\zeta + (n_3)_\zeta - m_{13} E_\zeta = m_{10}(FE_x - E_\zeta f_x) + m_7(GE_y - E_\zeta g_y) \tag{76.a}$$

$$\tag{76.b}$$

Note that either m_7 or m_{10} is zero for two-dimensional, axisymmetric, and quasi-three-dimensional flows.

The above equations are linearized using Newton-Rhapson's linearization technique [11]. The ζ-derivative terms are discretized using a central finite-difference scheme. An implicit second order backward finite-difference is used for the x- and y-derivative terms.. An implicit marching procedure, which is similar method used in Ref. [12], is used to solve the governing equations.

For abbreviation, finite-difference operators are defined as

$$\delta_\zeta F_k = \frac{\frac{\Delta\zeta(k-1)}{\Delta\zeta(k)}(F_{k+1} - F_k) + \frac{\Delta\zeta(k)}{\Delta\zeta(k-1)}(F_k - F_{k-1})}{\Delta\zeta_k + \Delta\zeta_{k-1}} \quad k = 2, 3, .., kmax - 1 \tag{77.a}$$

$$\Delta_\zeta(C_k\Delta_\zeta F_k) = \frac{2}{\Delta\zeta_k + \Delta\zeta_{k-1}}\left\{C_{k+1/2}\frac{F_{k+1}-F_k}{\Delta\zeta_k} - C_{k-1/2}\frac{F_k - F_{k-1}}{\Delta\zeta_{k-1}}\right\} \tag{77.b}$$

$$\delta_x F_i = \frac{F_i - \overline{F}_{i-1}}{\Delta x_i} \quad \text{if i=2} \tag{77.c}$$

$$\delta_x F_i = \frac{\{\Delta x_i^2 - (\Delta x_i + \Delta x_{i-1})^2\}F_i + (\Delta x_i + \Delta x_{i-1})^2\overline{F}_{i-1} - \Delta x_i^2\overline{F}_{i-2}}{(\Delta x_i)^2(\Delta x_i + \Delta x_{i-1}) - \Delta x_i(\Delta x_i + \Delta x_{i-1})^2} \quad \text{if i} \geq 3 \tag{77.d}$$

$$\delta_y F_j = \frac{F_j - \overline{F}_{j-1}}{\Delta y_j} \quad \text{if j=2} \tag{77.e}$$

$$\delta_y F_j = \frac{\left\{\Delta y_j^2 - (\Delta y_j + \Delta y_{j-1})^2\right\}F_j + (\Delta y_j + \Delta y_{j-1})^2\overline{F}_{j-1} - \Delta y_j^2\overline{F}_{j-2}}{(\Delta y_j)^2(\Delta y_j + \Delta y_{j-1}) - \Delta y_j(\Delta y_j + \Delta y_{j-1})^2} \quad \text{if j} \geq 3 \tag{77.f}$$

where $C_{k\pm1/2} = \frac{1}{2}(C_k + C_{k\pm1})$, $\Delta\zeta_k = \zeta_{k+1} - \zeta_k$, $\Delta x_i = x_i - x_{i-1}$, $\Delta y_j = y_j - y_{j-1}$, and i, j, and k represent the x, y, and ζ directions, respectively. The overlined quantities are the converged solution at the previous step ($i-1$, $i-2$, $j-1$, $j-2$).

The finite-difference equations for the Eqs. (74)-(76) are linearized as follows:

x-momentum equation

$$f_k - f_{k-1} - \frac{\Delta\zeta_{k-1}}{2}(F_k + F_{k-1}) = 0 \tag{78.a}$$

$$\begin{aligned}
&\Delta_\zeta(C_k\,\Delta_\zeta F_k) + m_1(\overline{f}_k\delta_\zeta F_k + \delta_\zeta\overline{F}_k f_k - \overline{f}_k\delta_\zeta\overline{F}_k) - m_2(2\overline{F}F_k - \overline{F}_k^2) - m_5(\overline{G}_k F_k \\
&+\overline{F}_k G_k - \overline{F}_k\overline{G}_k) + m_6(\overline{g}_k\delta_\zeta F_k + \delta_\zeta\overline{F}_k g_k - \overline{g}_k\delta_\zeta\overline{F}_k) - m_8(2\overline{G}G_k - \overline{G}_k^2) + m_{11}\bar{c}_k - m_{13}F_\zeta \\
&= m_{10}(\overline{F}_k\delta_x F_i + \delta_x\overline{F}_i F_k - \overline{F}_k\delta_x\overline{F}_i - \delta_\zeta\overline{F}_k\delta_x f_i - \delta_\zeta F_k\delta_x\overline{f}_i + \delta_\zeta\overline{F}_k\delta_x\overline{f}_i) \\
&\quad +m_7(\overline{G}_k\delta_y F_k + \delta_y\overline{F}_k G_k - \overline{G}_k\delta_y\overline{F}_k - \delta_\zeta\overline{F}_k\delta_y g_k - \delta_\zeta F_k\delta_y\overline{g}_k + \delta_\zeta\overline{F}_k\delta_y\overline{g}_k)
\end{aligned} \tag{78.b}$$

y-momentum equation

$$g_k - g_{k-1} - \frac{\Delta\zeta_{k-1}}{2}(G_k + G_{k-1}) = 0 \tag{79.a}$$

$$\begin{aligned}
&\Delta_\zeta(C_k\,\Delta_\zeta G_k) + m_1(\overline{f}_k\delta_\zeta G_k + \delta_\zeta\overline{G}_k f_k - \overline{f}_k\delta_\zeta\overline{G}_k) - m_3(2\overline{G}G_k - \overline{G}_k^2) - m_4(\overline{G}_k F_k \\
&+\overline{F}_k G_k - \overline{F}_k\overline{G}_k) + m_6(\overline{g}_k\delta_\zeta G_k + \delta_\zeta\overline{G}_k g_k - \overline{g}_k\delta_\zeta\overline{G}_k) - m_9(2\overline{F}F_k - \overline{F}_k^2) + m_{12}\bar{c}_k - m_{13}G_\zeta \\
&= m_{10}(\overline{F}_k\delta_x G_i + \delta_x\overline{G}_i F_k - \overline{F}_k\delta_x\overline{G}_i - \delta_\zeta\overline{G}_k\delta_x f_i - \delta_\zeta G_k\delta_x\overline{f}_i + \delta_\zeta\overline{G}_k\delta_x\overline{f}_i) \\
&\quad +m_7(\overline{G}_k\delta_y G_k + \delta_y\overline{G}_k G_k - \overline{G}_k\delta_y\overline{G}_k - \delta_\zeta\overline{G}_k\delta_y g_k - \delta_\zeta G_k\delta_y\overline{g}_k + \delta_\zeta\overline{G}_k\delta_y\overline{g}_k)
\end{aligned} \tag{79.b}$$

energy equation

$$\Delta_\zeta(n_{1,k}\,\Delta_\zeta E_k)+n_{2,k}\;\delta_\zeta E_k+\delta_\zeta n_{3,k}-m_{13}E_\zeta = m_{10}(F_k\delta_x E_i-\delta_\zeta E_k\delta_x f_i)+m_7(G_k\delta_y E_j-\delta_\zeta E_k\delta_y g_j) \tag{80}$$

where the overlined quantities are evaluated from the previous iteration. The energy equation does not require linearization since it is solved after the momentum equations.

The finite-difference momentum equations, Eqs. (78) and (79), are rearranged into a 2x2 block tridiagonal form as

$$h_k = h_{k-1} + \frac{\Delta\zeta_{k-1}}{2}(H_k + H_{k-1}) \tag{81.a}$$

$$-A_k H_{k-1} + B_k H_k - C_k H_{k+1} + a_k h_k = D_k \tag{81.b}$$

where

$$h_k = \begin{bmatrix} f_k \\ g_k \end{bmatrix}$$

$$H_k = \begin{bmatrix} F_k \\ G_k \end{bmatrix}$$

A_k, B_k, C_k, a_k are 2x2 matrices, and D_k is a vector.

These equations are solved by the Davis Modified Tridiagonal Algorithm (See Appendix A). The finite-difference energy equation, Eq. (80), is arranged into a linear tridiagonal matrix equation form as

$$B_k E_{k-1} + D_k E_k + A_k E_{k+1} = C_k \tag{82}$$

where A_k, B_k, C_k, and D_k are scalars.

This equation is solved using the Thomas Algorithm. The momentum equations and the energy equation are solved iteratively in an uncoupled manner until the converged solution is obtained. The converged solution is usually obtained within ten iterations. If the converged solution is not obtained within twenty iterations, the flow may have been separated.

5. RESULTS AND DISCUSSION

5.1 Boundary-layer Parameter Definition

The skin friction coefficients are defined and calculated from the following equations.

(a) for 2-D, axisymmetric flow and flow along a plane of symmetry:

$$C_{fx} = \frac{(\mu \partial u/\partial z)_w}{\frac{1}{2}\rho_e V_e^2} = \frac{2\mu_w u_e (\partial F/\partial \zeta)_w (\rho/\rho_e)_w (\rho_e u_e/\mu_e s)^{1/2}}{\rho_e V_e^2} \tag{83}$$

(b) for the flow along a leading-edge attachment line:

$$C_{fx} = \frac{(\mu \partial u/\partial z)_w}{\frac{1}{2}\rho_e V_e^2} = \frac{2\mu_w u_e (\partial F/\partial \zeta)_w (\rho/\rho_e)_w (\rho_e u_e/\mu_e)^{1/2}}{\rho_e V_e^2} \tag{84}$$

(c) for swept wing flow:

$$C_{fx} = \frac{(\mu \partial u/\partial z)_w}{\frac{1}{2}\rho_e u_e^2} = \frac{2\mu_w \mid u_e \mid (\partial F/\partial \zeta)_w (\rho/\rho_e)_w (\rho_e \mid u_e \mid /\mu_e x)^{1/2}}{\rho_e u_e^2} \tag{85.a}$$

$$C_{fy} = \frac{(\mu \partial v/\partial z)_w}{\frac{1}{2}\rho_e v_e^2} = \frac{2\mu_w v_e (\partial G/\partial \zeta)_w (\rho/\rho_e)_w (\rho_e \mid u_e \mid /\mu_e x)^{1/2}}{\rho_e v_e^2} \tag{85.b}$$

The derivartive terms; $(\partial F/\partial \zeta)_w$, and $(\partial G/\partial \zeta)_w$ are evaluated by second order one-sided differences at the wall, i.e.,

$$(\frac{\partial F}{\partial \zeta})_w = \frac{(\Delta\zeta_1 + \Delta\zeta_2)^2 F_2 - (\Delta\zeta_1)^2 F_3}{\Delta\zeta_1(\Delta\zeta_1 + \Delta\zeta_2)^2 - (\Delta\zeta_1 + \Delta\zeta_2)(\Delta\zeta_1)^2} \tag{86.a}$$

$$(\frac{\partial G}{\partial \zeta})_w = \frac{(\Delta\zeta_1 + \Delta\zeta_2)^2 G_2 - (\Delta\zeta_1)^2 G_3}{\Delta\zeta_1(\Delta\zeta_1 + \Delta\zeta_2)^2 - (\Delta\zeta_1 + \Delta\zeta_2)(\Delta\zeta_1)^2} \tag{86.b}$$

Displacement thickness is defined and calculated from the following equations.

(a) all the flows except the swept wing flow:

$$\delta_x^* = \int_0^\infty (1 - \frac{\rho V}{\rho_e V_e}) dz = \int_0^\infty (1 - \frac{\rho}{\rho_e} F) dz \tag{87}$$

(b) for swept wing flow:

$$\delta_x^* = \int_0^\infty (1 - \frac{\rho\, u}{\rho_e\, u_e}) dz = \int_0^\infty (1 - \frac{\rho}{\rho_e} F) dz \tag{88.a}$$

$$\delta_y^* = \int_0^\infty (1 - \frac{\rho\, v}{\rho_e\, v_e}) dz = \int_0^\infty (1 - \frac{\rho}{\rho_e} G) dz \tag{88.b}$$

Momentum thickness is defined and calculated in a similar manner as the displacement thickness.

Heat transfer is calculated from:

(a) for 2-D, axisymmetric flow and flow along plane of symmetry:

$$q_w = K(\frac{\partial T}{\partial y})_w = \frac{c_p \mu_w}{Pr}(\frac{\rho}{\rho_e})_w(\frac{\rho_e u_e}{\mu_e s})^{1/2}(\frac{\partial T}{\partial \zeta})_w \tag{89}$$

(b) for the flow along leading-edge attachment line::

$$q_w = K(\frac{\partial T}{\partial y})_w = \frac{c_p \mu_w}{Pr}(\frac{\rho}{\rho_e})_w(\frac{\rho_e u_e}{\mu_e})^{1/2}(\frac{\partial T}{\partial \zeta})_w \tag{90}$$

(c) for swept wing flow:

$$q_w = K(\frac{\partial T}{\partial y})_w = \frac{c_p \mu_w}{Pr}(\frac{\rho}{\rho_e})_w(\frac{\rho_e \mid u_e \mid}{\mu_e x})^{1/2}(\frac{\partial T}{\partial \zeta})_w \tag{91}$$

where $(\partial T/\partial \zeta)_w$ is obtained from:

$$(\frac{\partial T}{\partial \zeta})_w = \frac{[(\Delta\zeta_1)^2 - (\Delta\zeta_1 + \Delta\zeta_2)^2]T_1 + (\Delta\zeta_1 + \Delta\zeta_2)^2 T_2 - (\Delta\zeta_1)^2 T_3}{\Delta\zeta_1(\Delta\zeta_1 + \Delta\zeta_2)^2 - (\Delta\zeta_1 + \Delta\zeta_2)(\Delta\zeta_1)^2} \tag{92}$$

5.2 Test Cases

5.2.1 Two-Dimensional Flow

The subsonic flow past a NACA 0012 airfoil at 0 degrees angle of attack was selected as a two-dimensional flow test case with the following flow conditions (This flow condition is the same as that used in Ref. [4]):

$M_\infty = 0.5$

$\alpha = 0^o$

$p_\infty = 2116\, lb/ft^2$

$T_\infty = 520^o R$

$T_w = T_{aw}$

$c = 0.28266\, ft$

The free stream Reynolds number based on the chord length is 10^6.

The inviscid solution was obtained using the Euler code developed by Drela [13]. Figure 7 shows the skin friction coefficients. In this figure, skin friction based on the free stream velocity ($C_{f\infty} = \frac{(\mu \partial u/\partial z)_w}{\frac{1}{2}\rho_e V_\infty^2}$) is plotted to compare the results with Ref. [4]) These results were obtained using uniform grid spacing in the normal direction with $\Delta\zeta_1 = 0.1$ and $\zeta_e = 7.0$. The inviscid grid was used in the x-direction. The results are in good agreement with the result of Ref. [4] (not shown).

5.2.2 Axisymmetric Flow

The hypersonic flow over the sharp cone (half cone angle of 5 degrees) with mass transfer at the wall was selected as an axisymmetric flow test case with the following flow conditions (This flow condition is the same as that used in Ref. [4] and [14]):

$M_\infty = 7.4$

half cone angle $=5^o$

$\alpha = 0^o$

$p_\infty = 701.4\, N/m^2$

$T_\infty = 69.7^o K$

$T_w = 316.65^o$

From $X = 0$ to $X = 0.096\, m$, there is no mass transfer at the wall. From $X = 0.096\, m$, two types of mass transfer exist: $(\rho w)_w = 0$; $(\rho w)_w = -0.090117\, N\, sec/m^3$ or $C_q = -0.0020754$ (wall suction).

The inviscid pressure was obtained using the Euler code developed by M. D. Salas (unpublished work). The boundary-layer edge velocity (u_e/V_∞) from the Euler code is about 0.99176 and the initial velocity (u_e/V_∞ at i=1) calculated using Eq. (B1) is 0.99184. Therefore, for this flow, the initial edge velocity calculated assuming isentropic condition is very close (within 0.01 percent difference) to the inviscid velocity given by the Euler code. This seems to be because the shock angle is small (for this flow, about 9.2 degrees).

Figure 8 shows the skin friction coefficients on the cone with and without wall suction condition. These results were obtained using non-uniform (stretched) grid spacing in the

normal direction with $\Delta\zeta_1 = 0.005$ and $\Delta\zeta(k+1)/\Delta\zeta(k) = 1.05$. The step-size in the x-direction (Δx) varies from 0.001 (near the nose) to 0.01. The grid distribution used to obtain Fig.8 can be seen in PART II, section 6.3. The result is in good agreement with other result [4] (not shown).

5.2.3 Flow along Plane of Symmetry

An ellipsoid of revolution having a four to one ratio of major to minor axis ($a = 1m$, $b = 1/4m$) was selected as a test case, and the boundary-layer solutions were obtained for incompressible flow($M_\infty = 0.05$) at $\alpha = 6^o$.

For this body, the angle between the x and y coordinates (θ) is $\pi/2$. The metric coefficients can be obtained exactly, and the velocity components can be obtained analytically for the incompressible flow [15]:

$$h_1 = \left\{ \frac{1 + (X/a - 1)^2(t^2 - 1)}{1 - (X/a - 1)^2} \right\}^{1/2} \tag{93.a}$$

$$h_2 = b\sqrt{1 - (X/a - 1)^2} \tag{93.b}$$

$$u_e = V_\infty(V_0(t)\cos\alpha\cos\beta - V_{90}(t)\sin\alpha\sin\beta\cos\phi) \tag{93.c}$$

$$v_e = V_\infty(V_{90}(t)\sin\alpha\sin\phi) \tag{93.d}$$

where $t = b/a$. Note that x is measured along the axes X although x-direction is along the body surface; therefore $x = X$ in quantity. Here β is the angle between the line tangent to the ellipse and the positive X axis; it is given by

$$\cos\beta = \frac{\sqrt{1 - (X/a - 1)^2}}{\sqrt{1 + (X/a - 1)^2(t^2 - 1)}} \tag{94.a}$$

$$\beta < 0 \quad if \quad X/a > 1, \quad and \quad \beta > 0 \quad if \quad X/a < 1 \tag{94.b}$$

The parameters $V_0(t)$ and $V_{90}(t)$ are functions of t and are defined by

$$V_0(t) = \frac{(1 - t^2)^{3/2}}{\sqrt{1 - t^2} - \frac{1}{2}t^2 ln\left\{\frac{1+(1-t^2)^{1/2}}{1-(1-t^2)^{1/2}}\right\}} \tag{95.a}$$

$$V_{90}(t) = \frac{2V_0(t)}{2V_0(t) - 1} \tag{95.b}$$

The skin friction coefficients ($C_{f\infty}\sqrt{Re_\infty} = \frac{\nu(\partial u/\partial z)_w}{1/2V_\infty^2}\sqrt{\frac{V_\infty a}{\nu}}$, where $a = 1$) as a function of X at an angle of attack of 6 degrees are shown in Fig. 9. The present numerical results were obtained using the following grid distributions: Δx=0.002 near the nose followed by Δx=0.02 downstream, $\Delta y = 5^o$, and 61 grid points normal to surface uniformly spaced such that $\Delta\zeta$=0.1. The result is in good agreement with result given by Iyer [4] (note that Iyer's result must be multiplied by $1/\sqrt{2}$ for comparison due to the different definition of Re_∞).

5.2.4 Flow Along A Leading-edge Attachment Line

The subsonic flow past an infinite swept cylinder with a diameter of 0.75 feet and a sweep angle of 60^o at 0 degrees angle of attack was selected as a test case with the following flow conditions:

$M_\infty = 0.126675$

$\lambda = 60^o$

$\alpha = 0^o$

$p_\infty = 2116.8\, lb/ft^2$

$T_\infty = 520^o R$

$T_w = T_{aw}$

The inviscid solution was obtained from the analytical potential solution along with the sweep theory. For this flow, the x-coordinate is along the leading-edge, and the y-coordinate is normal to the leading-edge and measured from the center of cylinder. The metric coefficients are defined $h_1 = 1.0$ and $h_2 = 0.375$ where h_2 is the radius of the cylinder. The skin friction coefficient is the same along the leading-edge attachment line. The velocity profiles at various suction levels are plotted instead of the skin-friction coefficient for this test case. Figure 10 shows the results of applying suction C_q=0, −0.0005, −0.001, −0.002, −0.005, and −0.01. The Reynolds number based on the momentum thickness at the zero suction condition is about 203.

5.2.5 Swept-Wing Flow

The subsonic flow past a 'clean-up' glove of the swept-back tapered F-14 wing ([16]) was selected as a test case. The flow conditions are the same as that used as case 5 in Ref. [16]:

$M_\infty = 0.80$

$\lambda_1 = 22^o$, $\lambda_2 = 4.68^o$

$\alpha = 0.53^o$

$p_\infty = 785.3\, lb/ft^2$

$T_\infty = 430^o R$

$T_w = T_{aw}$

$c = 5.4256\, ft$

which makes the chord Reynolds number 15 Million.

Figure 11 shows the pressure distribution (measured) on this glove. The skin friction coefficient (C_{fy}) for zero suction as calculated using the present method and the Kaups-Cebeci code are compared in Fig. 12 and are in good agreement. The velocity profile (v) and its first and second normal derivatives at $X/c = 0.405$ (40-th station) calculated using two codes are shown in Fig. 13. The agreement is very good with the exception of small differences in the second normal derivative near the wall.

The logarithmic disturbance amplication factor N was calculated with the envelope method using the COSAL [18] linear stability analysis code to assess the effect of the different boundary-layer codes. The envelope method calculates the wave length and orientation angle combination that maximizes the disturbance growth for a fixed frequency. The curvature effect and non-parellel effect was not considered in this code. The N factor for a disturbance frequency of 3000 Hz was obtained using the result of the present method and of the Kaups-Cebeci code and are compared in Fig. 14. The difference is within 2 percent. For this flow, the most amplified disturbaces are cross-flow vortices (the wave angle and the inviscid streamline direction is about 85 degrees) up to the 60 percent chord location.

The skin friction coefficient obtained using Kaups-Cebeci code for this test case does not

show wiggles when suction is not applied. The skin friction coefficient obtained using Kaups-Cebeci code shows wiggles for some flow cases. The wiggles are propound especially when the pressure distribution near the stagnation point is not smooth or when suction is applied. The skin friction coefficient distributions with suction $C_q = -0.0007$ for $X/c = 0.051$ to 0.332 obtained using the two boundary-layer codes are compared in the Fig. 15. Immediately after the suction region, i.e., from $X/c = 0.33$, the skin friction coefficient obtained using the Kaups-Cebeci code shows an oscillation. The velocity and its normal derivatives at $X/c = 0.405$ (40-th step) are compared on Fig. 16. The first and second normal derivatives obtained using Kaups-Cebeci code are not smooth compared with those obtained using the present method.

6. CONCLUDING REMARKS

A computer program has been presented for solving the compressible, laminar boundary-layer equations for two-dimensional, axisymmetric, and quasi-three-dimensional flows which includes flow along the plane of symmetry, flow along the leading-edge attachment line, and swept wing flows with appropriate conical flow approximations. The method has been applied to a number of two-dimensional, axisymmetric, and quasi-three-dimensional flow cases over a range of speeds and validated. The results indicate that this boundary-layer code gives velocity and temperature profiles which are accurate, smooth, and continuous through the first and second normal derivatives. This code can be coupled with a stability analysis code and used to predict the onset of the boundary-layer transition which enables the assessment of the laminar flow control techniques. The CPU time for a typical swept wing with 48 streamwise station and 50 to 88 grid points across the boundary layer was about 4 seconds on the CRAY-2 or 1.5 seconds on the CRAY Y-MP computer.

Acknowledgement

The author would like to personally thank Prof. Fred R. DeJarnette at North Carolina State University and Dr. Fayette S. Collier at NASA Langley Research Center for the support of this work through Contract NAS1-19299. The author would also like to express his appreciation to Mr. Richard D. Wagner and Drs. Mujeeb Malik, Richard A. Wahls, Venkit Iyer, and Julius E. Harris at NASA Langley Research Center for their helps.

Appendix A. Block Tridiagonal Matrix Algorithm

The two vector equations to be solved are

$$h_k = h_{k-1} + \frac{\Delta\zeta_{k-1}}{2}(H_k + H_{k-1}) \tag{A1.a}$$

$$-A_k H_{k-1} + B_k H_k - C_k H_{k+1} + a_k h_k = D_k \tag{A1.b}$$

where A_k, B_k, C_k, and a_k are 2x2 matrices, H_k, h_k, and D_k are vectors. These equations are solved using the Davis Modified Tridiagonal Algorithm. The variables E_k, e_k and d_k are introduced such that

$$H_k = E_k H_{k-1} + \epsilon_k h_{k-1} + d_k \tag{A2}$$

where E_k and ϵ_k are 2x2 matrices, and d_k is a vector.

Using Eq. (A2), Eq. (A1.b) becomes

$$-A_k H_{k-1} + B_k H_k - C_k E_{k+1} H_k - C_k e_{k+1} h_k - C_k d_{k+1} + a_k h_k = D_k \tag{A3}$$

Define

$$R_k = a_k - C_k e_{k+1} \tag{A4}$$

Then, Eq. (A3) may be written as

$$-A_k H_{k-1} + (B_k - C_k E_{k+1}) H_k + R_k h_k = D_k + C_k d_{k+1} \tag{A5}$$

Substituting Eq. (A1.a) into Eq. (A5) gives

$$(-A_k + \frac{\Delta\zeta_{k-1}}{2} R_k) H_{k-1} + (B_k - C_k E_{k+1} + \frac{\Delta\zeta_{k-1}}{2} R_k) H_k + R_k h_{k-1} - D_k - C_k d_{k+1} = 0 \tag{A6}$$

Next, define

$$p_k = B_k - C_k E_{k+1} + \frac{\Delta\zeta_{k-1}}{2} R_k \tag{A7}$$

Solving Eq. (A6) for H_k,

$$H_k = p_k^{-1}(A_k - \frac{\Delta\zeta_{k-1}}{2} R_k) H_{k-1} - p_k^{-1} R_k h_{k-1} + p_k^{-1}(D_k + C_k d_{k+1}) \tag{A8}$$

Equating Eqs. (A2) and (A8) term by term yields

$$e_k = -p_k^{-1} R_k \tag{A9.a}$$

$$E_k = p_k^{-1} A_k + \frac{\Delta\zeta_{k-1}}{2} e_k \tag{A9.b}$$

$$d_k = p_k^{-1}(D_k + C_k d_{k+1}) \tag{A9.c}$$

The boundary condition at the edge of the boundary-layer (k=kmax) is

$$H_{kmax} = \begin{bmatrix} 1.0 \\ v_e/V_{ref} \text{ or } v_{ye}/V_{ref} \end{bmatrix}$$

This provides the conditions

$$d_{kmax} = \begin{bmatrix} 1.0 \\ v_e/V_{ref} \text{ or } v_{ye}/V_{ref} \end{bmatrix}$$

$$e_{kmax} = E_{kmax} = 0 \tag{A10}$$

The parameters of Eq. (A9) are first determined for decreasing values of k (kmax-1, kmax-2,...,2) beginning at the edge of the boundary-layer. Then Eqs. (A1.b) and (A2) are solved for increasing values of k (k=2,3,..., kmax) using the boundary conditions at the wall,

$$H_1 = h_1 = 0 \tag{A11}$$

Appendix B. Boundary-Layer Edge Conditions

B.1 Two-dimensional and Axisymmetric Flow

For an isentropic flow (when there is no shock between the free stream and the body), the boundary-layer edge velocity is obtained from C_p by the following equation.

$$u_e/V_\infty = \sqrt{1 - \frac{2}{(\gamma-1)M_\infty^2}\left\{\left(\frac{\gamma M_\infty^2 C_p}{2} + 1\right)^{\gamma-1/\gamma} - 1\right\}} \tag{B1}$$

However, for a non-isentropic flow (when there is a shock between the free stream and the body), the edge velocity is obtained from the C_p distribution by integration of the following surface Euler equation.

$$\frac{d(u_e/V_\infty)^2}{dx} = -\frac{\rho_\infty}{\rho_e}\frac{dC_p}{dx} \tag{B2}$$

which is another form of Eq. (21). This equation is integrated using the fourth-order Runge-Kutta method. For a blunted nose body at a supersonic free stream condition, we assume that there is a stagnation point where u_e is zero and the stagnation pressure was calculated assuming that the streamline to the stagnation point passed through the normal shock. For a sharp nose body at a supersonic free stream condition, the initial edge velocity (u_e at $i = 1$) was obtained from the Eq. (B1). This approximation is based on the assumption that the shock angle relative to the free stream is small. It would be better to replace this value if an accurate value (u_e at $i = 1$) is available and especially when shock angle is not small. To replace this value, put the value in the subroutine EDGECON.

In the code, if the free-stream Mach number is greater than RISENTD (0.7 is set in the code), the flow is assumed to be non-isentropic; and Eq. (B2) is integrated to obtain the boundary-layer edge velocity. However, if the velocity (u_e) is available along with the pressure distribution from the inviscid code, integration of Eq. (B2) is not needed. In that case, use option KUE=1.

B.2 Swept-wing Flow

The method to calculate the coordinate y is the same as used in Ref. [5]. The nondimensional wing thickness distribution $\bar{z}/c$ is assumed specified as a function of X/c on the airfoil surface. The boundary-layer calculations are done along the arc formed by the intersection of a sphere of radius $x = x_0$ and the conical wing surface. This chord intersects the sphere at the wing leading-edge as shown in Figs. 3, 4, and 5. A new variable ϕ is defined by (see Fig. 6)

$$X/c = 1 - cos\phi \tag{B3}$$

A negative value of X/c implies negative value of ϕ, and $\phi = 0$ designates the leading-edge.

The variable y is obtained from the integration of the following equations.

$$\frac{dy}{d\phi} = \frac{1}{x_0}\sqrt{(\frac{d\bar{x}}{d\phi})^2 + (\frac{d\bar{y}}{d\phi})^2 + (\frac{d\bar{z}}{d\phi})^2} \tag{B4}$$

For a swept-back wing with the spanwise conical flow assumption (Fig. 3),

$$x_0 = \frac{c}{cos\lambda_1(tan\lambda_1 - tan\lambda_2)} \tag{B5.a}$$

$$\frac{d\bar{x}}{d\phi} = \frac{-1}{cos\lambda_1 h^{1/2}}\left\{c\,sin\phi + \frac{[x_0\,sin\lambda_1 - c(1-cos\phi)]}{2h}\frac{dh}{d\phi}\right\} \tag{B5.b}$$

$$\frac{d\bar{y}}{d\phi} = -\frac{x_0}{2h^{3/2}}\frac{dh}{d\phi} \tag{B5.c}$$

$$\frac{d\bar{z}}{d\phi} = \frac{c}{cos\lambda_1 h^{1/2}}\left\{\frac{d(\bar{z}/c)_0}{d\phi} - \frac{(\bar{z}/c)_0}{2h}\frac{dh}{d\phi}\right\} \tag{B5.d}$$

$$h = 1 + \frac{c^2}{(x_0\,cos\lambda_1)^2}(\frac{\bar{z}}{c})_0^2 + \left\{tan\lambda_1 - \frac{c(1-cos\phi)}{x_0\,cos\lambda_1}\right\}^2 \tag{B5.e}$$

For a swept-forward wing with the spanwise conical flow assumption (Fig. 4),

$$x_0 = \frac{c}{cos\lambda_2(tan\lambda_1 - tan\lambda_2)} \tag{B6.a}$$

$$\frac{d\bar{x}}{d\phi} = \frac{-1}{cos\lambda_2 h^{1/2}}\left\{c\,sin\phi + \frac{[x_0\,sin(-\lambda_2) - c(1-cos\phi)]}{2h}\frac{dh}{d\phi}\right\} \tag{B6.b}$$

$$\frac{d\bar{y}}{d\phi} = -\frac{x_0}{2h^{3/2}}\frac{dh}{d\phi} \tag{B6.c}$$

$$\frac{d\bar{z}}{d\phi} = \frac{c}{cos\lambda_2 h^{1/2}}\left\{\frac{d(\bar{z}/c)_0}{d\phi} - \frac{(\bar{z}/c)_0}{2h}\frac{dh}{d\phi}\right\} \tag{B6.d}$$

$$h = 1 + \frac{c^2}{(x_0\,cos\lambda_2)^2}(\frac{\bar{z}}{c})_0^2 + \left\{tan(-\lambda_2) - \frac{c(1-cos\phi)}{x_0\,cos\lambda_2}\right\}^2 \tag{B6.e}$$

For a swept-back wing with the streamwise conical flow assumption (Fig. 5),

$$x_0 = \frac{c}{cos\lambda_1} \tag{B7.a}$$

$$\frac{d\bar{x}}{d\phi} = \frac{-1}{sin\lambda_1 h^{1/2}} \left\{ c\, sin\phi + \frac{[x_0\, cos\lambda_1 - c(1-cos\phi)]}{2h} \frac{dh}{d\phi} \right\} \tag{B7.b}$$

$$\frac{d\bar{y}}{d\phi} = -\frac{x_0}{2h^{3/2}} \frac{dh}{d\phi} \tag{B7.c}$$

$$\frac{d\bar{z}}{d\phi} = \frac{c}{sin\lambda_1 h^{1/2}} \left\{ \frac{d(\bar{z}/c)_0}{d\phi} - \frac{(\bar{z}/c)_0}{2h} \frac{dh}{d\phi} \right\} \tag{B7.d}$$

$$h = 1 + \frac{c^2}{(x_0\, sin\lambda_1)^2} (\frac{\bar{z}}{c})_0^2 + \left\{ cot\lambda_1 - \frac{c(1-cos\phi)}{x_0\, sin\lambda_1} \right\}^2 \tag{B7.e}$$

$(\bar{z}/c)_0$ denotes the ordinate of the defining airfoil and is obtained by cubic polynomial interpolation. Integration of the equations above starts from the stagnation line (leading-edge attchment line) where $y = 0$.

We solve the following surface Euler equations which are derived from Eq.(33).

$$\frac{d\,(u_e/V_\infty)}{d\,y} = v_e/V_\infty \tag{B8.a}$$

$$\frac{d(v_e/V_\infty)^2}{d\,y} = -2\,u_e v_e/V_\infty^2 - \frac{\rho_\infty}{\rho_e} \frac{d\,C_p}{d\,y} \tag{B8.b}$$

The equations above are integrated by the fourth order Runge-Kutta method with the initial conditions:

$$u_e/V_\infty = \pm\sqrt{1 - C_{ps}}\,, \qquad v_e = 0 \qquad \text{for isentropic flow} \tag{B9.a}$$

$$u_e/V_\infty = \pm\, sin\lambda_1\,, \qquad v_e = 0 \qquad \text{for non-isentropic flow} \tag{B9.b}$$

where C_{ps} is C_p at the stagnation line. Because the coordinate systems for swept wing flow are defined as in Figs. 3, 4, and 5, u_e is negative for swept-back wing flow with the spanwise conical flow assumption (Fig. 3) and u_e is positive for the other swept wing flow cases(Figs. 4 and 5). When there is a shock in front of the wing, it is better to replace the initial condition ($u_e/V_\infty = \pm sin\lambda_1$) by a more accurate value if it is available because this approximation is based on the assumption that shock is parallel to the stagnation line. To replace the initial condition, put the value in the subroutine WING.

It is not necessary to integrate Equation (B8.b) for isentropic flow since v_e can be obtained from known C_p and u_e. In the code, if free stream Mach number is less than RISENWG (0.7 is set in the code), the flow is assumed to be isentropic.

B.3 Temperature

The temperature at the edge of the boundary-layer can be obtained using the total inviscid velocity, i.e.,

$$T_e/T_\infty = 1 + \frac{\gamma - 1}{2} M_\infty^2 [1 - (\frac{V_e}{V_\infty})^2] \tag{B10}$$

Equation (B10) is derived from the inviscid energy equation and is valid for all speed regimes. Temperature at the boundary-layer edge is calculated using the above equation in the boundary-layer code.

PART II. USER'S MANUAL

1. PROGRAM DESCRIPTION

BLSTA was developed to solve the compressible, laminar boundary-layer equations for the two-dimensional flow (KASE=0), axisymmetric flow (KASE=1), and quasi-three-dimensional flows such as the flow along the planes of symmetry (KASE=2), the flow along the leading-edge attachment line (KASE=3), swept-back and swept-forward wing flows with the spanwise conical flow assumption (KASE=4), and swept-back delta wing flow with the streamwise conical flow assumption (KASE=5). Using BLSTA, the flows for wide speed range (from subsonic to hypersonic) can be solved; the post-shock conditions are not needed as a free-stream condition when there is a shock in front of the subject for supersonic flow. The velocity profiles and their normal derivatives are calculated to be used by the stability analysis codes as follows: e^{Malik} [17] code for KASE=0,1,2,3, and COSAL [18] or COSCUR [19] code for KASE=4,5.

The governing boundary-layer equations are in dimensional form; consequently, all inputs to BLSTA must be consistently dimensional. This code operates in either English units(ft, lb, sec, ^oR) or SI(MKS) units(m, kg, sec, ^oK). However, for swept wing flow (KASE= 4 and 5), use English units to be consistent with the stability analysis codes, COSAL or COSCUR, as these stability analysis codes(as written) use English units.

The code block, COMBLCK, which lists the common blocks, is designed for flexibility in changing the dimensions in the spatial coordinates(x and z) and to avoid listing the common blocks in each subroutine. This COMBLCK is included in the main program and most of the subroutines (except subroutine SY and interpolation subroutines) by an 'INCLUDE' statement. The dimensions of the common blocks are controlled by changing the parameters IMAXF and KMAXF in the COMBLCK. If either IMAX or KMAX, which are the actual number of grid points in the x and z-direction, respectively, happens to

exeed IMAXF or KMAXF, the boundary-layer calculation should stop and the corresponding parameters(IMAXF or KMAXF) should be increased so that they are greater than IMAX or KMAX. Also, it should be noted that KMAX, the number of grid points in the normal direction, may be increased automatically in the boundary-layer code initially (at i=1) and as marching downstream because of increasing ζ_e.

The flow chart of the BLSTA is shown on Fig.17. The convergence of the boundary-layer solution is checked at each i-th step in the subroutine SOLVE. If the convergence fails, the flow is most probably separated. The skin friction coefficients (C_{fx} or C_{fy}) are a measure of the boundary-layer separation and it decreases rapidly near the separation.

BLPARA	calculates the boundary-layer parameters for KASE=0,1,2.
BLPAR3	calculates the boundary-layer parameters for KASE=3.
BLPAR4	calculates the boundary-layer parameters for KASE=4,5.
COEF	calculates the coefficients m_1 through m_{13} for KASE=0,1,2, i≥2
COEF1	calculates the coefficients m_1 through m_{13} for KASE=0,1,2, i=1
COEFLE	calculates the coefficients m_1 through m_{13} for KASE=3, i≥2
COEFLE1	calculates the coefficients m_1 through m_{13} for KASE=3, i=1
COWING	calculates the coefficients m_1 through m_{13} for KASE=4,5, i≥2
COWING1	calculates the coefficients m_1 through m_{13} for KASE=4,5, i=1
CUBINT	cubic polynomial interpolation subroutine
DERIVY	calculates first and second normal derivatives to be used in the stability analysis codes
EDGECON	For a given C_p distribution, locates the stagnation point and calculates the boundary-layer edge velocity(u_e) for KASE=0,1
INPUT	reads in input file
INTEG	integration subroutine
LININT	linear interpolation subroutine (used if INTEV $\neq$ 0)
NTRID	solves block tridiagonal matrix equations using Davis Modified Tridiagonal Algorithm
OUTCOS	writes the velocity profiles and its normal derivatives on COSLNPUT which is to be read by the COSAL or COSCUR stability analysis code when KASE=4,5.
OUTEMAL	writes the velocity profiles and its normal derivatives on BFLOW which is to be read by the e^{Malik} stability analysis code when KASE=0,1,2,3.
OUTPUT	writes the input echos, velocity profiles, boundary-layer edge conditions, and boundary-layer parameters on FORT.30

SOLVE	calculates the coefficients for the tridiagonal systems of equations and solves the momentum equations and energy equation iteratively.
SPLINE	derivative subroutine
STAGPT	solves the stagnation point flow (key parameter is C^*).
SY	solves the tridiagonal systems of equations using Thomas Algorithm
WING	calculates velocity components for a given C_p distribution (for KASE=4,5)

3. PARAMETER AND VARIABLE DIRECTORY

A(I)	X/c for defining airfoil, where c=chord. (for KASE=4,5)
AINF	speed of sound
BC(I,K)	$C(=\rho\mu/\rho_e\mu_e)$ at (x_i, z_k)
BLTH(I)	δ, boundary-layer thickness where V/V_e =BLTK
BLTK	V/V_e value for defining boundary-layer thickness, 0.995 is set in the code.
CAVD(I,J)	V_e, boundary-layer edge total velocity
CFX(I)	C_{fx}
CFY(I)	C_{fy} (for KASE=4,5)
COSTH(I,J)	$\cos\theta$
CP	c_p, specific heat
CPD(I,J)	Cp, pressure coefficient
CQD(I)	Cq, suction coefficient
CSTAR	$C^*(= B/A)$
DK1DY	$\partial(K_1\cos\theta)/\partial y$
DSPTX(I)	δ_x^*, displacement thickness in x-direction
DSPTY(I)	δ_y^*, displacement thickness in y-direction (for KASE=4,5)
DSTZ	length scale $(l) = \sqrt{\nu_e x/u_e}$ (KASE=0,1,2,3), $= \delta_y^*$ (KASE=4,5)
DX	$\Delta x_i, = x_i - x_{i-1}$
DY(J)	Δy_j
DZETA(K)	$\Delta\zeta_k, = \zeta_{k+1} - \zeta_k$
DZETA1	$\Delta\zeta_1$
GAMMA	γ
H(1,I,K)	F at the point (x_i, z_k)
H(2,I,K)	G at the point (x_i, z_k)
H(3,I,K)	E at the point (x_i, z_k)

HN(1,I,K)	the solution for F from subroutine NTRID
HN(2,I,K)	the solution for G from subroutine NTRID
HS(1,I,K)	f at the point (x_i, z_k)
HS(2,I,K)	g at the point (x_i, z_k)
H1(I,J)	h_1 at the point (x_i, y_j)
H2(I,J)	h_2 at the point (x_i, y_j)
I	index for the boundary-layer grid in the x direction
IL	i-th step where the boundary-layer calculation stops (not necessarily the same as IMAX or ISTOP)
IMAX	number of boundary-layer grid points in the x-direction
IMAXF	maximum possible number of grid points in the x-direction, given in COMBLCK
J	index for the boundary-layer grid in the y direction
K	index for the boundary-layer grid in the ζ direction
KASE	index for case of the flow =0 for two-dimensional flow =1 for axisymmetric flow =2 for the flow along the plane of symmetry =3 for the flow along the leading-edge attachment line =4 for the swept wing flow with the spanwise conical flow assumption =5 for the delta wing flow with the streamwise conical flow assumption
KMAX	number of grid points in the z-direction (may be changed as i increases) (KMAX $\leq$ KMAXF)
KMAXF	maximum possible number of grid points in the z-direction, given in COMBLCK
KROW	=1 when wall mass injection exists =0 when there is no wall mass injection

KSHALE	=1 when the shape of nose is sharp (when there is no stagnation point)
	=0 when the shape of nose is blunted (when there is a stagnation point)
KTW	=1 when the wall temperature is given as a boundary condition
	=0 for adiabatic wall condition
KUE	=1 when the inviscid velocity is given as input (for KASE=0,1)
	=0 when the inviscid velocity is not given as input
MKS	=0 when using the English units ($ft, lb, sec, {}^{\circ}R$)
	=1 when using SI units ($m, kg, sec, {}^{\circ}K$)
M1,..,M13	$m_1, .., m_{13}$
NI	number of input stations for the streamwise airfoil (for KASE=4,5)
PE(I)	p, pressure
PI	π
PINF	p_∞, free stream pressure
PR	Pr, Prandtl Number
QW(I)	q_w
RISENTD	free-stream Mach number below which isentropic condition is used to calculate the edge velocity for 2-D and Axisymmetric flow (0.7 is set in the code)
RISENWG	free-stream Mach number below which isentropic condition is used to calculate the edge velocity for swept-wing flow (0.7 is set in the code)
RK	$\kappa (= \Delta\zeta_{k+1}/\Delta\zeta_k)$
RKAPA(I)	Kappa value
RMINF	M_∞
RMYUED(I)	μ_e
RNUINF	ν_∞
ROED(I)	ρ_e
ROERO(I,K)	ρ_e/ρ
ROINF	ρ_∞

ROWW(I)	$(\rho w)_w$
RR	gas constant
SWLE	leading-edge sweep angle in degrees
SWTE	trailing-edge sweep angle in degrees
S1(I,J)	s
TD(I,K)	temperature inside the boundary-layer at (x_i, z_k)
TE(I)	boundary-layer edge temperature
THMOX(I)	momentum thickness in x-direction, defined as $\int_0^\infty \frac{\rho}{\rho_e}\frac{u}{u_e}(1-\frac{u}{u_e})dz$
THMOY(I)	momentum thickness in y-direction, defined as $\int_0^\infty \frac{\rho}{\rho_e}\frac{v}{v_e}(1-\frac{v}{v_e})dz$
	for KASE=4,5
TINF	T_∞
TWALL(I)	T_w
TWTADB(I)	T_w/T_{aw}
UE(I,J)	u_e or u_e/V_∞
UKMAX1	KMAX and ζ_e (=ζ(KMAX)) are to be increased as going downstream
	so that $(u/u_e)_{k=KMAX-1}$ is greater than this value, typically 0.99999
VE(I,J)	v_e or v_e/V_∞
VINF	V_∞
VMAX(I)	maximum crosswise velocity
XC(I)	X/c (KASE=0,1,4,5) or x (KASE=2,3)
XD(I)	x for KASE=0,1,2,3, y for KASE=4,5
XKI(I)	cross-flow Reynolds number, defined as $\rho_e\, c_{max}\, \delta_{0.01}/\mu_e$
XPD(I,J)	x'
X0	x (for KASE=4,5)
Y(I)	$\bar{z}/c$ for defining airfoil (for KASE=4,5 only)
YC(I)	y'/c for 2-D flow, where c= chord
	$(r-r_{le})/c$ for axisymmetric flow, where c= chord

YD(J)	y
YPD(I,J)	y' for 2-D flow, r for axisymmetric flow
ZACT(I,K)	z
ZETA(K)	ζ
ZETAE	ζ_e

4. INPUT DESCRIPTION

Inputs to BLSTA are read through subroutine INPUT. There are three input formats which differ depending on type of the flow. The necessary input parameters are described below. For supersonic flow, and when a shock is present between the free stream and the body, we do not have to replace the free stream condition by the post-shock condition, i.e., the undisturbed free stream condition is still used for the free stream condition.

4.1 Two-dimensional and Axisymmetric Flow

KASE =0 for two-dimensional flow
=1 for axisymmetric flow

ISTOP i-th step to stop the computaion

MKS =1 when using the SI (MKS) Units ($m, kg, sec, ^{o}K$)
=0 when using the English Units ($ft, lb, sec, ^{o}R$)

KSHALE =1 when the shape of the nose or leading-edge is sharp (if there is no stagnation point)
=0 when the shape of the nose or leading-edge is blunted (if there is a stagnation point)

KTW =1 when the wall temperature is given as a boundary condition (TWTADB(I) must be specified.)
=0 when adiabatic wall condition is used (TWTADB(I) is not needed. Although it might be specified in the input, it will be neglected.)

KROW =1 when wall mass injection exists (CQD(I) must be specified)
=0 when there is no wall mass injection (CQD(I) is not needed. Although CQD(I) might be specified below, it will be neglected.)

KUE =1 when the inviscid velocity is given as input (recommended when there is a shock in front of the body)

	=0 when the inviscid velocity is not given as input
PR	Prandtl Number
RMINF	M_∞ (free stream Mach number)
PINF	P_∞ (free stream pressure) in N/m^2 (if MKS=1) or in lb/ft^2 (if MKS=0)
TINF	T_∞ (free stream temperature) in ^oK (if MKS=1) or in ^oR if (MKS=0)
UKMAX1	ZETAE and KMAX will be increased in BLSTA so that $(u/u_e)_{KMAX-1}$ is greater than this value, typically 0.99999.
ZETAE	ζ_e at i=1 (guess value, note that ZETAE and KMAX is increased as required even at i=1, and as i increases)
DZETA1	$\Delta\zeta(1)$
RK	$\Delta\zeta(k+1)/\Delta\zeta(k)$
IMAX	number of input stations where C_p is specified
CHORD	chord in m(if MKS=1) or in ft(if MKS=0)
RLE	0 for 2-D flow r_{le}, radius of leading-edge, measured from axes of rotation for axisymmetric body, in m(if MKS=1) or in ft(if MKS=0)
INTEV	number of additional points for the boundary-layer grid between each input stations
ISTABW	=0 output stations for the stability analysis will be the same as the inviscid grid points(input stations). =1 output stations for the stability analysis will be the same as the boundary-layer grid points (used when INTEV $\neq$ 0)
XC(I)	X/c, where c= chord

YC(I)	y'/c for 2-D flow, where c= chord
	$(r - r_{l\epsilon})/c$ for axisymmetric flow, where c= chord
CPD(I,1)	C_p $(= (p - p_\infty)/\frac{1}{2}\rho_\infty V_\infty^2)$
CQD(I)	C_q $(= (\rho w)_w/\rho_\infty V_\infty)$, $C_q < 0$ for suction
TWTADB(I)	T_w/T_{aw} (This is a required input if KTW=1)
UE(I,1)	u_ϵ/V_∞ (This is required input if KUE=1)

For a blunt leading-edge body (KSHALE=0), the first input station does not have to be the stagnation point; however, the input stations must enclose the stagnation point. The code locates the stagnation point and starts the boundary-layer calculations from the stagnation point (The code resets i=1 at the stagnation point). For an axisymmetric flow, the first input station should be slightly downstream of the nose tip to avoid $h_2 = 0$. For an axisymmetric nacelle application, use nonzero $r_{l\epsilon}$ which is the radius of the nacelle leading-edge measured from the center of rotation of the body.

In the code, TWALL(I), which will be used as the wall boundary condition, is calculated from the input TWTADB(I) $(= T_w/T_{aw})$ value and the adibatic wall temperature (T_{aw}) which is approximated by the following equation.

$$T_{aw} = T_\epsilon(1 + \frac{\gamma - 1}{2}\sqrt{Pr}\, M_\epsilon^2) \tag{II.1}$$

This equation gives a fairly accutare value for T_{aw}. However, to apply a more precise wall temperature condition, specify values directly to TWALL(I).

4.2 Flow Along Plane of Symmetry and Along Leading-Edge Attachment Line

KASE =2 for the flow along the plane of symmetry
=3 for the flow along leading-edge attachment line

ISTOP i-th step to stop the computaion

MKS =1 when using the SI (MKS) Units ($m, kg, sec, ^oK$)
=0 when using the English Units ($ft, lb, sec, ^oR$)

KSHALE =1 when the shape of nose or leading-edge is sharp (if there is no stagnation point)
=0 when the shape of nose or leading-edge is blunted (if there is a stagnation point)

KTW =1 when the wall temperature is given as a boundary condition (TWTADB(I) must be specified.)
=0 when adiabatic wall condition is used (TWTADB(I) is not needed. Although it might be specified in the input, it will be neglected.)

KROW =1 when wall mass injection exists (CQD(I) must be specified)
=0 when there is no wall mass injection (CQD(I) is not needed. Although CQD(I) might be specified below, it will be neglected.)

PR Prandtl Number

RMINF M_∞ (free stream Mach number)

PINF P_∞ (free stream pressure) in N/m^2 (if MKS=1) or in lb/ft^2 (if MKS=0)

TINF T_∞ (free stream temperature) in ^oK (if MKS=1) or in ^oR if (MKS=0)

UKMAX1 ZETAE and KMAX will be increased in BLSTA so that $(u/u_e)_{KMAX-1}$ is greater than this value, typically 0.99999.

ZETAE ζ_e at i=1 (guess value, note that ZETAE and KMAX is increased as

	required even at i=1, and as i increases)
DZETA1	$\Delta\zeta(1)$
RK	$\Delta\zeta(k+1)/\Delta\zeta(k)$
IMAX	number of input stations where C_p is specified
XD(I)	x
YD(J)	y
XPD(I,J)	x' (for reference)
YPD(I,J)	y' (for reference)
S1(I,J)	s
UE(I,J)	u_e/V_∞
VE(I,J)	v_e/V_∞
H1(I,J)	h_1
H2(I,J)	h_2
COSTH(I,J)	$cos\theta$
CPD(I,1)	C_p $(= (p-p_\infty)/\frac{1}{2}\rho_\infty V_\infty^2)$
CQD(I)	C_q $(= (\rho w)_w/\rho_\infty V_\infty)$, $C_q < 0$ for suction
TWTADB(I)	T_w/T_{aw} (This is a required input if KTW=1)

The location of the first input station should be slightly downstream of the stagnation point or nose tip for the flow along the plane of symmetry (KASE=2). j=1 designates the plane of symmetry or the leading-edge attachment line. j=2 is off the plane of symmetry or off the leading-edge attachment line.

To apply a more precise wall temperature condition, specify values directly to TWALL(I) because T_{aw} was approximated by the Eq. (II.1).

4.3 Swept Wing Flow

Input parameters written in the input file for swept wing flows are the same as Kaups-Cebeci code [5] input except the first two lines.

KASE =4 for swept wing flow with the spanwise conical flow assumption
=5 for delta wing flow with the streamwise conical flow assumption

KTW =1 when the wall temperature is given as a boundary condition (TWTADB(I) must be specified.)
=0 when adiabatic wall condition is used (TWTADB(I) is not needed. Although it might be specified in the input, it will be neglected.)

KROW =1 when wall mass injection exists (CQD(I) must be specified below)
=0 when there is no wall mass injection (CQD(I) is not needed. Although CQD(I) might be specified below, it will be neglected.)

INTEV number of additional points for the boundary-layer grid between each inviscid input station. If you want 2 more boundary-layer grid points between each inviscid input station, set INTEV=2. This is useful if the inviscid grid is sparce or highly nonuniform. If you want the boundary-layer grid the same as the inviscid grid, set INTEV=0. Setting INTEV $>$ 0 may cause early convergence failure if the pressure distribution is not reasonable near the stagnation point.

ISTABW =0 output stations for the stability analysis will be the same as the inviscid grid points(input stations).
=1 output stations for the stability analysis will be the same as the boundary-layer grid points (used when INTEV $\neq$ 0)

NI number of input stations for the airfoil

IMAX number of input stations where pressure is specified

ZETAE	Estimated value of ζ_e at the first station.
DZETA1	$\Delta\zeta(1)$
RK	$\Delta\zeta(k+1)/\Delta\zeta(k)$
CHORD	chord length in ft for the airfoil
SWLE	leading-edge sweep angle in degrees (negative for swept-forward wing)
SWTE	trailing-edge sweep angle in degrees (negative for swept-forward wing) (not used for KASE=5)
RMINF	M_∞ (free stream Mach number)
UREF	V_∞ (free stream velocity) in ft/sec, input only if $M_\infty = 0$.
PINF	P_∞ (free stream pressure) in lb/ft^2
TINF	T_∞ (free stream temperature) in ^oR
PR	Prandtl Number
A(I)	X/c for defining airfoil, where c= chord. A(I)=0.0 must be input if calculations contain the leading edge. Total of NI points
Y(I)	$\bar{z}/c$ for defining airfoil, where c= chord. Y(I)=0.0 must be input if calculations contain the leading edge. Total of NI points
XC(I)	X/c of input stations, total of IMAX points, must include the stagnation line at $I = 1$.
CPD(I,1)	C_p values at X/c of input stations, total of IMAX points
CQD(I)	C_q values $(= (\rho w)_w/\rho_\infty V_\infty)$, $C_q < 0$ for suction. Total of IMAX points.
TWTADB(I)	T_w/T_{aw} values, total of IMAX points. Required if KTW=1
RKAPA(I)	Kappa value, total of IMAX points. Required for COSCUR stability code.

The following concerning sweep angles λ_1 and λ_2 must be observed.

$$\lambda_1 > 0, \quad \lambda_1 > \lambda_2 \qquad \text{for swept-back wing flow (KASE=4)} \qquad \text{(II.2.a)}$$

$$\lambda_1 < 0, \quad \lambda_2 < 0, \quad \lambda_1 > \lambda_2 \qquad \text{for swept-forward wing flow (KASE=4)} \qquad \text{(II.2.b)}$$

$$\lambda_1 > 0 \qquad \text{for delta wing flow (KASE=5)} \qquad \text{(II.2.c)}$$

As described in PART I, Appendix B, this code does not assume isentropic flow to calculate the velocity components when the free stream Mach number is greater than RISENWG; therefore, supersonic flow can be solved without replacing the free stream condition by the condition downstream of the shock. The sweep angle does not need to be changed either.

Airfoil coordinates and the pressure input for KASE=4 are along the streamwise direction as shown on Figs. 3 and 4. However, airfoil coordinates and the pressure input for KASE=5 should be along the direction as indicated on Fig. 5. A few extra points ahead of the stagnation point should be included in the definition of the airfoil for proper interpolation of the geometrical data near the stagnation point.

The first input station must be the stagnation point and the pressure coefficient at this point can be obtained analytically by the following equation for isentropic flow (subsonic flow).

$$C_{ps} = \left\{ (1 + \frac{\gamma - 1}{2} M_\infty^2 cos^2 \lambda_1)^{\gamma/(\gamma-1)} - 1 \right\} / \frac{\gamma}{2} M_\infty^2 \qquad \text{(II.3)}$$

For the swept wing flows, a variable normal grid is necessary because ζ_e increases rapidly as i increases. The present code employs a stretched normal grid which applies a constant ratio between two adjacent grid spacings, i.e., $\Delta\zeta(k+1)/\Delta\zeta(k) = \kappa = const.$ The total number of points across the boundary layer, KMAX, can be calculated by the following equation:

$$\text{KMAX} = \frac{ln[1 + (\kappa - 1)(\zeta_e/\Delta\zeta_1)]}{ln\kappa} \qquad \text{(II.4)}$$

A uniform normal grid, of course, can be obtained by setting $\kappa = 1$. For typical swept wing flows, $\kappa = 1.05$ is a reasonable value. For a quick estimate of input ZETAE (ζ_e) for a typical swept wing, the following guide may be useful although it may differ depending on

the velocity gradient at the stagnation point.

$$\lambda_1 - \lambda_2 \approx 0.01 \text{ (in degrees)} \rightarrow \zeta_e \leq 0.01 \quad \text{(II.5.a)}$$

$$\lambda_1 - \lambda_2 \approx 1.0 \text{ (in degrees)} \rightarrow \zeta_e \leq 0.1 \quad \text{(II.5.b)}$$

$$\lambda_1 - \lambda_2 \approx 10. \text{ (in degrees)} \rightarrow \zeta_e \leq 0.2 \quad \text{(II.5.c)}$$

$$\lambda_1 - \lambda_2 \approx 20. \text{ (in degrees)} \rightarrow \zeta_e \leq 0.4 \quad \text{(II.5.d)}$$

$$\lambda_1 - \lambda_2 \geq 30. \text{ (in degrees)} \rightarrow \zeta_e \leq 1.0 \quad \text{(II.5.e)}$$

Assuming $\kappa = 1.05$, if we choose $\Delta\zeta_1 = \zeta_e/500$, we have 67 grid points at the stagnation point.

In the code, TWALL(I), which will be used as the wall boundary condition, is calculated from the input TWTADB(I) ($= T_w/T_{aw}$) value and the adibatic wall temperature (T_{aw}) which is approximated by the Eq. (II.1). Equation (II.1) gives a fairly accutare value for T_{aw}. However, to apply a more precise wall temperature condition, specify values directly to TWALL(I).

BLSTA can use either SI unit or English unit. However, since the stability analysis codes, COSAL and COSCUR use English units, English units should be used for this case (swept wing flows, KASE=4 and 5).

5. OUTPUT DESCRIPTION

5.1 Standard Output

The standard output from BLSTA is written on FORT.30 by subroutine OUTPUT.

(1) The flow condition and other input parameters are echoed. This includes

KASE, ISTOP, MKS, KSHALE, KTW, KROW, PR, RMINF, PINF, TINF,

UKMAX1, ZETAE, DZETA1, RK, IMAX, CHORD, RLE, INTEV, and ISTABW.

NI, SWLE, SWTE is added for KASE=4 and 5.

Also the calculated free-stream conditions, CP(c_p, specific heat), ROINF(ρ_∞),

RMYUINF (μ_∞), RNUINF(ν_∞), AINF(a_∞), VINF(V_∞) are printed.

(2) The velocity and temperature profiles for all the i step (i=1,..,IL) are printed:

ζ, F (= u/u_e), G (= v/V_{ref} or v_y/V_{ref}), T/T_e (= ρ_e/ρ) for k=1,2,..,KMAX, i=1,2,..,IL

(3) The boundary-layer edge conditions are printed:

u_e, v_e, P_e, T_e, ρ_e, μ_e, ν_e, V_e, and M_e for i=1,2,..,IL

(4) The boundary-layer parameters are printed:

XC(X/c), CFX(C_{fx}), BLTH(δ), DSPTX(δ_x^*), THMOX(x-momentum thickness),

CFY(C_{fy}), DSPTY(δ_y^*), THMOY(y-momentum thickness), QW(q_w), TWALL(T_w)

for i=1,2,..,IL

The unit for q_w is W/m^2 (if MKS=1) or $Btu/sec/ft^2$ (if MKS=0).

5.2 Output to Stability Analysis Codes

The profiles of the flows of KASE=0,1,2,3 are written by the subroutine OUTEMAL on BFLOW which can be read by the 2-D and Axisymmetric, spatial, linear stability analysis code, e^{Malik} [17].

BFLOW

IMAXW	number of output stations
IPS	station number
KMAX	number of points inside the boundary layer
DSTZ	length scale $l = \sqrt{\nu_e x/u_e}$
REY	Reynolds number, $= u_e l/\nu_e$ where $l = \sqrt{\nu_e x/u_e}$
RES	Length Reynolds number, $= (u_e l/\nu_e)^2$
EPSXR	nondimensional streamwise curvature, $= l\kappa$
	$\kappa > 0$ for convex, $\kappa < 0$ for concave
DRDX	dr/ds, where r is local radius of body and s measured along the body
YPD(I,1)	r; local radius of body
THMOX(I)	momentum thickness
BLTH(I)	boundary-layer thickness
RETHETA	momentum thickness Reynolds number (Re_θ)
RETHM	Re_θ/M_e
PR	Prandtl Number
MKS	=1 when using the SI (MKS) Units ($m, kg, sec, ^oK$)
	=0 when using the English Units ($ft, lb, sec, ^oR$)
TE(I)	boundary-layer edge temperature (T_e)
RMYUED(I)	boundary-layer edge viscosity (μ_e)
UE(I,1)	u_e
S1(I,1)	s
XC(I)	X/c (added for reference)
ZACT(I,K)/DSTZ	actual distance normal to the wall devided by length scale, z/l

H(1,I,K)	u/u_e
UP(K)	$d(u/u_e)/d(z/l)$
UDP(K)	$d^2(u/u_e)/d(z/l)^2$
ROERO(I,K)	$\rho_e/\rho\,(=T/T_e)$
TP(K)	$d(T/T_e)/d(z/l)$
TDP(K)	$d^2(T/T_e)/d(z/l)^2$

The profiles of the flows for KASE=4,5 (swept wings) are written by subroutine OUTCOS on COSLNPUT which can be read by the 3-D, temporal, linear stability analysis codes, COSAL [18] and COSCUR [19].

COSLNPUT

IMAXW	number of output stations
X0	x
CHORD	chord length in ft for the airfoil
SWLE	leading-edge sweep angle
VINF	V_∞
XC(I)	X/c
XD(I)	y
VE(I,1)	v_e
RRW(I)	s : arc length along x coordinate
IPS	station number
KMAX	number of points inside the boundary layer
DSTZ	length scale $l = \delta_y^*$
REY	Reynolds number, $= v_e l/\nu_e$, where $l = \delta_y^*$

XKI(I)	cross-flow Reynolds number, $= \rho_e\, c_{max}\, \delta_{0.01}/\mu_e$, for COSCUR code
EPS	δ_y^* RKAPA(I)/($c\,sin$(SWLE)), for COSCUR code
UTDEL	δ/c, for COSCUR code
CAVD(I,1)	V_e
PE(I)	p_e
TE(I)	T_e
ROED(I)	ρ_e
RMYUED(I)	μ_e
TWALL(I)	T_w
ROED(I)/ROERO(I,1)	ρ_w
ZACT(I,K)/DSTZ	z/l
VTEMP(K)	v/v_e
VP(K)	$d(v/v_e)/d(z/l)$
VDP(K)	$d^2(v/v_e)/d(z/l)^2$
UTEMP(K)	$-u/v_e$
UP(K)	$d(-u/v_e)/d(z/l)$
UDP(K)	$d^2(-u/v_e)/d(z/l)^2$
ROERO(I,K)	$\rho_e/\rho\,(= T/T_e)$
TP(K)	$d(T/T_e)/d(z/l)$
TDP(K)	$d^2(T/T_e)/d(z/l)^2$

6. SAMPLE CASE INPUT

6.1 Flat plate

```
Flat plate
0
istop mks kshale  ktw krow  kue
 21    0    1      0    0    0
pr    rminf       pinf      tinf    ukmax1    zetae      dzeta1 rk
0.72  2.0         25334.3   518.4   0.999999   8.0       0.1    1.0
imax  chord rle intev istabw
 21    1.    0.  0       0
x/c          y/c          cp             cq          twtadb
0.000000     0.0          0.000000       0.000000    1.0
0.010000     0.0          0.000000       0.000000    1.0
0.020000     0.0          0.000000       0.000000    1.0
0.030000     0.0          0.000000       0.000000    1.0
0.040000     0.0          0.000000       0.000000    1.0
0.050000     0.0          0.000000       0.000000    1.0
0.060000     0.0          0.000000       0.000000    1.0
0.070000     0.0          0.000000       0.000000    1.0
0.080000     0.0          0.000000       0.000000    1.0
0.090000     0.0          0.000000       0.000000    1.0
0.100000     0.0          0.000000       0.000000    1.0
0.110000     0.0          0.000000       0.000000    1.0
0.120000     0.0          0.000000       0.000000    1.0
0.130000     0.0          0.000000       0.000000    1.0
0.140000     0.0          0.000000       0.000000    1.0
0.150000     0.0          0.000000       0.000000    1.0
0.160000     0.0          0.000000       0.000000    1.0
0.170000     0.0          0.000000       0.000000    1.0
0.180000     0.0          0.000000       0.000000    1.0
0.190000     0.0          0.000000       0.000000    1.0
0.200000     0.0          0.000000       0.000000    1.0
```

6.2 NACA 0012 airfoil

This input file was used to generate the result presented in PART I, section 5.2.1.

```
NACA 0012 airfoil
0
istop mks  kshale ktw krow  kue
85     0    0      0   0     0
pr    rminf      pinf      tinf    ukmax1  zetae  dzeta1 rk
0.72  0.5       2116.0     520.0   0.99999 7.0    0.100  1.0
imax  chord   rle intev istabw
 85   0.28266 0.  0      0
   x/c            y/c            cp            cq            twtadb
   0.000000     0.000000     1.064070     0.000000     1.000000
   0.000775     0.004841     0.892081     0.000000     1.000000
   0.002955     0.009464     0.610767     0.000000     1.000000
   0.006215     0.013564     0.324677     0.000000     1.000000
   0.010168     0.017176     0.104429     0.000000     1.000000
   0.014600     0.020384    -0.047884     0.000000     1.000000
   0.019392     0.023265    -0.152775     0.000000     1.000000
   0.024453     0.025893    -0.232184     0.000000     1.000000
   0.029746     0.028308    -0.292468     0.000000     1.000000
   0.035235     0.030530    -0.333274     0.000000     1.000000
   0.040894     0.032593    -0.363119     0.000000     1.000000
   0.046701     0.034525    -0.389434     0.000000     1.000000
   0.052644     0.036337    -0.411557     0.000000     1.000000
   0.058707     0.038036    -0.428407     0.000000     1.000000
   0.064883     0.039631    -0.440971     0.000000     1.000000
   0.071161     0.041134    -0.450779     0.000000     1.000000
   0.077527     0.042547    -0.457964     0.000000     1.000000
   0.083979     0.043883    -0.464400     0.000000     1.000000
   0.090506     0.045144    -0.470200     0.000000     1.000000
   0.097100     0.046333    -0.475096     0.000000     1.000000
   0.103757     0.047452    -0.477730     0.000000     1.000000
   0.117234     0.049494    -0.479044     0.000000     1.000000
   0.130892     0.051303    -0.479344     0.000000     1.000000
   0.144698     0.052898    -0.477948     0.000000     1.000000
   0.158623     0.054293    -0.474022     0.000000     1.000000
   0.172644     0.055505    -0.469354     0.000000     1.000000
   0.186741     0.056548    -0.463392     0.000000     1.000000
   0.200899     0.057432    -0.456391     0.000000     1.000000
   0.215106     0.058169    -0.449168     0.000000     1.000000
   0.229351     0.058767    -0.439979     0.000000     1.000000
   0.243625     0.059238    -0.430423     0.000000     1.000000
   0.257924     0.059598    -0.422939     0.000000     1.000000
   0.272242     0.059843    -0.413984     0.000000     1.000000
   0.286573     0.059980    -0.403774     0.000000     1.000000
   0.300918     0.060020    -0.394188     0.000000     1.000000
   0.315270     0.059967    -0.384397     0.000000     1.000000
   0.329629     0.059825    -0.374046     0.000000     1.000000
   0.343992     0.059600    -0.363322     0.000000     1.000000
   0.358359     0.059299    -0.353406     0.000000     1.000000
   0.372730     0.058926    -0.343330     0.000000     1.000000
   0.387100     0.058483    -0.333330     0.000000     1.000000
   0.401472     0.057975    -0.323081     0.000000     1.000000
```

0.415846	0.057406	-0.313969	0.000000	1.000000
0.430217	0.056774	-0.303939	0.000000	1.000000
0.444588	0.056083	-0.293325	0.000000	1.000000
0.458957	0.055336	-0.282234	0.000000	1.000000
0.473326	0.054544	-0.273298	0.000000	1.000000
0.487695	0.053701	-0.263542	0.000000	1.000000
0.502059	0.052810	-0.252860	0.000000	1.000000
0.516423	0.051879	-0.244331	0.000000	1.000000
0.530785	0.050902	-0.234945	0.000000	1.000000
0.545145	0.049879	-0.224334	0.000000	1.000000
0.559501	0.048818	-0.214411	0.000000	1.000000
0.573856	0.047721	-0.205009	0.000000	1.000000
0.588207	0.046587	-0.195108	0.000000	1.000000
0.602554	0.045420	-0.185450	0.000000	1.000000
0.616900	0.044224	-0.177266	0.000000	1.000000
0.631242	0.042991	-0.167714	0.000000	1.000000
0.645577	0.041724	-0.157628	0.000000	1.000000
0.659910	0.040428	-0.148539	0.000000	1.000000
0.674235	0.039102	-0.139062	0.000000	1.000000
0.688554	0.037745	-0.129007	0.000000	1.000000
0.702865	0.036361	-0.119126	0.000000	1.000000
0.717166	0.034953	-0.110205	0.000000	1.000000
0.731454	0.033514	-0.099750	0.000000	1.000000
0.745729	0.032049	-0.089578	0.000000	1.000000
0.759983	0.030562	-0.080102	0.000000	1.000000
0.774215	0.029045	-0.068917	0.000000	1.000000
0.788415	0.027504	-0.057411	0.000000	1.000000
0.802579	0.025945	-0.046723	0.000000	1.000000
0.816697	0.024364	-0.035715	0.000000	1.000000
0.830753	0.022760	-0.023096	0.000000	1.000000
0.844735	0.021138	-0.009978	0.000000	1.000000
0.858622	0.019503	0.003225	0.000000	1.000000
0.872391	0.017860	0.016574	0.000000	1.000000
0.886011	0.016207	0.031380	0.000000	1.000000
0.899451	0.014549	0.047433	0.000000	1.000000
0.912667	0.012891	0.064860	0.000000	1.000000
0.925617	0.011241	0.084260	0.000000	1.000000
0.938253	0.009608	0.105485	0.000000	1.000000
0.950523	0.007999	0.129255	0.000000	1.000000
0.962379	0.006421	0.157685	0.000000	1.000000
0.973779	0.004881	0.192978	0.000000	1.000000
0.984674	0.003386	0.242692	0.000000	1.000000
0.995024	0.001952	0.343002	0.000000	1.000000

6.3 Hypersonic cone

This input file was used to generate the result presented in PART I, section 5.2.2.

```
Hypersonic cone
1
istop mks kshale  ktw krow  kue
 58   1    1      1    1     0
pr    rminf     pinf     tinf      ukmax1  zetae   zetal  rk
0.72  7.4       701.4    69.7     0.99999  5.0     0.005  1.05
imax  chord rle intev  istabw
 58    1.     0.  0      0
      x/c        (r-rle)/c      cp           cq          twtadb
    0.005000     0.000437     0.020200     0.000000     0.440700
    0.006000     0.000525     0.020200     0.000000     0.440700
    0.007000     0.000612     0.020200     0.000000     0.440700
    0.008000     0.000700     0.020200     0.000000     0.440700
    0.009000     0.000787     0.020200     0.000000     0.440700
    0.010000     0.000875     0.020200     0.000000     0.440700
    0.012000     0.001050     0.020200     0.000000     0.440700
    0.014000     0.001225     0.020200     0.000000     0.440700
    0.016000     0.001400     0.020200     0.000000     0.440700
    0.018000     0.001575     0.020200     0.000000     0.440700
    0.020000     0.001750     0.020200     0.000000     0.440700
    0.022000     0.001925     0.020200     0.000000     0.440700
    0.024000     0.002100     0.020200     0.000000     0.440700
    0.026000     0.002275     0.020200     0.000000     0.440700
    0.028000     0.002450     0.020200     0.000000     0.440700
    0.030000     0.002625     0.020200     0.000000     0.440700
    0.035000     0.003062     0.020200     0.000000     0.440700
    0.040000     0.003500     0.020200     0.000000     0.440700
    0.045000     0.003937     0.020200     0.000000     0.440700
    0.050000     0.004374     0.020200     0.000000     0.440700
    0.055000     0.004812     0.020200     0.000000     0.440700
    0.060000     0.005249     0.020200     0.000000     0.440700
    0.065000     0.005687     0.020200     0.000000     0.440700
    0.070000     0.006124     0.020200     0.000000     0.440700
    0.075000     0.006562     0.020200     0.000000     0.440700
    0.080000     0.006999     0.020200     0.000000     0.440700
    0.085000     0.007437     0.020200     0.000000     0.440700
    0.090000     0.007874     0.020200     0.000000     0.440700
    0.095000     0.008311     0.020200     0.000000     0.440700
    0.097000     0.008486     0.020200    -0.0020754    0.440700
    0.099000     0.008661     0.020200    -0.0020754    0.440700
    0.101000     0.008836     0.020200    -0.0020754    0.440700
    0.103000     0.009011     0.020200    -0.0020754    0.440700
    0.105000     0.009186     0.020200    -0.0020754    0.440700
    0.107000     0.009361     0.020200    -0.0020754    0.440700
    0.109000     0.009536     0.020200    -0.0020754    0.440700
    0.111000     0.009711     0.020200    -0.0020754    0.440700
    0.113000     0.009886     0.020200    -0.0020754    0.440700
    0.115000     0.010061     0.020200    -0.0020754    0.440700
    0.125000     0.010936     0.020200    -0.0020754    0.440700
    0.135000     0.011811     0.020200    -0.0020754    0.440700
    0.145000     0.012686     0.020200    -0.0020754    0.440700
```

0.155000	0.013561	0.020200	-0.0020754	0.440700
0.165000	0.014436	0.020200	-0.0020754	0.440700
0.175000	0.015311	0.020200	-0.0020754	0.440700
0.185000	0.016185	0.020200	-0.0020754	0.440700
0.195000	0.017060	0.020200	-0.0020754	0.440700
0.205000	0.017935	0.020200	-0.0020754	0.440700
0.215000	0.018810	0.020200	-0.0020754	0.440700
0.225000	0.019685	0.020200	-0.0020754	0.440700
0.235000	0.020560	0.020200	-0.0020754	0.440700
0.245000	0.021435	0.020200	-0.0020754	0.440700
0.255000	0.022310	0.020200	-0.0020754	0.440700
0.265000	0.023184	0.020200	-0.0020754	0.440700
0.275000	0.024059	0.020200	-0.0020754	0.440700
0.285000	0.024934	0.020200	-0.0020754	0.440700
0.295000	0.025809	0.020200	-0.0020754	0.440700
0.305000	0.026684	0.020200	-0.0020754	0.440700

```
Engine nacelle external flow
1
istop mks   kshale   ktw krow   kue
 56     0      0       0    0     0
pr     rminf pinf      tinf     ukmax1    zetae    dzetal rk
0.72   0.82  498.145   394.013  0.99999   5.0      0.05   1.0
imax   chord rle   intev istabw
 56    14.3  4.25  0       0
```

x/c	(r-rle)/c	cp	cq	twtadb
0.0238683256	-0.0204869641	0.6151417248	0.0000000000	1.0
0.0164744072	-0.0168793666	0.7887464320	0.0000000000	1.0
0.0103140282	-0.0128975952	0.9718194839	0.0000000000	1.0
0.0055795044	-0.0086236824	1.1049125354	0.0000000000	1.0
0.0021887510	-0.0045658737	1.1124471984	0.0000000000	1.0
0.0000000000	0.0000000000	0.7048278453	0.0000000000	1.0
0.0014599675	0.0051387024	-0.0842995853	0.0000000000	1.0
0.0056109715	0.0085813903	-0.5854369694	0.0000000000	1.0
0.0111811832	0.0113131167	-0.6227023027	0.0000000000	1.0
0.0176661613	0.0141906722	-0.5492159541	0.0000000000	1.0
0.0251549880	0.0170536214	-0.5007490775	0.0000000000	1.0
0.0335803651	0.0199254323	-0.4527134120	0.0000000000	1.0
0.0428933413	0.0227864298	-0.4200126030	0.0000000000	1.0
0.0530431706	0.0256447006	-0.4025171908	0.0000000000	1.0
0.0639960788	0.0284675950	-0.3966051721	0.0000000000	1.0
0.0757221834	0.0312211987	-0.3897372348	0.0000000000	1.0
0.0881880014	0.0339075743	-0.3754882614	0.0000000000	1.0
0.1013622347	0.0365418465	-0.3572414199	0.0000000000	1.0
0.1152177741	0.0391388779	-0.3416229385	0.0000000000	1.0
0.1297320899	0.0417051878	-0.3326261400	0.0000000000	1.0
0.1448862411	0.0442393140	-0.3309526130	0.0000000000	1.0
0.1606642699	0.0467312006	-0.3353721378	0.0000000000	1.0
0.1770521761	0.0491657984	-0.3430597205	0.0000000000	1.0
0.1940369963	0.0515277730	-0.3516655119	0.0000000000	1.0
0.2116064374	0.0538032291	-0.3601120215	0.0000000000	1.0
0.2297489695	0.0559787605	-0.3682139709	0.0000000000	1.0
0.2484536975	0.0580415091	-0.3760610538	0.0000000000	1.0
0.2677103674	0.0599788028	-0.3837500080	0.0000000000	1.0
0.2875092786	0.0617779173	-0.3913308636	0.0000000000	1.0
0.3078412841	0.0634258019	-0.3988228827	0.0000000000	1.0
0.3286977320	0.0649087944	-0.4062423817	0.0000000000	1.0
0.3500704366	0.0662123468	-0.4135845297	0.0000000000	1.0
0.3719516374	0.0673206586	-0.4207987245	0.0000000000	1.0
0.3943339817	0.0682164201	-0.4277360508	0.0000000000	1.0
0.4172104607	0.0688805972	-0.4340833245	0.0000000000	1.0
0.4405743102	0.0692928918	-0.4394972038	0.0000000000	1.0
0.4644189467	0.0694321954	-0.4438936907	0.0000000000	1.0
0.4887377690	0.0692782623	-0.4479707927	0.0000000000	1.0
0.5135242811	0.0688102521	-0.4536920492	0.0000000000	1.0
0.5387721440	0.0680053963	-0.4641817715	0.0000000000	1.0
0.5644758112	0.0668267161	-0.4817351890	0.0000000000	1.0
0.5906321308	0.0651894933	-0.5025687672	0.0000000000	1.0
0.6172386384	0.0629741575	-0.5127644663	0.0000000000	1.0
0.6442919546	0.0600429897	-0.4899800994	0.0000000000	1.0

0.6717855835	0.0562771302	-0.4192777548	0.0000000000	1.0
0.6997076802	0.0516424902	-0.3117699386	0.0000000000	1.0
0.7280428406	0.0461947096	-0.1975039140	0.0000000000	1.0
0.7567745415	0.0400791629	-0.0960932589	0.0000000000	1.0
0.7858881302	0.0335065360	-0.0073313301	0.0000000000	1.0
0.8153729797	0.0267229901	0.0716443622	0.0000000000	1.0
0.8452233688	0.0199787301	0.1392549527	0.0000000000	1.0
0.8754380855	0.0135004870	0.1947019608	0.0000000000	1.0
0.9060191458	0.0074787590	0.2388075692	0.0000000000	1.0
0.9369702317	0.0020876729	0.2754120815	0.0000000000	1.0
0.9682957072	-0.0024966698	0.2995486827	0.0000000000	1.0
1.0000000000	-0.0060581764	0.3146850653	0.0000000000	1.0

6.5 Ellipsoid of revolution along windward plane of symmetry

This is reduced input file from which was used to generate the result presented in PART I, section 5.2.3.

```
Ellipsoid of revolution, windward plane of symmetry
2
istop mks  kshale   ktw krow
 20    0     0        0    0
pr     rminf       pinf       tinf     ukmax1    zetae  dzeta1 rk
0.72   0.05        2116.      520.0    0.99999    6.0     0.1   1.0
imax
      20
 0.400000E-02  0.450000E-02  0.500000E-02  0.550000E-02  0.600000E-02
 0.800000E-02  0.100000E-01  0.120000E-01  0.140000E-01  0.160000E-01
 0.180000E-01  0.200000E-01  0.220000E-01  0.240000E-01  0.260000E-01
 0.280000E-01  0.300000E-01  0.320000E-01  0.340000E-01  0.360000E-01
 0.000000E+00  0.872665E-01
  1    1  0.400000E-02  0.000000E+00  0.226936E-01  0.180332E+00
          0.000000E+00  0.296069E+01  0.223383E-01  0.000000E+00
  1    2  0.400000E-02  0.194691E-02  0.226936E-01  0.181028E+00
          0.169429E-01  0.296069E+01  0.223383E-01  0.000000E+00
  2    1  0.450000E-02  0.000000E+00  0.241363E-01  0.201077E+00
          0.000000E+00  0.281027E+01  0.236904E-01  0.000000E+00
  2    2  0.450000E-02  0.206475E-02  0.241363E-01  0.201768E+00
          0.169429E-01  0.281027E+01  0.236904E-01  0.000000E+00
  3    1  0.500000E-02  0.000000E+00  0.255099E-01  0.220376E+00
          0.000000E+00  0.268387E+01  0.249687E-01  0.000000E+00
  3    2  0.500000E-02  0.217617E-02  0.255099E-01  0.221063E+00
          0.169429E-01  0.268387E+01  0.249687E-01  0.000000E+00
  4    1  0.550000E-02  0.000000E+00  0.268248E-01  0.238433E+00
          0.000000E+00  0.257585E+01  0.261841E-01  0.000000E+00
  4    2  0.550000E-02  0.228210E-02  0.268248E-01  0.239115E+00
          0.169429E-01  0.257585E+01  0.261841E-01  0.000000E+00
  5    1  0.600000E-02  0.000000E+00  0.280893E-01  0.255407E+00
          0.000000E+00  0.248224E+01  0.273450E-01  0.000000E+00
  5    2  0.600000E-02  0.238328E-02  0.280893E-01  0.256084E+00
          0.169429E-01  0.248224E+01  0.273450E-01  0.000000E+00
  6    1  0.800000E-02  0.000000E+00  0.327760E-01  0.314700E+00
          0.000000E+00  0.220441E+01  0.315595E-01  0.000000E+00
  6    2  0.800000E-02  0.275059E-02  0.327760E-01  0.315359E+00
          0.169429E-01  0.220441E+01  0.315595E-01  0.000000E+00
  7    1  0.100000E-01  0.000000E+00  0.369999E-01  0.363744E+00
          0.000000E+00  0.201946E+01  0.352668E-01  0.000000E+00
  7    2  0.100000E-01  0.307371E-02  0.369999E-01  0.364387E+00
          0.169429E-01  0.201946E+01  0.352668E-01  0.000000E+00
  8    1  0.120000E-01  0.000000E+00  0.409054E-01  0.405468E+00
          0.000000E+00  0.188610E+01  0.386135E-01  0.000000E+00
  8    2  0.120000E-01  0.336539E-02  0.409054E-01  0.406095E+00
          0.169429E-01  0.188610E+01  0.386135E-01  0.000000E+00
  9    1  0.140000E-01  0.000000E+00  0.445763E-01  0.441657E+00
          0.000000E+00  0.178476E+01  0.416863E-01  0.000000E+00
  9    2  0.140000E-01  0.363320E-02  0.445763E-01  0.442270E+00
          0.169429E-01  0.178476E+01  0.416863E-01  0.000000E+00
```

```
10    1  0.160000E-01  0.000000E+00  0.480659E-01  0.473498E+00
         0.000000E+00  0.170481E+01  0.445421E-01  0.000000E+00
10    2  0.160000E-01  0.388210E-02  0.480659E-01  0.474097E+00
         0.169429E-01  0.170481E+01  0.445421E-01  0.000000E+00
11    1  0.180000E-01  0.000000E+00  0.514106E-01  0.501827E+00
         0.000000E+00  0.163993E+01  0.472202E-01  0.000000E+00
11    2  0.180000E-01  0.411551E-02  0.514106E-01  0.502413E+00
         0.169429E-01  0.163993E+01  0.472202E-01  0.000000E+00
12    1  0.200000E-01  0.000000E+00  0.546367E-01  0.527258E+00
         0.000000E+00  0.158612E+01  0.497494E-01  0.000000E+00
12    2  0.200000E-01  0.433594E-02  0.546367E-01  0.527832E+00
         0.169429E-01  0.158612E+01  0.497494E-01  0.000000E+00
13    1  0.220000E-01  0.000000E+00  0.577635E-01  0.550259E+00
         0.000000E+00  0.154070E+01  0.521512E-01  0.000000E+00
13    2  0.220000E-01  0.454528E-02  0.577635E-01  0.550822E+00
         0.169429E-01  0.154070E+01  0.521512E-01  0.000000E+00
14    1  0.240000E-01  0.000000E+00  0.608060E-01  0.571195E+00
         0.000000E+00  0.150180E+01  0.544426E-01  0.000000E+00
14    2  0.240000E-01  0.474499E-02  0.608060E-01  0.571747E+00
         0.169429E-01  0.150180E+01  0.544426E-01  0.000000E+00
15    1  0.260000E-01  0.000000E+00  0.637758E-01  0.590356E+00
         0.000000E+00  0.146808E+01  0.566370E-01  0.000000E+00
15    2  0.260000E-01  0.493624E-02  0.637758E-01  0.590897E+00
         0.169429E-01  0.146808E+01  0.566370E-01  0.000000E+00
16    1  0.280000E-01  0.000000E+00  0.666825E-01  0.607975E+00
         0.000000E+00  0.143855E+01  0.587452E-01  0.000000E+00
16    2  0.280000E-01  0.511998E-02  0.666825E-01  0.608506E+00
         0.169429E-01  0.143855E+01  0.587452E-01  0.000000E+00
17    1  0.300000E-01  0.000000E+00  0.695335E-01  0.624245E+00
         0.000000E+00  0.141246E+01  0.607762E-01  0.000000E+00
17    2  0.300000E-01  0.529700E-02  0.695335E-01  0.624767E+00
         0.169429E-01  0.141246E+01  0.607762E-01  0.000000E+00
18    1  0.320000E-01  0.000000E+00  0.723352E-01  0.639327E+00
         0.000000E+00  0.138922E+01  0.627375E-01  0.000000E+00
18    2  0.320000E-01  0.546794E-02  0.723352E-01  0.639840E+00
         0.169429E-01  0.138922E+01  0.627375E-01  0.000000E+00
19    1  0.340000E-01  0.000000E+00  0.750928E-01  0.653354E+00
         0.000000E+00  0.136840E+01  0.646355E-01  0.000000E+00
19    2  0.340000E-01  0.563336E-02  0.750928E-01  0.653859E+00
         0.169429E-01  0.136840E+01  0.646355E-01  0.000000E+00
20    1  0.360000E-01  0.000000E+00  0.778108E-01  0.666441E+00
         0.000000E+00  0.134962E+01  0.664756E-01  0.000000E+00
20    2  0.360000E-01  0.579373E-02  0.778108E-01  0.666938E+00
         0.169429E-01  0.134962E+01  0.664756E-01  0.000000E+00
0.967481E+00  0.959568E+00  0.951434E+00  0.943149E+00  0.934767E+00
0.900964E+00  0.867690E+00  0.835596E+00  0.804939E+00  0.775800E+00
0.748170E+00  0.721999E+00  0.697215E+00  0.673736E+00  0.651480E+00
0.630367E+00  0.610318E+00  0.591261E+00  0.573128E+00  0.555857E+00
0.000000E+00  0.000000E+00  0.000000E+00  0.000000E+00  0.000000E+00
0.000000E+00  0.000000E+00  0.000000E+00  0.000000E+00  0.000000E+00
0.000000E+00  0.000000E+00  0.000000E+00  0.000000E+00  0.000000E+00
0.000000E+00  0.000000E+00  0.000000E+00  0.000000E+00  0.000000E+00
0.100000E+01  0.100000E+01  0.100000E+01  0.100000E+01  0.100000E+01
0.100000E+01  0.100000E+01  0.100000E+01  0.100000E+01  0.100000E+01
0.100000E+01  0.100000E+01  0.100000E+01  0.100000E+01  0.100000E+01
0.100000E+01  0.100000E+01  0.100000E+01  0.100000E+01  0.100000E+01
```

6.6 Ellipsoid of revolution along leeward plane of symmetry

This is reduced input file from which was used to generate the result presented in PART I, section 5.2.3.

```
Ellipsoid of revolution, leeward plane of symmetry
2
istop mks  kshale   ktw krow
20    0     0       0    0
pr    rminf       pinf      tinf     ukmax1   zetae  dzeta1    rk
0.72  0.05        2116.     520.0    0.99999   6.0    0.1      1.0
imax
 20
 0.400000E-02  0.450000E-02  0.500000E-02  0.550000E-02  0.600000E-02
 0.800000E-02  0.100000E-01  0.120000E-01  0.140000E-01  0.160000E-01
 0.180000E-01  0.200000E-01  0.220000E-01  0.240000E-01  0.260000E-01
 0.280000E-01  0.300000E-01  0.320000E-01  0.340000E-01  0.360000E-01
 0.314159E+01  0.305433E+01
  1   37  0.400000E-02 -0.766260E-16  0.226936E-01  0.546279E+00
         -0.666833E-15  0.296069E+01  0.223383E-01  0.000000E+00
  1   36  0.400000E-02  0.194691E-02  0.226936E-01  0.545583E+00
          0.169429E-01  0.296069E+01  0.223383E-01  0.000000E+00
  2   37  0.450000E-02 -0.812639E-16  0.241363E-01  0.564425E+00
         -0.666833E-15  0.281027E+01  0.236904E-01  0.000000E+00
  2   36  0.450000E-02  0.206475E-02  0.241363E-01  0.563734E+00
          0.169429E-01  0.281027E+01  0.236904E-01  0.000000E+00
  3   37  0.500000E-02 -0.856490E-16  0.255099E-01  0.581176E+00
         -0.666833E-15  0.268387E+01  0.249687E-01  0.000000E+00
  3   36  0.500000E-02  0.217617E-02  0.255099E-01  0.580490E+00
          0.169429E-01  0.268387E+01  0.249687E-01  0.000000E+00
  4   37  0.550000E-02 -0.898181E-16  0.268248E-01  0.596734E+00
         -0.666833E-15  0.257585E+01  0.261841E-01  0.000000E+00
  4   36  0.550000E-02  0.228210E-02  0.268248E-01  0.596053E+00
          0.169429E-01  0.257585E+01  0.261841E-01  0.000000E+00
  5   37  0.600000E-02 -0.938002E-16  0.280893E-01  0.611256E+00
         -0.666833E-15  0.248224E+01  0.273450E-01  0.000000E+00
  5   36  0.600000E-02  0.238328E-02  0.280893E-01  0.610579E+00
          0.169429E-01  0.248224E+01  0.273450E-01  0.000000E+00
  6   37  0.800000E-02 -0.108257E-15  0.327760E-01  0.661190E+00
         -0.666833E-15  0.220441E+01  0.315595E-01  0.000000E+00
  6   36  0.800000E-02  0.275059E-02  0.327760E-01  0.660531E+00
          0.169429E-01  0.220441E+01  0.315595E-01  0.000000E+00
  7   37  0.100000E-01 -0.120974E-15  0.369999E-01  0.701525E+00
         -0.666833E-15  0.201946E+01  0.352668E-01  0.000000E+00
  7   36  0.100000E-01  0.307371E-02  0.369999E-01  0.700883E+00
          0.169429E-01  0.201946E+01  0.352668E-01  0.000000E+00
  8   37  0.120000E-01 -0.132454E-15  0.409054E-01  0.735119E+00
         -0.666833E-15  0.188610E+01  0.386135E-01  0.000000E+00
  8   36  0.120000E-01  0.336539E-02  0.409054E-01  0.734492E+00
          0.169429E-01  0.188610E+01  0.386135E-01  0.000000E+00
  9   37  0.140000E-01 -0.142994E-15  0.445763E-01  0.763693E+00
         -0.666833E-15  0.178476E+01  0.416863E-01  0.000000E+00
  9   36  0.140000E-01  0.363320E-02  0.445763E-01  0.763081E+00
          0.169429E-01  0.178476E+01  0.416863E-01  0.000000E+00
```

```
10  37  0.160000E-01 -0.152791E-15  0.480659E-01  0.788382E+00
       -0.666833E-15  0.170481E+01  0.445421E-01  0.000000E+00
10  36  0.160000E-01  0.388210E-02  0.480659E-01  0.787783E+00
        0.169429E-01  0.170481E+01  0.445421E-01  0.000000E+00
11  37  0.180000E-01 -0.161977E-15  0.514106E-01  0.809974E+00
       -0.666833E-15  0.163993E+01  0.472202E-01  0.000000E+00
11  36  0.180000E-01  0.411551E-02  0.514106E-01  0.809388E+00
        0.169429E-01  0.163993E+01  0.472202E-01  0.000000E+00
12  37  0.200000E-01 -0.170653E-15  0.546367E-01  0.829047E+00
       -0.666833E-15  0.158612E+01  0.497494E-01  0.000000E+00
12  36  0.200000E-01  0.433594E-02  0.546367E-01  0.828473E+00
        0.169429E-01  0.158612E+01  0.497494E-01  0.000000E+00
13  37  0.220000E-01 -0.178892E-15  0.577635E-01  0.846032E+00
       -0.666833E-15  0.154070E+01  0.521512E-01  0.000000E+00
13  36  0.220000E-01  0.454528E-02  0.577635E-01  0.845469E+00
        0.169429E-01  0.154070E+01  0.521512E-01  0.000000E+00
14  37  0.240000E-01 -0.186752E-15  0.608060E-01  0.861264E+00
       -0.666833E-15  0.150180E+01  0.544426E-01  0.000000E+00
14  36  0.240000E-01  0.474499E-02  0.608060E-01  0.860712E+00
        0.169429E-01  0.150180E+01  0.544426E-01  0.000000E+00
15  37  0.260000E-01 -0.194279E-15  0.637758E-01  0.875005E+00
       -0.666833E-15  0.146808E+01  0.566370E-01  0.000000E+00
15  36  0.260000E-01  0.493624E-02  0.637758E-01  0.874464E+00
        0.169429E-01  0.146808E+01  0.566370E-01  0.000000E+00
16  37  0.280000E-01 -0.201511E-15  0.666825E-01  0.887468E+00
       -0.666833E-15  0.143855E+01  0.587452E-01  0.000000E+00
16  36  0.280000E-01  0.511998E-02  0.666825E-01  0.886936E+00
        0.169429E-01  0.143855E+01  0.587452E-01  0.000000E+00
17  37  0.300000E-01 -0.208478E-15  0.695335E-01  0.898823E+00
       -0.666833E-15  0.141246E+01  0.607762E-01  0.000000E+00
17  36  0.300000E-01  0.529700E-02  0.695335E-01  0.898300E+00
        0.169429E-01  0.141246E+01  0.607762E-01  0.000000E+00
18  37  0.320000E-01 -0.215205E-15  0.723352E-01  0.909211E+00
       -0.666833E-15  0.138922E+01  0.627375E-01  0.000000E+00
18  36  0.320000E-01  0.546794E-02  0.723352E-01  0.908697E+00
        0.169429E-01  0.138922E+01  0.627375E-01  0.000000E+00
19  37  0.340000E-01 -0.221716E-15  0.750928E-01  0.918751E+00
       -0.666833E-15  0.136840E+01  0.646355E-01  0.000000E+00
19  36  0.340000E-01  0.563336E-02  0.750928E-01  0.918246E+00
        0.169429E-01  0.136840E+01  0.646355E-01  0.000000E+00
20  37  0.360000E-01 -0.228028E-15  0.778108E-01  0.927540E+00
       -0.666833E-15  0.134962E+01  0.664756E-01  0.000000E+00
20  36  0.360000E-01  0.579373E-02  0.778108E-01  0.927044E+00
        0.169429E-01  0.134962E+01  0.664756E-01  0.000000E+00
0.701579E+00  0.681424E+00  0.662234E+00  0.643908E+00  0.626366E+00
0.562828E+00  0.507862E+00  0.459600E+00  0.416773E+00  0.378454E+00
0.343942E+00  0.312681E+00  0.284230E+00  0.258225E+00  0.234365E+00
0.212401E+00  0.192118E+00  0.173336E+00  0.155897E+00  0.139669E+00
0.000000E+00  0.000000E+00  0.000000E+00  0.000000E+00  0.000000E+00
0.000000E+00  0.000000E+00  0.000000E+00  0.000000E+00  0.000000E+00
0.000000E+00  0.000000E+00  0.000000E+00  0.000000E+00  0.000000E+00
0.000000E+00  0.000000E+00  0.000000E+00  0.000000E+00  0.000000E+00
0.100000E+01  0.100000E+01  0.100000E+01  0.100000E+01  0.100000E+01
0.100000E+01  0.100000E+01  0.100000E+01  0.100000E+01  0.100000E+01
0.100000E+01  0.100000E+01  0.100000E+01  0.100000E+01  0.100000E+01
0.100000E+01  0.100000E+01  0.100000E+01  0.100000E+01  0.100000E+01
```

6.7 Infinite swept cylider along the leading-edge attachment line

This input file was used to generate the result presented in PART I, section 5.2.4.

```
Infinite swept cylinder leading-edge attachment line
3
istop mks kshale   ktw krow
 4     0   0        0    0
pr    rminf      pinf      tinf    ukmax1  zetae  dzetal rk
0.72  0.126675   2116.8    520.0  0.99999  3.5    0.001  1.05
imax
       10
 0.100000E-01  0.200000E-01  0.300000E-01  0.400000E-01  0.500000E-01
 0.600000E-01  0.700000E-01  0.800000E-01  0.900000E-01  0.100000E+00
 0.000000E+00  0.174533E-01
  1    1  0.000000E+00  0.000000E+00  0.100000E-01  0.866025E+00
          0.359535E-11  0.100000E+01  0.375000E+00  0.000000E+00
  1    2  0.000000E+00  0.000000E+00  0.100000E-01  0.866025E+00
          0.174547E-01  0.100000E+01  0.375000E+00  0.000000E+00
  2    1  0.000000E+00  0.000000E+00  0.200000E-01  0.866025E+00
          0.359535E-11  0.100000E+01  0.375000E+00  0.000000E+00
  2    2  0.000000E+00  0.000000E+00  0.200000E-01  0.866025E+00
          0.174547E-01  0.100000E+01  0.375000E+00  0.000000E+00
  3    1  0.000000E+00  0.000000E+00  0.300000E-01  0.866025E+00
          0.359535E-11  0.100000E+01  0.375000E+00  0.000000E+00
  3    2  0.000000E+00  0.000000E+00  0.300000E-01  0.866025E+00
          0.174547E-01  0.100000E+01  0.375000E+00  0.000000E+00
  4    1  0.000000E+00  0.000000E+00  0.400000E-01  0.866025E+00
          0.359535E-11  0.100000E+01  0.375000E+00  0.000000E+00
  4    2  0.000000E+00  0.000000E+00  0.400000E-01  0.866025E+00
          0.174547E-01  0.100000E+01  0.375000E+00  0.000000E+00
  5    1  0.000000E+00  0.000000E+00  0.500000E-01  0.866025E+00
          0.359535E-11  0.100000E+01  0.375000E+00  0.000000E+00
  5    2  0.000000E+00  0.000000E+00  0.500000E-01  0.866025E+00
          0.174547E-01  0.100000E+01  0.375000E+00  0.000000E+00
  6    1  0.000000E+00  0.000000E+00  0.600000E-01  0.866025E+00
          0.359535E-11  0.100000E+01  0.375000E+00  0.000000E+00
  6    2  0.000000E+00  0.000000E+00  0.600000E-01  0.866025E+00
          0.174547E-01  0.100000E+01  0.375000E+00  0.000000E+00
  7    1  0.000000E+00  0.000000E+00  0.700000E-01  0.866025E+00
          0.359535E-11  0.100000E+01  0.375000E+00  0.000000E+00
  7    2  0.000000E+00  0.000000E+00  0.700000E-01  0.866025E+00
          0.174547E-01  0.100000E+01  0.375000E+00  0.000000E+00
  8    1  0.000000E+00  0.000000E+00  0.800000E-01  0.866025E+00
          0.359535E-11  0.100000E+01  0.375000E+00  0.000000E+00
  8    2  0.000000E+00  0.000000E+00  0.800000E-01  0.866025E+00
          0.174547E-01  0.100000E+01  0.375000E+00  0.000000E+00
  9    1  0.000000E+00  0.000000E+00  0.900000E-01  0.866025E+00
          0.359535E-11  0.100000E+01  0.375000E+00  0.000000E+00
  9    2  0.000000E+00  0.000000E+00  0.900000E-01  0.866025E+00
          0.174547E-01  0.100000E+01  0.375000E+00  0.000000E+00
 10    1  0.000000E+00  0.000000E+00  0.100000E+00  0.866025E+00
          0.359535E-11  0.100000E+01  0.375000E+00  0.000000E+00
 10    2  0.000000E+00  0.000000E+00  0.100000E+00  0.866025E+00
          0.174547E-01  0.100000E+01  0.375000E+00  0.000000E+00
```

```
0.250251E+00  0.250251E+00  0.250251E+00  0.250251E+00  0.250251E+00
0.250251E+00  0.250251E+00  0.250251E+00  0.250251E+00  0.250251E+00
0.000000E+00  0.000000E+00  0.000000E+00  0.000000E+00  0.000000E+00
0.000000E+00  0.000000E+00  0.000000E+00  0.000000E+00  0.000000E+00
0.100000E+01  0.100000E+01  0.100000E+01  0.100000E+01  0.100000E+01
0.100000E+01  0.100000E+01  0.100000E+01  0.100000E+01  0.100000E+01
```

6.8 Swept-back wing

This input file was used to generate the result presented in PART I, section 5.2.5.

```
 F-14 VSTFE CLEAN-UP GLOVE
 4
 0 1 0 0
51  48  0.20000  0.0010000   1.05
  5.425594    22.18     4.68     .80     .0  785.30000  430.00000     .72
       .1616606      -.0262935
       .1414880      -.0257465
       .1213054      -.0250774
       .1011129      -.0242459
       .0809103      -.0231646
       .0606977      -.0216108
       .0404044      -.0194493
       .0202426      -.0156186
       .0100719      -.0121270
       .0050211      -.0091629
       .0019336      -.0058652
       .0000000       .0000000
       .0019336       .0061704
       .0050211       .0097646
       .0100719       .0136796
       .0202426       .0192767
       .0404044       .0271152
       .0606977       .0329864
       .0809103       .0379677
       .1011129       .0422232
       .1213054       .0459822
       .1414880       .0493646
       .1616606       .0524201
       .1818233       .0551935
       .2019760       .0576876
       .2221187       .0599615
       .2422515       .0619935
       .2623744       .0638032
       .2824873       .0653983
       .3025903       .0667787
       .3226834       .0679643
       .3427665       .0688854
       .3628398       .0697315
       .3829032       .0703230
       .4029567       .0707373
       .4230003       .0709645
       .4430340       .0710145
       .4630579       .0708873
       .4830719       .0705982
       .5030761       .0701466
       .5230704       .0695354
       .5630296       .0678540
       .6029494       .0656117
       .6428300       .0628557
       .6826715       .0596285
       .7025776       .0577982
```

.7224739	.0559902		
.7423604	.0540278		
.7622372	.0519857		
.7821042	.0498664		
.8019615	.0476850		
.0001219	.9828369	.0000000	1.000000
.0008643	.9291969	.0000000	1.000000
.0016067	.8558530	.0000000	1.000000
.0023491	.7860392	.0000000	1.000000
.0030916	.7235947	.0000000	1.000000
.0038340	.6685212	.0000000	1.000000
.0060612	.5306466	.0000000	1.000000
.0082885	.4146636	.0000000	1.000000
.0105158	.3174372	.0000000	1.000000
.0127431	.2479026	.0000000	1.000000
.0149703	.1841853	.0000000	1.000000
.0171976	.1250204	.0000000	1.000000
.0194249	.0695431	.0000000	1.000000
.0246218	-.0133144	.0000000	1.000000
.0298188	-.0815164	.0000000	1.000000
.0350158	-.1439954	.0000000	1.000000
.0402127	-.2019712	.0000000	1.000000
.0454097	-.2352954	.0000000	1.000000
.0506067	-.2656347	-.0007000	1.000000
.0558036	-.2944504	-.0007000	1.000000
.0669400	-.3357120	-.0007000	1.000000
.0780763	-.3613739	-.0007000	1.000000
.0892127	-.3837189	-.0007000	1.000000
.1003490	-.4043051	-.0007000	1.000000
.1114854	-.4173073	-.0007000	1.000000
.1226217	-.4298466	-.0007000	1.000000
.1337581	-.4457382	-.0007000	1.000000
.1448944	-.4610751	-.0007000	1.000000
.1656823	-.4949900	-.0007000	1.000000
.1864701	-.5317120	-.0007000	1.000000
.2072580	-.5662568	-.0007000	1.000000
.2280459	-.5959700	-.0007000	1.000000
.2488337	-.6247629	-.0007000	1.000000
.2696216	-.6515539	-.0007000	1.000000
.2904094	-.6774718	-.0007000	1.000000
.3111973	-.7032281	-.0007000	1.000000
.3319851	-.7290463	-.0007000	1.000000
.3527730	-.7545299	.0000000	1.000000
.3787578	-.7868917	.0000000	1.000000
.4047426	-.8187169	.0000000	1.000000
.4307275	-.8478254	.0000000	1.000000
.4567123	-.8746795	.0000000	1.000000
.4826971	-.8885065	.0000000	1.000000
.5086819	-.8964149	.0000000	1.000000
.5230704	-.8887564	.0000000	1.000000
.5391213	-.8802513	.0000000	1.000000
.5695606	-.8642401	.0000000	1.000000
.6000000	-.8483981	.0000000	1.000000

7. SAMPLE CASE OUTPUT

To reduce the size of output data, only the boundary-layer parameters written on file FORT.30 will be shown.

7.1 Flat plate

i	x/c cfy	cfx dspty	blth thmoy	dsptx twall	thmox qw
1	0.000000E+00	0.000000E+00	0.000000E+00	0.000000E+00	0.000000E+00
	0.000000E+00	0.000000E+00	0.000000E+00	0.000000E+00	0.000000E+00
2	0.100000E-01	0.484239E-03	0.517312E-04	0.251080E-04	0.483610E-05
	0.000000E+00	0.000000E+00	0.000000E+00	0.868923E+03	-0.150288E+01
3	0.200000E-01	0.342408E-03	0.731589E-04	0.355080E-04	0.683927E-05
	0.000000E+00	0.000000E+00	0.000000E+00	0.868923E+03	-0.106270E+01
4	0.300000E-01	0.279575E-03	0.896010E-04	0.434883E-04	0.837636E-05
	0.000000E+00	0.000000E+00	0.000000E+00	0.868923E+03	-0.867689E+00
5	0.400000E-01	0.242119E-03	0.103462E-03	0.502160E-04	0.967219E-05
	0.000000E+00	0.000000E+00	0.000000E+00	0.868923E+03	-0.751441E+00
6	0.500000E-01	0.216558E-03	0.115674E-03	0.561431E-04	0.108138E-04
	0.000000E+00	0.000000E+00	0.000000E+00	0.868923E+03	-0.672109E+00
7	0.600000E-01	0.197690E-03	0.126715E-03	0.615017E-04	0.118460E-04
	0.000000E+00	0.000000E+00	0.000000E+00	0.868923E+03	-0.613549E+00
8	0.700000E-01	0.183025E-03	0.136868E-03	0.664295E-04	0.127951E-04
	0.000000E+00	0.000000E+00	0.000000E+00	0.868923E+03	-0.568036E+00
9	0.800000E-01	0.171204E-03	0.146318E-03	0.710161E-04	0.136785E-04
	0.000000E+00	0.000000E+00	0.000000E+00	0.868923E+03	-0.531349E+00
10	0.900000E-01	0.161413E-03	0.155194E-03	0.753239E-04	0.145083E-04
	0.000000E+00	0.000000E+00	0.000000E+00	0.868923E+03	-0.500960E+00
11	0.100000E+00	0.153130E-03	0.163588E-03	0.793984E-04	0.152931E-04
	0.000000E+00	0.000000E+00	0.000000E+00	0.868923E+03	-0.475253E+00
12	0.110000E+00	0.146003E-03	0.171573E-03	0.832737E-04	0.160395E-04
	0.000000E+00	0.000000E+00	0.000000E+00	0.868923E+03	-0.453136E+00
13	0.120000E+00	0.139788E-03	0.179202E-03	0.869766E-04	0.167527E-04
	0.000000E+00	0.000000E+00	0.000000E+00	0.868923E+03	-0.433844E+00
14	0.130000E+00	0.134304E-03	0.186519E-03	0.905281E-04	0.174368E-04
	0.000000E+00	0.000000E+00	0.000000E+00	0.868923E+03	-0.416824E+00
15	0.140000E+00	0.129418E-03	0.193560E-03	0.939455E-04	0.180950E-04
	0.000000E+00	0.000000E+00	0.000000E+00	0.868923E+03	-0.401662E+00
16	0.150000E+00	0.125030E-03	0.200354E-03	0.972428E-04	0.187301E-04
	0.000000E+00	0.000000E+00	0.000000E+00	0.868923E+03	-0.388042E+00
17	0.160000E+00	0.121060E-03	0.206925E-03	0.100432E-03	0.193444E-04
	0.000000E+00	0.000000E+00	0.000000E+00	0.868923E+03	-0.375720E+00
18	0.170000E+00	0.117445E-03	0.213293E-03	0.103523E-03	0.199397E-04
	0.000000E+00	0.000000E+00	0.000000E+00	0.868923E+03	-0.364502E+00
19	0.180000E+00	0.114136E-03	0.219477E-03	0.106524E-03	0.205178E-04
	0.000000E+00	0.000000E+00	0.000000E+00	0.868923E+03	-0.354233E+00
20	0.190000E+00	0.111092E-03	0.225491E-03	0.109443E-03	0.210801E-04
	0.000000E+00	0.000000E+00	0.000000E+00	0.868923E+03	-0.344785E+00
21	0.200000E+00	0.108279E-03	0.231349E-03	0.112286E-03	0.216277E-04
	0.000000E+00	0.000000E+00	0.000000E+00	0.868923E+03	-0.336054E+00

7.2 NACA 0012 airfoil

i	x/c cfy	cfx dspty	blth thmoy	dsptx twall	thmox qw
1	0.000000E+00	0.000000E+00	0.000000E+00	0.000000E+00	0.000000E+00
	0.000000E+00	0.000000E+00	0.000000E+00	0.000000E+00	0.000000E+00
2	0.775000E-03	0.495157E-01	0.852824E-04	0.215699E-04	0.952800E-05
	0.000000E+00	0.000000E+00	0.000000E+00	0.545375E+03	-0.729836E+01
3	0.295500E-02	0.250882E-01	0.102382E-03	0.266100E-04	0.114849E-04
	0.000000E+00	0.000000E+00	0.000000E+00	0.544426E+03	-0.130195E+02
4	0.621500E-02	0.166742E-01	0.119106E-03	0.318478E-04	0.134165E-04
	0.000000E+00	0.000000E+00	0.000000E+00	0.543406E+03	-0.148705E+02
5	0.101680E-01	0.121680E-01	0.138414E-03	0.381869E-04	0.156829E-04
	0.000000E+00	0.000000E+00	0.000000E+00	0.542555E+03	-0.121798E+02
6	0.146000E-01	0.941305E-02	0.159176E-03	0.452794E-04	0.181766E-04
	0.000000E+00	0.000000E+00	0.000000E+00	0.541932E+03	-0.877449E+01
7	0.193920E-01	0.766982E-02	0.179854E-03	0.525144E-04	0.207107E-04
	0.000000E+00	0.000000E+00	0.000000E+00	0.541490E+03	-0.642159E+01
8	0.244530E-01	0.650778E-02	0.200040E-03	0.595256E-04	0.231665E-04
	0.000000E+00	0.000000E+00	0.000000E+00	0.541160E+03	-0.497353E+01
9	0.297460E-01	0.560452E-02	0.220015E-03	0.666347E-04	0.256091E-04
	0.000000E+00	0.000000E+00	0.000000E+00	0.540912E+03	-0.363998E+01
10	0.352350E-01	0.488171E-02	0.240048E-03	0.739434E-04	0.280756E-04
	0.000000E+00	0.000000E+00	0.000000E+00	0.540734E+03	-0.253464E+01
11	0.408940E-01	0.437027E-02	0.259342E-03	0.809198E-04	0.304633E-04
	0.000000E+00	0.000000E+00	0.000000E+00	0.540601E+03	-0.201267E+01
12	0.467010E-01	0.399905E-02	0.277574E-03	0.873951E-04	0.327215E-04
	0.000000E+00	0.000000E+00	0.000000E+00	0.540491E+03	-0.175704E+01
13	0.526440E-01	0.367386E-02	0.295311E-03	0.937532E-04	0.349129E-04
	0.000000E+00	0.000000E+00	0.000000E+00	0.540399E+03	-0.143119E+01
14	0.587070E-01	0.337700E-02	0.313138E-03	0.100198E-03	0.370848E-04
	0.000000E+00	0.000000E+00	0.000000E+00	0.540327E+03	-0.108580E+01
15	0.648830E-01	0.312142E-02	0.330562E-03	0.106644E-03	0.392359E-04
	0.000000E+00	0.000000E+00	0.000000E+00	0.540271E+03	-0.826581E+00
16	0.711610E-01	0.290185E-02	0.347783E-03	0.113038E-03	0.413584E-04
	0.000000E+00	0.000000E+00	0.000000E+00	0.540228E+03	-0.629495E+00
17	0.775270E-01	0.272025E-02	0.364579E-03	0.119258E-03	0.434362E-04
	0.000000E+00	0.000000E+00	0.000000E+00	0.540195E+03	-0.505497E+00
18	0.839790E-01	0.257701E-02	0.380758E-03	0.125154E-03	0.454434E-04
	0.000000E+00	0.000000E+00	0.000000E+00	0.540167E+03	-0.456180E+00
19	0.905060E-01	0.245206E-02	0.396351E-03	0.130836E-03	0.473884E-04
	0.000000E+00	0.000000E+00	0.000000E+00	0.540143E+03	-0.403273E+00
20	0.971000E-01	0.232289E-02	0.412124E-03	0.136626E-03	0.493140E-04
	0.000000E+00	0.000000E+00	0.000000E+00	0.540123E+03	-0.289249E+00
21	0.103757E+00	0.219169E-02	0.427771E-03	0.142646E-03	0.512520E-04
	0.000000E+00	0.000000E+00	0.000000E+00	0.540110E+03	-0.156901E+00
22	0.117234E+00	0.198242E-02	0.458722E-03	0.154454E-03	0.550697E-04
	0.000000E+00	0.000000E+00	0.000000E+00	0.540099E+03	-0.379250E-01
23	0.130892E+00	0.182297E-02	0.488208E-03	0.165712E-03	0.587479E-04
	0.000000E+00	0.000000E+00	0.000000E+00	0.540097E+03	0.133113E-01
24	0.144698E+00	0.167648E-02	0.517222E-03	0.176968E-03	0.623528E-04
	0.000000E+00	0.000000E+00	0.000000E+00	0.540104E+03	0.910654E-01
25	0.158623E+00	0.154640E-02	0.545901E-03	0.188243E-03	0.659050E-04
	0.000000E+00	0.000000E+00	0.000000E+00	0.540118E+03	0.151775E+00

26	0.172644E+00	0.143449E-02	0.573779E-03	0.199399E-03	0.693890E-04
	0.000000E+00	0.000000E+00	0.000000E+00	0.540138E+03	0.189371E+00
27	0.186741E+00	0.132994E-02	0.601694E-03	0.210683E-03	0.728367E-04
	0.000000E+00	0.000000E+00	0.000000E+00	0.540164E+03	0.230475E+00
28	0.200899E+00	0.123895E-02	0.628882E-03	0.221905E-03	0.762361E-04
	0.000000E+00	0.000000E+00	0.000000E+00	0.540192E+03	0.252147E+00
29	0.215106E+00	0.114714E-02	0.656482E-03	0.233532E-03	0.796277E-04
	0.000000E+00	0.000000E+00	0.000000E+00	0.540225E+03	0.286715E+00
30	0.229351E+00	0.105472E-02	0.684224E-03	0.245795E-03	0.830536E-04
	0.000000E+00	0.000000E+00	0.000000E+00	0.540263E+03	0.319619E+00
31	0.243625E+00	0.998273E-03	0.710749E-03	0.256948E-03	0.863605E-04
	0.000000E+00	0.000000E+00	0.000000E+00	0.540300E+03	0.290747E+00
32	0.257924E+00	0.948108E-03	0.736188E-03	0.267649E-03	0.895620E-04
	0.000000E+00	0.000000E+00	0.000000E+00	0.540336E+03	0.279839E+00
33	0.272242E+00	0.872308E-03	0.763204E-03	0.279913E-03	0.928435E-04
	0.000000E+00	0.000000E+00	0.000000E+00	0.540374E+03	0.315149E+00
34	0.286573E+00	0.806571E-03	0.790449E-03	0.292504E-03	0.961393E-04
	0.000000E+00	0.000000E+00	0.000000E+00	0.540416E+03	0.316246E+00
35	0.300918E+00	0.754748E-03	0.816888E-03	0.304733E-03	0.993817E-04
	0.000000E+00	0.000000E+00	0.000000E+00	0.540457E+03	0.303006E+00
36	0.315270E+00	0.696915E-03	0.844151E-03	0.317695E-03	0.102641E-03
	0.000000E+00	0.000000E+00	0.000000E+00	0.540499E+03	0.303635E+00
37	0.329629E+00	0.634864E-03	0.872225E-03	0.331716E-03	0.105947E-03
	0.000000E+00	0.000000E+00	0.000000E+00	0.540543E+03	0.302272E+00
38	0.343992E+00	0.586320E-03	0.899933E-03	0.345480E-03	0.109221E-03
	0.000000E+00	0.000000E+00	0.000000E+00	0.540587E+03	0.284722E+00
39	0.358359E+00	0.546420E-03	0.926862E-03	0.358838E-03	0.112436E-03
	0.000000E+00	0.000000E+00	0.000000E+00	0.540630E+03	0.266901E+00
40	0.372730E+00	0.502311E-03	0.954566E-03	0.372916E-03	0.115655E-03
	0.000000E+00	0.000000E+00	0.000000E+00	0.540673E+03	0.255835E+00
41	0.387100E+00	0.455670E-03	0.983070E-03	0.387973E-03	0.118891E-03
	0.000000E+00	0.000000E+00	0.000000E+00	0.540716E+03	0.243281E+00
42	0.401472E+00	0.422837E-03	0.101051E-02	0.402210E-03	0.122065E-03
	0.000000E+00	0.000000E+00	0.000000E+00	0.540758E+03	0.223411E+00
43	0.415846E+00	0.386999E-03	0.103841E-02	0.417052E-03	0.125216E-03
	0.000000E+00	0.000000E+00	0.000000E+00	0.540799E+03	0.209451E+00
44	0.430217E+00	0.321864E-03	0.107186E-02	0.437166E-03	0.128571E-03
	0.000000E+00	0.000000E+00	0.000000E+00	0.540842E+03	0.196891E+00
45	0.444588E+00	0.242323E-03	0.111228E-02	0.463352E-03	0.132141E-03
	0.000000E+00	0.000000E+00	0.000000E+00	0.540889E+03	0.165820E+00
46	0.458957E+00	0.206234E-03	0.114607E-02	0.484547E-03	0.135414E-03
	0.000000E+00	0.000000E+00	0.000000E+00	0.540933E+03	0.135557E+00
47	0.473326E+00	0.184615E-03	0.117689E-02	0.502658E-03	0.138538E-03
	0.000000E+00	0.000000E+00	0.000000E+00	0.540973E+03	0.117190E+00
48	0.487695E+00	0.000000E+00	0.000000E+00	0.000000E+00	0.000000E+00
	0.000000E+00	0.000000E+00	0.000000E+00	0.000000E+00	0.000000E+00

i	x/c	cfx	blth	dsptx	thmox
	cfy	dspty	thmoy	twall	qw
1	0.500000E-02	0.000000E+00	0.000000E+00	0.000000E+00	0.000000E+00
	0.000000E+00	0.000000E+00	0.000000E+00	0.316999E+03	0.000000E+00
2	0.600000E-02	0.628591E-02	0.130625E-03	0.100913E-03	0.538282E-05
	0.000000E+00	0.000000E+00	0.000000E+00	0.316999E+03	0.101339E+06
3	0.700000E-02	0.474071E-02	0.172452E-03	0.133553E-03	0.711912E-05
	0.000000E+00	0.000000E+00	0.000000E+00	0.316999E+03	0.764025E+05
4	0.800000E-02	0.407778E-02	0.199896E-03	0.154997E-03	0.825610E-05
	0.000000E+00	0.000000E+00	0.000000E+00	0.316999E+03	0.657031E+05
5	0.900000E-02	0.367952E-02	0.221067E-03	0.171620E-03	0.913739E-05
	0.000000E+00	0.000000E+00	0.000000E+00	0.316999E+03	0.592819E+05
6	0.100000E-01	0.340323E-02	0.239033E-03	0.185525E-03	0.987604E-05
	0.000000E+00	0.000000E+00	0.000000E+00	0.316999E+03	0.548330E+05
7	0.120000E-01	0.302557E-02	0.268638E-03	0.208605E-03	0.111012E-04
	0.000000E+00	0.000000E+00	0.000000E+00	0.316999E+03	0.487516E+05
8	0.140000E-01	0.276607E-02	0.293948E-03	0.228179E-03	0.121416E-04
	0.000000E+00	0.000000E+00	0.000000E+00	0.316999E+03	0.445744E+05
9	0.160000E-01	0.256892E-02	0.316509E-03	0.245801E-03	0.130806E-04
	0.000000E+00	0.000000E+00	0.000000E+00	0.316999E+03	0.414023E+05
10	0.180000E-01	0.241072E-02	0.337936E-03	0.262080E-03	0.139495E-04
	0.000000E+00	0.000000E+00	0.000000E+00	0.316999E+03	0.388572E+05
11	0.200000E-01	0.227945E-02	0.357772E-03	0.277311E-03	0.147630E-04
	0.000000E+00	0.000000E+00	0.000000E+00	0.316999E+03	0.367445E+05
12	0.220000E-01	0.216802E-02	0.376294E-03	0.291676E-03	0.155302E-04
	0.000000E+00	0.000000E+00	0.000000E+00	0.316999E+03	0.349501E+05
13	0.240000E-01	0.207179E-02	0.393850E-03	0.305306E-03	0.162579E-04
	0.000000E+00	0.000000E+00	0.000000E+00	0.316999E+03	0.333998E+05
14	0.260000E-01	0.198757E-02	0.410864E-03	0.318301E-03	0.169515E-04
	0.000000E+00	0.000000E+00	0.000000E+00	0.316999E+03	0.320423E+05
15	0.280000E-01	0.191302E-02	0.427084E-03	0.330744E-03	0.176154E-04
	0.000000E+00	0.000000E+00	0.000000E+00	0.316999E+03	0.308406E+05
16	0.300000E-01	0.184643E-02	0.442612E-03	0.342701E-03	0.182531E-04
	0.000000E+00	0.000000E+00	0.000000E+00	0.316999E+03	0.297668E+05
17	0.350000E-01	0.170687E-02	0.478839E-03	0.370748E-03	0.197485E-04
	0.000000E+00	0.000000E+00	0.000000E+00	0.316999E+03	0.275162E+05
18	0.400000E-01	0.159549E-02	0.512077E-03	0.396637E-03	0.211283E-04
	0.000000E+00	0.000000E+00	0.000000E+00	0.316999E+03	0.257198E+05
19	0.450000E-01	0.150338E-02	0.543287E-03	0.420941E-03	0.224236E-04
	0.000000E+00	0.000000E+00	0.000000E+00	0.316999E+03	0.242346E+05
20	0.500000E-01	0.142559E-02	0.573147E-03	0.443917E-03	0.236481E-04
	0.000000E+00	0.000000E+00	0.000000E+00	0.316999E+03	0.229803E+05
21	0.550000E-01	0.135890E-02	0.601427E-03	0.465707E-03	0.248093E-04
	0.000000E+00	0.000000E+00	0.000000E+00	0.316999E+03	0.219052E+05
22	0.600000E-01	0.130070E-02	0.628449E-03	0.486554E-03	0.259202E-04
	0.000000E+00	0.000000E+00	0.000000E+00	0.316999E+03	0.209668E+05
23	0.650000E-01	0.124949E-02	0.654282E-03	0.506501E-03	0.269832E-04
	0.000000E+00	0.000000E+00	0.000000E+00	0.316999E+03	0.201412E+05
24	0.700000E-01	0.120381E-02	0.679158E-03	0.525724E-03	0.280075E-04
	0.000000E+00	0.000000E+00	0.000000E+00	0.316999E+03	0.194048E+05
25	0.750000E-01	0.116288E-02	0.703091E-03	0.544229E-03	0.289936E-04
	0.000000E+00	0.000000E+00	0.000000E+00	0.316999E+03	0.187450E+05

26	0.800000E-01	0.112581E-02	0.726265E-03	0.562157E-03	0.299488E-04
	0.000000E+00	0.000000E+00	0.000000E+00	0.316999E+03	0.181473E+05
27	0.850000E-01	0.109213E-02	0.748665E-03	0.579492E-03	0.308726E-04
	0.000000E+00	0.000000E+00	0.000000E+00	0.316999E+03	0.176044E+05
28	0.900000E-01	0.106125E-02	0.770447E-03	0.596355E-03	0.317710E-04
	0.000000E+00	0.000000E+00	0.000000E+00	0.316999E+03	0.171067E+05
29	0.950000E-01	0.103284E-02	0.791632E-03	0.612760E-03	0.326452E-04
	0.000000E+00	0.000000E+00	0.000000E+00	0.316999E+03	0.166487E+05
30	0.970000E-01	0.173760E-02	0.753936E-03	0.573713E-03	0.319390E-04
	0.000000E+00	0.000000E+00	0.000000E+00	0.316999E+03	0.268610E+05
31	0.990000E-01	0.206746E-02	0.718314E-03	0.539133E-03	0.306585E-04
	0.000000E+00	0.000000E+00	0.000000E+00	0.316999E+03	0.317821E+05
32	0.101000E+00	0.227347E-02	0.690004E-03	0.512221E-03	0.294100E-04
	0.000000E+00	0.000000E+00	0.000000E+00	0.316999E+03	0.349898E+05
33	0.103000E+00	0.241863E-02	0.668187E-03	0.491556E-03	0.283353E-04
	0.000000E+00	0.000000E+00	0.000000E+00	0.316999E+03	0.373565E+05
34	0.105000E+00	0.252802E-02	0.650370E-03	0.475395E-03	0.274318E-04
	0.000000E+00	0.000000E+00	0.000000E+00	0.316999E+03	0.392156E+05
35	0.107000E+00	0.261392E-02	0.636766E-03	0.462452E-03	0.266692E-04
	0.000000E+00	0.000000E+00	0.000000E+00	0.316999E+03	0.407277E+05
36	0.109000E+00	0.268318E-02	0.625154E-03	0.451868E-03	0.260194E-04
	0.000000E+00	0.000000E+00	0.000000E+00	0.316999E+03	0.419839E+05
37	0.111000E+00	0.274005E-02	0.615407E-03	0.443074E-03	0.254606E-04
	0.000000E+00	0.000000E+00	0.000000E+00	0.316999E+03	0.430422E+05
38	0.113000E+00	0.278733E-02	0.607552E-03	0.435683E-03	0.249768E-04
	0.000000E+00	0.000000E+00	0.000000E+00	0.316999E+03	0.439427E+05
39	0.115000E+00	0.282702E-02	0.600424E-03	0.429418E-03	0.245556E-04
	0.000000E+00	0.000000E+00	0.000000E+00	0.316999E+03	0.447144E+05
40	0.125000E+00	0.295952E-02	0.574461E-03	0.407479E-03	0.229890E-04
	0.000000E+00	0.000000E+00	0.000000E+00	0.316999E+03	0.473867E+05
41	0.135000E+00	0.302481E-02	0.559251E-03	0.396181E-03	0.220893E-04
	0.000000E+00	0.000000E+00	0.000000E+00	0.316999E+03	0.488197E+05
42	0.145000E+00	0.305333E-02	0.552099E-03	0.391620E-03	0.216500E-04
	0.000000E+00	0.000000E+00	0.000000E+00	0.316999E+03	0.495480E+05
43	0.155000E+00	0.306254E-02	0.550301E-03	0.390896E-03	0.214881E-04
	0.000000E+00	0.000000E+00	0.000000E+00	0.316999E+03	0.498811E+05
44	0.165000E+00	0.306189E-02	0.551563E-03	0.392237E-03	0.214830E-04
	0.000000E+00	0.000000E+00	0.000000E+00	0.316999E+03	0.499955E+05
45	0.175000E+00	0.305632E-02	0.555210E-03	0.394647E-03	0.215631E-04
	0.000000E+00	0.000000E+00	0.000000E+00	0.316999E+03	0.499912E+05
46	0.185000E+00	0.304839E-02	0.559412E-03	0.397593E-03	0.216884E-04
	0.000000E+00	0.000000E+00	0.000000E+00	0.316999E+03	0.499233E+05
47	0.195000E+00	0.303956E-02	0.564093E-03	0.400756E-03	0.218349E-04
	0.000000E+00	0.000000E+00	0.000000E+00	0.316999E+03	0.498252E+05
48	0.205000E+00	0.303049E-02	0.569255E-03	0.403985E-03	0.219903E-04
	0.000000E+00	0.000000E+00	0.000000E+00	0.316999E+03	0.497136E+05
49	0.215000E+00	0.302154E-02	0.574115E-03	0.407193E-03	0.221477E-04
	0.000000E+00	0.000000E+00	0.000000E+00	0.316999E+03	0.495980E+05
50	0.225000E+00	0.301291E-02	0.578621E-03	0.410333E-03	0.223033E-04
	0.000000E+00	0.000000E+00	0.000000E+00	0.316999E+03	0.494836E+05
51	0.235000E+00	0.300468E-02	0.583684E-03	0.413379E-03	0.224548E-04
	0.000000E+00	0.000000E+00	0.000000E+00	0.316999E+03	0.493732E+05
52	0.245000E+00	0.299689E-02	0.588395E-03	0.416318E-03	0.226011E-04
	0.000000E+00	0.000000E+00	0.000000E+00	0.316999E+03	0.492682E+05
53	0.255000E+00	0.298954E-02	0.592743E-03	0.419147E-03	0.227417E-04
	0.000000E+00	0.000000E+00	0.000000E+00	0.316999E+03	0.491690E+05

54	0.265000E+00	0.298258E-02	0.596735E-03	0.421872E-03	0.228769E-04
	0.000000E+00	0.000000E+00	0.000000E+00	0.316999E+03	0.490751E+05
55	0.275000E+00	0.297607E-02	0.600944E-03	0.424479E-03	0.230059E-04
	0.000000E+00	0.000000E+00	0.000000E+00	0.316999E+03	0.489877E+05
56	0.285000E+00	0.296995E-02	0.605068E-03	0.426978E-03	0.231291E-04
	0.000000E+00	0.000000E+00	0.000000E+00	0.316999E+03	0.489059E+05
57	0.295000E+00	0.296419E-02	0.608888E-03	0.429374E-03	0.232468E-04
	0.000000E+00	0.000000E+00	0.000000E+00	0.316999E+03	0.488291E+05
58	0.305000E+00	0.295875E-02	0.612409E-03	0.431673E-03	0.233594E-04
	0.000000E+00	0.000000E+00	0.000000E+00	0.316999E+03	0.487570E+05

i	x/c cfy	cfx dspty	blth thmoy	dsptx twall	thmox qw
1	0.373416E-02	0.000000E+00	0.000000E+00	0.000000E+00	0.000000E+00
	0.000000E+00	0.000000E+00	0.000000E+00	0.000000E+00	0.000000E+00
2	0.218875E-02	0.162810E-01	0.649704E-03	0.164296E-03	0.727296E-04
	0.000000E+00	0.000000E+00	0.000000E+00	0.446464E+03	-0.193601E+00
3	0.000000E+00	0.604084E-02	0.778570E-03	0.201441E-03	0.856589E-04
	0.000000E+00	0.000000E+00	0.000000E+00	0.443914E+03	-0.109754E+01
4	0.145997E-02	0.367783E-02	0.951187E-03	0.263736E-03	0.100272E-03
	0.000000E+00	0.000000E+00	0.000000E+00	0.438654E+03	-0.212606E+01
5	0.561097E-02	0.235163E-02	0.130662E-02	0.398167E-03	0.134613E-03
	0.000000E+00	0.000000E+00	0.000000E+00	0.434196E+03	-0.112155E+01
6	0.111812E-01	0.125468E-02	0.174349E-02	0.598226E-03	0.185629E-03
	0.000000E+00	0.000000E+00	0.000000E+00	0.433090E+03	-0.349651E-01
7	0.176662E-01	0.701414E-03	0.217831E-02	0.823670E-03	0.239134E-03
	0.000000E+00	0.000000E+00	0.000000E+00	0.433571E+03	0.867581E-01
8	0.251550E-01	0.503271E-03	0.257521E-02	0.102513E-02	0.287813E-03
	0.000000E+00	0.000000E+00	0.000000E+00	0.434200E+03	0.584770E-01
9	0.335804E-01	0.410599E-03	0.294645E-02	0.120198E-02	0.334112E-03
	0.000000E+00	0.000000E+00	0.000000E+00	0.434770E+03	0.426648E-01
10	0.428933E-01	0.389267E-03	0.327812E-02	0.133903E-02	0.377128E-03
	0.000000E+00	0.000000E+00	0.000000E+00	0.435183E+03	0.279242E-01
11	0.530432E-01	0.395935E-03	0.357713E-02	0.144198E-02	0.416248E-03
	0.000000E+00	0.000000E+00	0.000000E+00	0.435428E+03	0.151245E-01
12	0.639961E-01	0.392345E-03	0.387022E-02	0.153890E-02	0.452737E-03
	0.000000E+00	0.000000E+00	0.000000E+00	0.435557E+03	0.904173E-02
13	0.757222E-01	0.359495E-03	0.418669E-02	0.165871E-02	0.489669E-03
	0.000000E+00	0.000000E+00	0.000000E+00	0.435659E+03	0.130545E-01
14	0.881880E-01	0.312134E-03	0.452897E-02	0.180597E-02	0.528775E-03
	0.000000E+00	0.000000E+00	0.000000E+00	0.435793E+03	0.182800E-01
15	0.101362E+00	0.276467E-03	0.486913E-02	0.195564E-02	0.568240E-03
	0.000000E+00	0.000000E+00	0.000000E+00	0.435946E+03	0.181670E-01
16	0.115218E+00	0.265231E-03	0.517285E-02	0.207565E-02	0.605288E-03
	0.000000E+00	0.000000E+00	0.000000E+00	0.436074E+03	0.136696E-01
17	0.129732E+00	0.273282E-03	0.543096E-02	0.215548E-02	0.638392E-03
	0.000000E+00	0.000000E+00	0.000000E+00	0.436149E+03	0.669523E-02
18	0.144886E+00	0.289138E-03	0.565398E-02	0.220556E-02	0.667044E-03
	0.000000E+00	0.000000E+00	0.000000E+00	0.436161E+03	-0.144470E-02
19	0.160664E+00	0.302779E-03	0.585929E-02	0.224417E-02	0.691956E-03
	0.000000E+00	0.000000E+00	0.000000E+00	0.436118E+03	-0.864108E-02
20	0.177052E+00	0.308940E-03	0.606272E-02	0.228630E-02	0.714780E-03
	0.000000E+00	0.000000E+00	0.000000E+00	0.436040E+03	-0.129254E-01
21	0.194037E+00	0.307959E-03	0.627200E-02	0.233826E-02	0.737101E-03
	0.000000E+00	0.000000E+00	0.000000E+00	0.435946E+03	-0.144695E-01
22	0.211606E+00	0.302694E-03	0.648871E-02	0.239965E-02	0.759753E-03
	0.000000E+00	0.000000E+00	0.000000E+00	0.435851E+03	-0.146568E-01
23	0.229749E+00	0.295679E-03	0.670995E-02	0.246756E-02	0.782921E-03
	0.000000E+00	0.000000E+00	0.000000E+00	0.435760E+03	-0.145427E-01
24	0.248454E+00	0.288261E-03	0.693435E-02	0.253932E-02	0.806510E-03
	0.000000E+00	0.000000E+00	0.000000E+00	0.435672E+03	-0.144964E-01
25	0.267710E+00	0.280948E-03	0.715934E-02	0.261331E-02	0.830392E-03
	0.000000E+00	0.000000E+00	0.000000E+00	0.435588E+03	-0.145445E-01

26	0.287509E+00	0.273879E-03	0.738459E-02	0.268874E-02	0.854485E-03
	0.000000E+00	0.000000E+00	0.000000E+00	0.435507E+03	-0.146367E-01
27	0.307841E+00	0.267085E-03	0.761104E-02	0.276523E-02	0.878752E-03
	0.000000E+00	0.000000E+00	0.000000E+00	0.435427E+03	-0.147443E-01
28	0.328698E+00	0.260551E-03	0.783843E-02	0.284269E-02	0.903194E-03
	0.000000E+00	0.000000E+00	0.000000E+00	0.435349E+03	-0.148422E-01
29	0.350070E+00	0.254176E-03	0.806708E-02	0.292135E-02	0.927858E-03
	0.000000E+00	0.000000E+00	0.000000E+00	0.435272E+03	-0.148569E-01
30	0.371952E+00	0.247719E-03	0.829838E-02	0.300203E-02	0.952871E-03
	0.000000E+00	0.000000E+00	0.000000E+00	0.435197E+03	-0.146227E-01
31	0.394334E+00	0.240749E-03	0.853478E-02	0.308644E-02	0.978486E-03
	0.000000E+00	0.000000E+00	0.000000E+00	0.435126E+03	-0.138521E-01
32	0.417210E+00	0.232856E-03	0.877912E-02	0.317678E-02	0.100505E-02
	0.000000E+00	0.000000E+00	0.000000E+00	0.435062E+03	-0.123398E-01
33	0.440574E+00	0.224178E-03	0.903265E-02	0.327404E-02	0.103282E-02
	0.000000E+00	0.000000E+00	0.000000E+00	0.435006E+03	-0.103677E-01
34	0.464419E+00	0.216113E-03	0.929317E-02	0.337450E-02	0.106154E-02
	0.000000E+00	0.000000E+00	0.000000E+00	0.434959E+03	-0.909932E-02
35	0.488738E+00	0.211817E-03	0.954539E-02	0.346570E-02	0.108994E-02
	0.000000E+00	0.000000E+00	0.000000E+00	0.434909E+03	-0.107338E-01
36	0.513524E+00	0.215325E-03	0.976756E-02	0.352770E-02	0.111567E-02
	0.000000E+00	0.000000E+00	0.000000E+00	0.434839E+03	-0.181953E-01
37	0.538772E+00	0.227689E-03	0.994758E-02	0.354934E-02	0.113653E-02
	0.000000E+00	0.000000E+00	0.000000E+00	0.434723E+03	-0.331862E-01
38	0.564476E+00	0.240595E-03	0.101185E-01	0.355615E-02	0.115374E-02
	0.000000E+00	0.000000E+00	0.000000E+00	0.434554E+03	-0.481426E-01
39	0.590632E+00	0.233491E-03	0.103707E-01	0.362707E-02	0.117656E-02
	0.000000E+00	0.000000E+00	0.000000E+00	0.434386E+03	-0.374389E-01
40	0.617239E+00	0.173675E-03	0.109444E-01	0.394885E-02	0.123058E-02
	0.000000E+00	0.000000E+00	0.000000E+00	0.434385E+03	0.149628E-01
41	0.644292E+00	0.000000E+00	0.000000E+00	0.000000E+00	0.000000E+00
	0.000000E+00	0.000000E+00	0.000000E+00	0.000000E+00	0.000000E+00

7.5 Ellipsoid of revolution along windward plane of symmetry

i	x/c	cfx	blth	dsptx	thmox
	cfy	dspty	thmoy	twall	qw
1	0.400000E-02	0.000000E+00	0.000000E+00	0.000000E+00	0.000000E+00
	0.000000E+00	0.000000E+00	0.000000E+00	0.000000E+00	0.000000E+00
2	0.450000E-02	0.762597E-01	0.115106E-02	0.294283E-03	0.130723E-03
	0.000000E+00	0.000000E+00	0.000000E+00	0.520259E+03	-0.274508E-02
3	0.500000E-02	0.728950E-01	0.106555E-02	0.273060E-03	0.120332E-03
	0.000000E+00	0.000000E+00	0.000000E+00	0.520259E+03	-0.335102E-02
4	0.550000E-02	0.680647E-01	0.101057E-02	0.264054E-03	0.115054E-03
	0.000000E+00	0.000000E+00	0.000000E+00	0.520258E+03	-0.377599E-02
5	0.600000E-02	0.634669E-01	0.984121E-03	0.260747E-03	0.112725E-03
	0.000000E+00	0.000000E+00	0.000000E+00	0.520258E+03	-0.414369E-02
6	0.800000E-02	0.502922E-01	0.951446E-03	0.260638E-03	0.111134E-03
	0.000000E+00	0.000000E+00	0.000000E+00	0.520256E+03	-0.535532E-02
7	0.100000E-01	0.420724E-01	0.965137E-03	0.267585E-03	0.113716E-03
	0.000000E+00	0.000000E+00	0.000000E+00	0.520255E+03	-0.624270E-02
8	0.120000E-01	0.364407E-01	0.995366E-03	0.276117E-03	0.117206E-03
	0.000000E+00	0.000000E+00	0.000000E+00	0.520254E+03	-0.687253E-02
9	0.140000E-01	0.323392E-01	0.102208E-02	0.284682E-03	0.120716E-03
	0.000000E+00	0.000000E+00	0.000000E+00	0.520253E+03	-0.731235E-02
10	0.160000E-01	0.292091E-01	0.105039E-02	0.292961E-03	0.124077E-03
	0.000000E+00	0.000000E+00	0.000000E+00	0.520252E+03	-0.760958E-02
11	0.180000E-01	0.267302E-01	0.107384E-02	0.300960E-03	0.127294E-03
	0.000000E+00	0.000000E+00	0.000000E+00	0.520251E+03	-0.779689E-02
12	0.200000E-01	0.247096E-01	0.110036E-02	0.308734E-03	0.130398E-03
	0.000000E+00	0.000000E+00	0.000000E+00	0.520250E+03	-0.789926E-02
13	0.220000E-01	0.230253E-01	0.112447E-02	0.316328E-03	0.133413E-03
	0.000000E+00	0.000000E+00	0.000000E+00	0.520249E+03	-0.793640E-02
14	0.240000E-01	0.215956E-01	0.114627E-02	0.323768E-03	0.136357E-03
	0.000000E+00	0.000000E+00	0.000000E+00	0.520248E+03	-0.792337E-02
15	0.260000E-01	0.203640E-01	0.116935E-02	0.331073E-03	0.139239E-03
	0.000000E+00	0.000000E+00	0.000000E+00	0.520247E+03	-0.787136E-02
16	0.280000E-01	0.192900E-01	0.119281E-02	0.338258E-03	0.142065E-03
	0.000000E+00	0.000000E+00	0.000000E+00	0.520246E+03	-0.778976E-02
17	0.300000E-01	0.183441E-01	0.121460E-02	0.345326E-03	0.144841E-03
	0.000000E+00	0.000000E+00	0.000000E+00	0.520245E+03	-0.768674E-02
18	0.320000E-01	0.175036E-01	0.123509E-02	0.352284E-03	0.147568E-03
	0.000000E+00	0.000000E+00	0.000000E+00	0.520244E+03	-0.756745E-02
19	0.340000E-01	0.167511E-01	0.125490E-02	0.359137E-03	0.150251E-03
	0.000000E+00	0.000000E+00	0.000000E+00	0.520244E+03	-0.743644E-02
20	0.360000E-01	0.161442E-01	0.127630E-02	0.365285E-03	0.152765E-03
	0.000000E+00	0.000000E+00	0.000000E+00	0.520243E+03	-0.750395E-02

7.6 Ellipsoid of revolution along leeward plane of symmetry

i	x/c	cfx	blth	dsptx	thmox
	cfy	dspty	thmoy	twall	qw
1	0.400000E-02	0.000000E+00	0.000000E+00	0.000000E+00	0.000000E+00
	0.000000E+00	0.000000E+00	0.000000E+00	0.000000E+00	0.000000E+00
2	0.450000E-02	0.321218E-01	0.784167E-03	0.217507E-03	0.918193E-04
	0.000000E+00	0.000000E+00	0.000000E+00	0.520253E+03	-0.876983E-02
3	0.500000E-02	0.292291E-01	0.821668E-03	0.231428E-03	0.970987E-04
	0.000000E+00	0.000000E+00	0.000000E+00	0.520250E+03	-0.839545E-02
4	0.550000E-02	0.274982E-01	0.850371E-03	0.240952E-03	0.101107E-03
	0.000000E+00	0.000000E+00	0.000000E+00	0.520248E+03	-0.850976E-02
5	0.600000E-02	0.261933E-01	0.875234E-03	0.248208E-03	0.104313E-03
	0.000000E+00	0.000000E+00	0.000000E+00	0.520247E+03	-0.864227E-02
6	0.800000E-02	0.225559E-01	0.945531E-03	0.268665E-03	0.113260E-03
	0.000000E+00	0.000000E+00	0.000000E+00	0.520243E+03	-0.905064E-02
7	0.100000E-01	0.201938E-01	0.996408E-03	0.283017E-03	0.119414E-03
	0.000000E+00	0.000000E+00	0.000000E+00	0.520241E+03	-0.926889E-02
8	0.120000E-01	0.184437E-01	0.103881E-02	0.294983E-03	0.124414E-03
	0.000000E+00	0.000000E+00	0.000000E+00	0.520239E+03	-0.929852E-02
9	0.140000E-01	0.170506E-01	0.107739E-02	0.306002E-03	0.128910E-03
	0.000000E+00	0.000000E+00	0.000000E+00	0.520238E+03	-0.918767E-02
10	0.160000E-01	0.158981E-01	0.111213E-02	0.316576E-03	0.133153E-03
	0.000000E+00	0.000000E+00	0.000000E+00	0.520236E+03	-0.898171E-02
11	0.180000E-01	0.149219E-01	0.114456E-02	0.326881E-03	0.137243E-03
	0.000000E+00	0.000000E+00	0.000000E+00	0.520235E+03	-0.871521E-02
12	0.200000E-01	0.140812E-01	0.117782E-02	0.336977E-03	0.141224E-03
	0.000000E+00	0.000000E+00	0.000000E+00	0.520233E+03	-0.841304E-02
13	0.220000E-01	0.133477E-01	0.120929E-02	0.346896E-03	0.145116E-03
	0.000000E+00	0.000000E+00	0.000000E+00	0.520232E+03	-0.809191E-02
14	0.240000E-01	0.127009E-01	0.123931E-02	0.356655E-03	0.148931E-03
	0.000000E+00	0.000000E+00	0.000000E+00	0.520231E+03	-0.776332E-02
15	0.260000E-01	0.121253E-01	0.126807E-02	0.366265E-03	0.152677E-03
	0.000000E+00	0.000000E+00	0.000000E+00	0.520230E+03	-0.743518E-02
16	0.280000E-01	0.116091E-01	0.129757E-02	0.375739E-03	0.156361E-03
	0.000000E+00	0.000000E+00	0.000000E+00	0.520229E+03	-0.711269E-02
17	0.300000E-01	0.111429E-01	0.132689E-02	0.385087E-03	0.159989E-03
	0.000000E+00	0.000000E+00	0.000000E+00	0.520229E+03	-0.679867E-02
18	0.320000E-01	0.107194E-01	0.135515E-02	0.394315E-03	0.163563E-03
	0.000000E+00	0.000000E+00	0.000000E+00	0.520228E+03	-0.649590E-02
19	0.340000E-01	0.103326E-01	0.138247E-02	0.403430E-03	0.167088E-03
	0.000000E+00	0.000000E+00	0.000000E+00	0.520227E+03	-0.620523E-02
20	0.360000E-01	0.100190E-01	0.140831E-02	0.411904E-03	0.170474E-03
	0.000000E+00	0.000000E+00	0.000000E+00	0.520227E+03	-0.612996E-02

7.7 Infinite swept cylider along the leading-edge attachment line

i	x/c cfy	cfx dspty	blth thmoy	dsptx twall	thmox qw
1	0.100000E-01	0.227267E-02	0.212016E-02	0.663990E-03	0.260441E-03
	0.000000E+00	0.000000E+00	0.000000E+00	0.521493E+03	-0.888370E-08
2	0.200000E-01	0.227267E-02	0.212016E-02	0.663990E-03	0.260441E-03
	0.000000E+00	0.000000E+00	0.000000E+00	0.521493E+03	0.222093E-07
3	0.300000E-01	0.227267E-02	0.212016E-02	0.663990E-03	0.260441E-03
	0.000000E+00	0.000000E+00	0.000000E+00	0.521493E+03	0.888370E-08
4	0.400000E-01	0.227267E-02	0.212016E-02	0.663990E-03	0.260441E-03
	0.000000E+00	0.000000E+00	0.000000E+00	0.521493E+03	0.177674E-07

7.8 Swept-back wing

i	x/c cfy	cfx dspty	blth thmoy	dsptx twall	thmox qw
1	0.121900E-03	0.648001E-02	0.479884E-03	0.152013E-03	0.585255E-04
	0.000000E+00	0.000000E+00	0.000000E+00	0.483938E+03	-0.351638E-04
2	0.864300E-03	0.619005E-02	0.494110E-03	0.160975E-03	0.617156E-04
	0.236945E-01	0.103222E-03	0.445461E-04	0.483524E+03	-0.729616E-01
3	0.160670E-02	0.594413E-02	0.508753E-03	0.170342E-03	0.649066E-04
	0.150014E-01	0.110595E-03	0.471944E-04	0.483074E+03	-0.132228E+00
4	0.234910E-02	0.573117E-02	0.524839E-03	0.179489E-03	0.679731E-04
	0.114673E-01	0.117804E-03	0.497426E-04	0.482617E+03	-0.171745E+00
5	0.309160E-02	0.551083E-02	0.542727E-03	0.189243E-03	0.712194E-04
	0.940938E-02	0.125769E-03	0.525154E-04	0.482191E+03	-0.184495E+00
6	0.383400E-02	0.531356E-02	0.563707E-03	0.198824E-03	0.744109E-04
	0.809523E-02	0.133637E-03	0.552665E-04	0.481805E+03	-0.187440E+00
7	0.606120E-02	0.488254E-02	0.617817E-03	0.224182E-03	0.827832E-04
	0.601189E-02	0.153936E-03	0.623367E-04	0.480814E+03	-0.188232E+00
8	0.828850E-02	0.456890E-02	0.670657E-03	0.247221E-03	0.902216E-04
	0.490637E-02	0.172218E-03	0.685211E-04	0.479963E+03	-0.178061E+00
9	0.105158E-01	0.428030E-02	0.726227E-03	0.270905E-03	0.977276E-04
	0.411003E-02	0.191890E-03	0.749336E-04	0.479238E+03	-0.147379E+00
10	0.127431E-01	0.402506E-02	0.780888E-03	0.293860E-03	0.105010E-03
	0.355803E-02	0.211491E-03	0.813126E-04	0.478655E+03	-0.119317E+00
11	0.149703E-01	0.384535E-02	0.829711E-03	0.314394E-03	0.111547E-03
	0.321903E-02	0.228496E-03	0.869714E-04	0.478138E+03	-0.111213E+00
12	0.171976E-01	0.370054E-02	0.874538E-03	0.333489E-03	0.117558E-03
	0.296348E-02	0.243966E-03	0.920822E-04	0.477658E+03	-0.104321E+00
13	0.194249E-01	0.355980E-02	0.918225E-03	0.352891E-03	0.123488E-03
	0.271542E-02	0.260184E-03	0.971654E-04	0.477223E+03	-0.895337E-01
14	0.246218E-01	0.324529E-02	0.102787E-02	0.397694E-03	0.137203E-03
	0.224944E-02	0.299421E-03	0.109347E-03	0.476467E+03	-0.578648E-01
15	0.298188E-01	0.303573E-02	0.112438E-02	0.437282E-03	0.149344E-03
	0.198989E-02	0.333533E-03	0.120144E-03	0.475862E+03	-0.489781E-01
16	0.350158E-01	0.288465E-02	0.121123E-02	0.473053E-03	0.160250E-03
	0.181834E-02	0.363505E-03	0.129691E-03	0.475315E+03	-0.443263E-01
17	0.402127E-01	0.273238E-02	0.130095E-02	0.510916E-03	0.171375E-03
	0.163004E-02	0.396591E-03	0.139528E-03	0.474844E+03	-0.330507E-01
18	0.454097E-01	0.257720E-02	0.139031E-02	0.548686E-03	0.182438E-03
	0.145231E-02	0.431381E-03	0.149611E-03	0.474499E+03	-0.222588E-01
19	0.506067E-01	0.353363E-02	0.140956E-02	0.534318E-03	0.187133E-03
	0.183446E-02	0.418741E-03	0.151633E-03	0.474589E+03	-0.111386E+00
20	0.558036E-01	0.393445E-02	0.143290E-02	0.525487E-03	0.189579E-03
	0.191825E-02	0.413101E-03	0.151966E-03	0.474764E+03	-0.123242E+00
21	0.669400E-01	0.432097E-02	0.150220E-02	0.523764E-03	0.194247E-03
	0.189381E-02	0.419399E-03	0.154702E-03	0.475206E+03	-0.121451E+00
22	0.780763E-01	0.450060E-02	0.157116E-02	0.530200E-03	0.198671E-03
	0.182969E-02	0.433497E-03	0.159095E-03	0.475667E+03	-0.116441E+00
23	0.892127E-01	0.462176E-02	0.163121E-02	0.538715E-03	0.202695E-03
	0.177914E-02	0.448325E-03	0.163785E-03	0.476083E+03	-0.114545E+00
24	0.100349E+00	0.471450E-02	0.169362E-02	0.548166E-03	0.206462E-03
	0.173047E-02	0.463284E-03	0.168500E-03	0.476451E+03	-0.111563E+00
25	0.111485E+00	0.478874E-02	0.174453E-02	0.556812E-03	0.209783E-03
	0.168803E-02	0.476993E-03	0.172948E-03	0.476799E+03	-0.108508E+00

26	0.122622E+00	0.487009E-02	0.179429E-02	0.564001E-03	0.212525E-03
	0.166666E-02	0.488101E-03	0.176765E-03	0.477103E+03	-0.109966E+00
27	0.133758E+00	0.495858E-02	0.183724E-02	0.570528E-03	0.214842E-03
	0.165488E-02	0.497413E-03	0.179963E-03	0.477356E+03	-0.113198E+00
28	0.144894E+00	0.504627E-02	0.187373E-02	0.576336E-03	0.216784E-03
	0.164594E-02	0.505215E-03	0.182584E-03	0.477570E+03	-0.116654E+00
29	0.165682E+00	0.522451E-02	0.193499E-02	0.586482E-03	0.219823E-03
	0.163740E-02	0.517367E-03	0.186338E-03	0.477881E+03	-0.125483E+00
30	0.186470E+00	0.541044E-02	0.199060E-02	0.596669E-03	0.222523E-03
	0.162572E-02	0.528528E-03	0.189273E-03	0.478120E+03	-0.133606E+00
31	0.207258E+00	0.559782E-02	0.204009E-02	0.606964E-03	0.225085E-03
	0.160746E-02	0.539779E-03	0.191920E-03	0.478334E+03	-0.139685E+00
32	0.228046E+00	0.578921E-02	0.208417E-02	0.616575E-03	0.227413E-03
	0.158923E-02	0.550490E-03	0.194349E-03	0.478548E+03	-0.145350E+00
33	0.248834E+00	0.599498E-02	0.212460E-02	0.625776E-03	0.229560E-03
	0.157469E-02	0.560698E-03	0.196592E-03	0.478753E+03	-0.152037E+00
34	0.269622E+00	0.621346E-02	0.216111E-02	0.634319E-03	0.231463E-03
	0.156244E-02	0.570148E-03	0.198581E-03	0.478949E+03	-0.159236E+00
35	0.290409E+00	0.644903E-02	0.219391E-02	0.642279E-03	0.233141E-03
	0.155357E-02	0.578784E-03	0.200293E-03	0.479133E+03	-0.167645E+00
36	0.311197E+00	0.670440E-02	0.222294E-02	0.649792E-03	0.234626E-03
	0.154753E-02	0.586686E-03	0.201721E-03	0.479302E+03	-0.177352E+00
37	0.331985E+00	0.698122E-02	0.224805E-02	0.657027E-03	0.235965E-03
	0.154312E-02	0.594063E-03	0.202905E-03	0.479456E+03	-0.188119E+00
38	0.352773E+00	0.394345E-02	0.254270E-02	0.837342E-03	0.272363E-03
	0.860034E-03	0.767111E-03	0.240279E-03	0.478408E+03	-0.670153E-02
39	0.378758E+00	0.313802E-02	0.279693E-02	0.994587E-03	0.306064E-03
	0.676153E-03	0.911435E-03	0.273455E-03	0.476932E+03	-0.559573E-02
40	0.404743E+00	0.285078E-02	0.302247E-02	0.112313E-02	0.336483E-03
	0.600065E-03	0.102506E-02	0.302347E-03	0.475778E+03	-0.507192E-02
41	0.430727E+00	0.270359E-02	0.323873E-02	0.123934E-02	0.365323E-03
	0.549513E-03	0.112561E-02	0.328922E-03	0.474868E+03	-0.452597E-02
42	0.456712E+00	0.260168E-02	0.345275E-02	0.135522E-02	0.394160E-03
	0.498313E-03	0.122766E-02	0.354951E-03	0.474151E+03	-0.323506E-02
43	0.482697E+00	0.251322E-02	0.367205E-02	0.147118E-02	0.423057E-03
	0.442710E-03	0.133404E-02	0.380867E-03	0.473632E+03	-0.164004E-02
44	0.508682E+00	0.239502E-02	0.393646E-02	0.161111E-02	0.456416E-03
	0.365094E-03	0.147390E-02	0.410803E-03	0.473351E+03	0.642064E-03
45	0.523070E+00	0.232022E-02	0.407961E-02	0.169164E-02	0.475463E-03
	0.318873E-03	0.155986E-02	0.427664E-03	0.473302E+03	0.150493E-02
46	0.539121E+00	0.227911E-02	0.423750E-02	0.177448E-02	0.496192E-03
	0.285474E-03	0.164967E-02	0.446153E-03	0.473282E+03	0.151861E-02
47	0.569561E+00	0.226365E-02	0.451179E-02	0.191354E-02	0.532796E-03
	0.244581E-03	0.180120E-02	0.479014E-03	0.473267E+03	0.137205E-02
48	0.600000E+00	0.229420E-02	0.475976E-02	0.204084E-02	0.567603E-03
	0.215248E-03	0.194051E-02	0.510110E-03	0.473277E+03	0.128328E-02

References

[1] Aircraft Drag Prediction and Reduction, AGARD Report No. 723, July, 1985.

[2] Research in Natural Laminar Flow and Laminar-Flow Control, Compiled by Jerry N. Hefner and Frances E. Sabo, NASA CP-2487, Parts 1, 2, and 3, Proceedings of a Symposium held at Langley Research Center, March 16-19, 1987.

[3] Wie, Y. S., "A Three-Dimensional, Compressible, Boundary-Layer Method for General Fuselages," Volume I; Numerical Method, Volume II; User's Manual, NASA CR-4292, May 1990.

[4] Iyer, V., "Computation of Three-Dimensional Compressible Boundary Layers to Fourth-Order Accuracy on Wings and Fuselages," NASA CR-4269, Jan. 1990.

[5] Kaups, K. ,and Cebeci, T., " Compressible Laminar Boundary Layers with Suction on Swept and Tapered Wings," Journal of Aircraft, Vol. 14, No.7, July 1977, pp.661-667.

[6] Wie, Y. S., Collier, F. S. Jr., Wagner, R. D., Viken, J. K. and Pfenninger, W., "Design of A Hybrid Laminar Flow Control Nacelle," AIAA Paper No. 92-0400, Jan., 1992.

[7] Wie, Y. S. and Collier, F. S. Jr., "Instability of a Swept Leading-Edge Attachment-Line Boundary-Layer," To be presented at ASME Fluids Engineering Conference, June 20-23, 1993, Washington, D.C.

[8] Wie, Y. S. and Harris, J. E., "Numerical Solution of The Boundary-Layer Equations for A General Aviation Fuselage," Journal of Aircraft, Vol.28, No. 12, Dec. 1991. pp.861-868, see also AIAA Paper No. 90-0305, Jan, 1990.

[9] Cebeci, T., Kaups, K., and Ramsey, J., A., "A General Method for Calculating Three-Dimensional Compressible Laminar and Turbulent Boundary Layers on Arbitrary Wings," NASA CR-2777, Jan. 1977.

[10] Howarth, F. R. S., "The Boundary Layer in Three-Dimensional Flow, Part II: The Flow Near a Stagnation Point," Philosophical Magazine, Ser. 7, Vol. 42, No. 335, pp. 1433-1440, 1951.

[11] Blottner, F. G., "Computational Techniques for Boundary Layers, AGARD Lecture Series," No. 73, 1975.

[12] Flugge-Lotz, I., and Blottner, F. G., "Computation of the Compressible Laminar Boundary-Layer Flow Including Displacement-Thickness Interaction Using Finite-Difference Methods," AFOSR 2206, U.S. Air Force, Jan. 1962.

[13] Drela, M., "Two-Dimensional Transonic Aerodynamic Design and Analysis Using The Euler Equations," Ph. D. Dissertation, Massachusetts Institute of Technology, Dec. 1985.

[14] Harris, J. E., and Blanchard, D. K.,"Computer Program for Solving Laminar, Transitional, or Turbulent Compressible Boundary-Layer Equations for Two-Dimensional and Axisymmetric Flow," NASA TM 83207, Feb. 1982.

[15] Cebeci, T., Khattab, A. K., and Stewartson, K., "Three-Dimensional Laminar Boundary Layers and OK of Accessibility," Journal of Fluid Mechanics, Vol. 107, 1981, pp. 57-87.

[16] Collier, F. S. Jr., Bartlett, D. W., Wagner, R. D., Tat, V. V., and Anderson, B. T., "Correlation of Boundary-Layer Stability Analysis with Flight Transition Data," IUTAM Third Symposium on Laminar-Turbulent Transition, Toulouse, France, sept., 1989.

[17] Malik, Mujeeb R.,"e^{Malik}: A New Spatial Stability Analysis Program for Transition Prediction Using the e^N Method," High Technology Rept. HTC-8902, 1989.

[18] Malik, Mujeeb R.,"COSAL-A Black Box Compressible Stability Analysis Code for Transition Prediction in Three-Dimensional Boundary Layers," NASA CR-165925, 1982.

[19] Collier, F. S. Jr.,"Effect of Curvature on Three-Dimensional Boundary Layers. Ph. D. Dissertation," Virginia Polytechnic Institute and State University, May 1988.

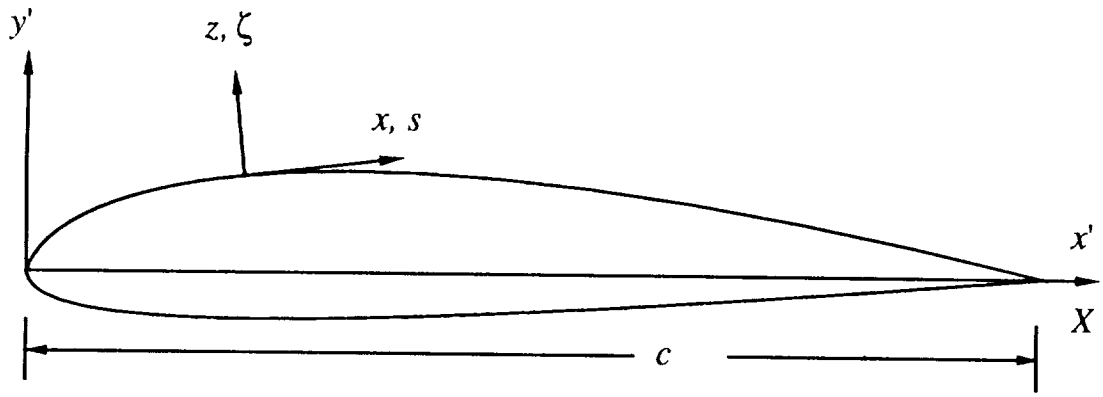

Two-Dimensional Flow

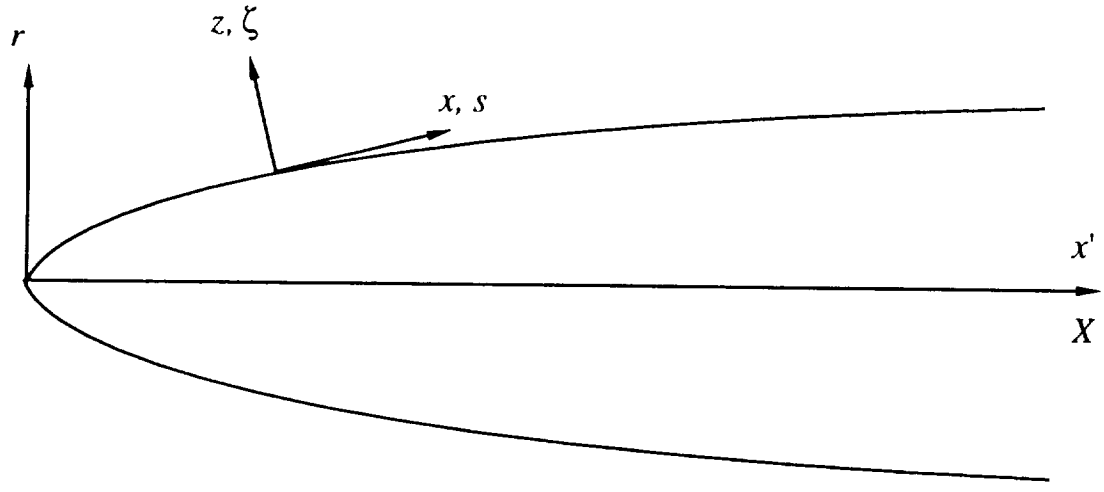

Axisymmetric Flow

Figure 1. Coordinate System for 2-D and Axisymmetric Flow

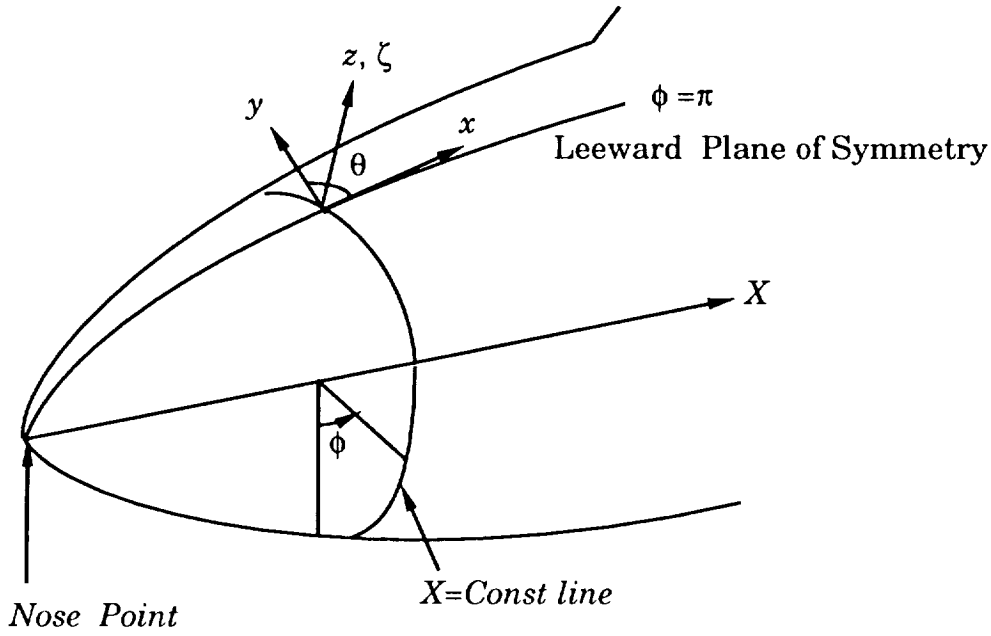

Flow Along Plane of Symmetry

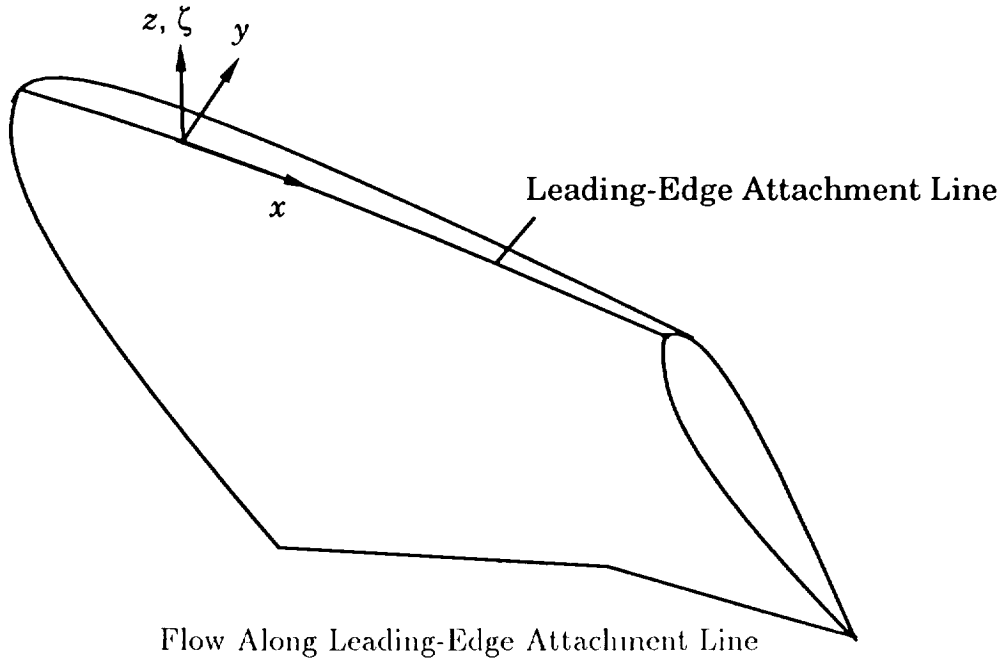

Flow Along Leading-Edge Attachment Line

Figure 2. Coordinate System for the Flow Along Plane of Symmetry and Along Leading-Edge Attachment Line

C-2

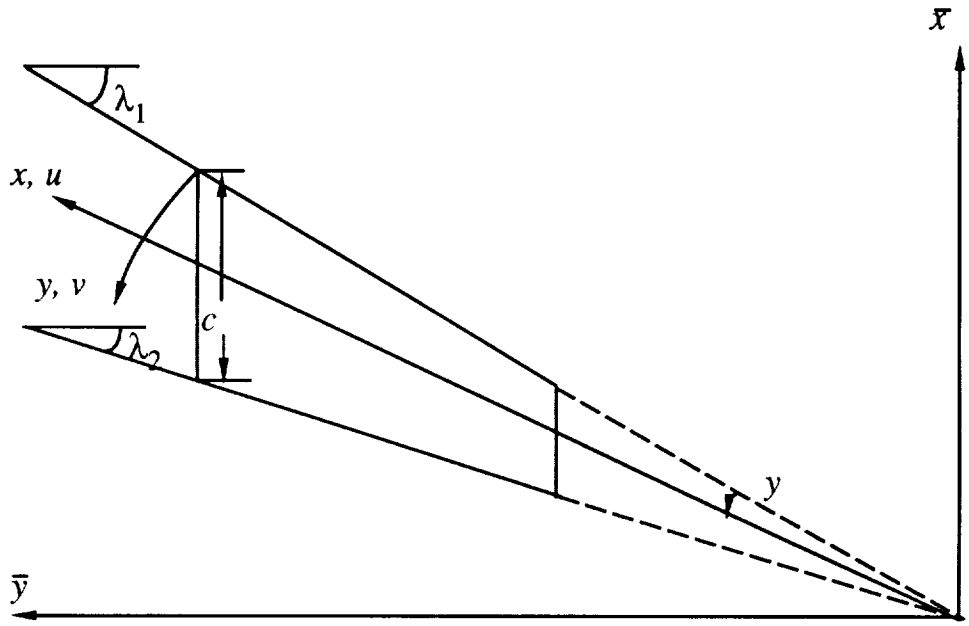

Figure 3. Coordinate System for the Swept-Back Wing Flow

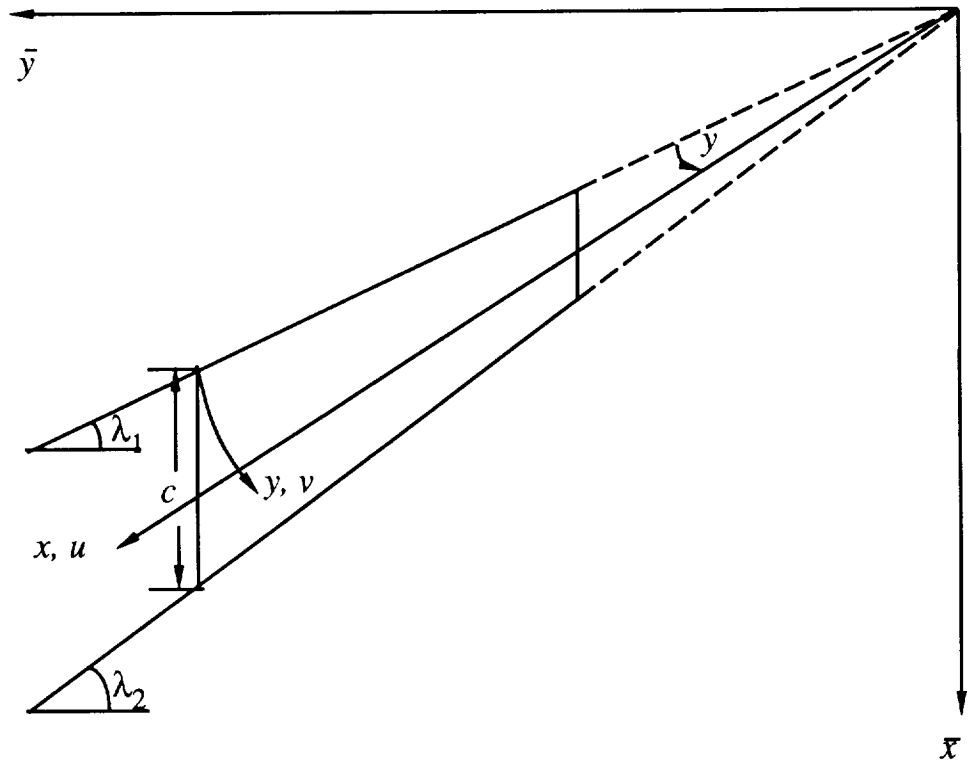

Figure 4. Coordinate System for the Swept-Forward Wing Flow

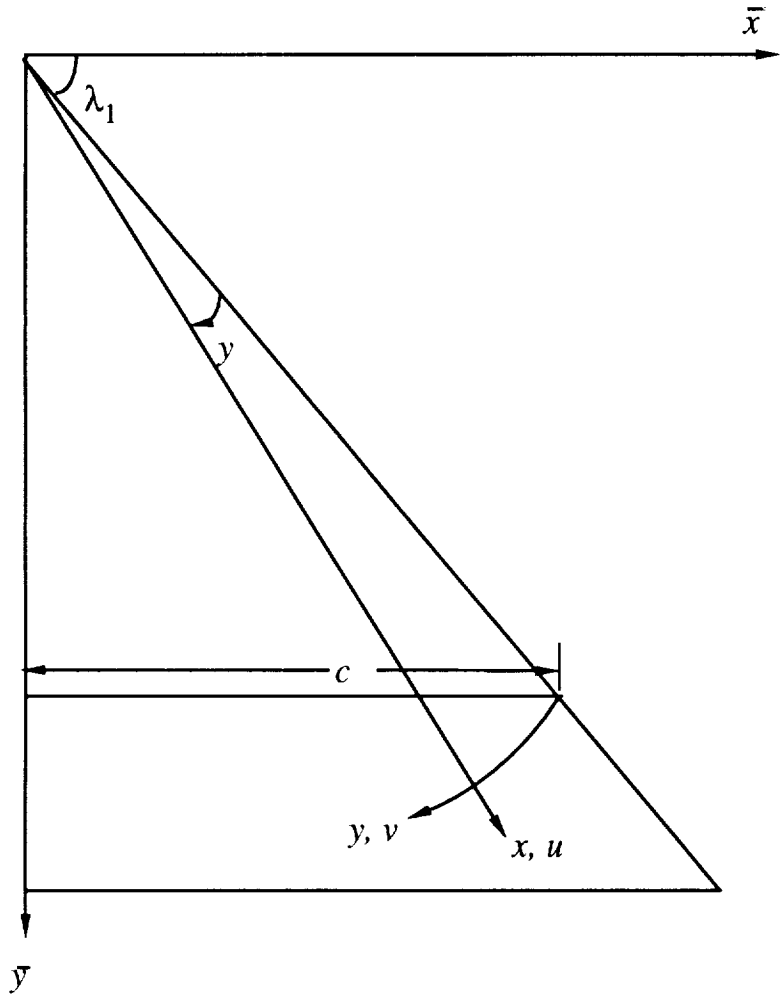

Figure 5. Coordinate System for the Delta Wing Flow

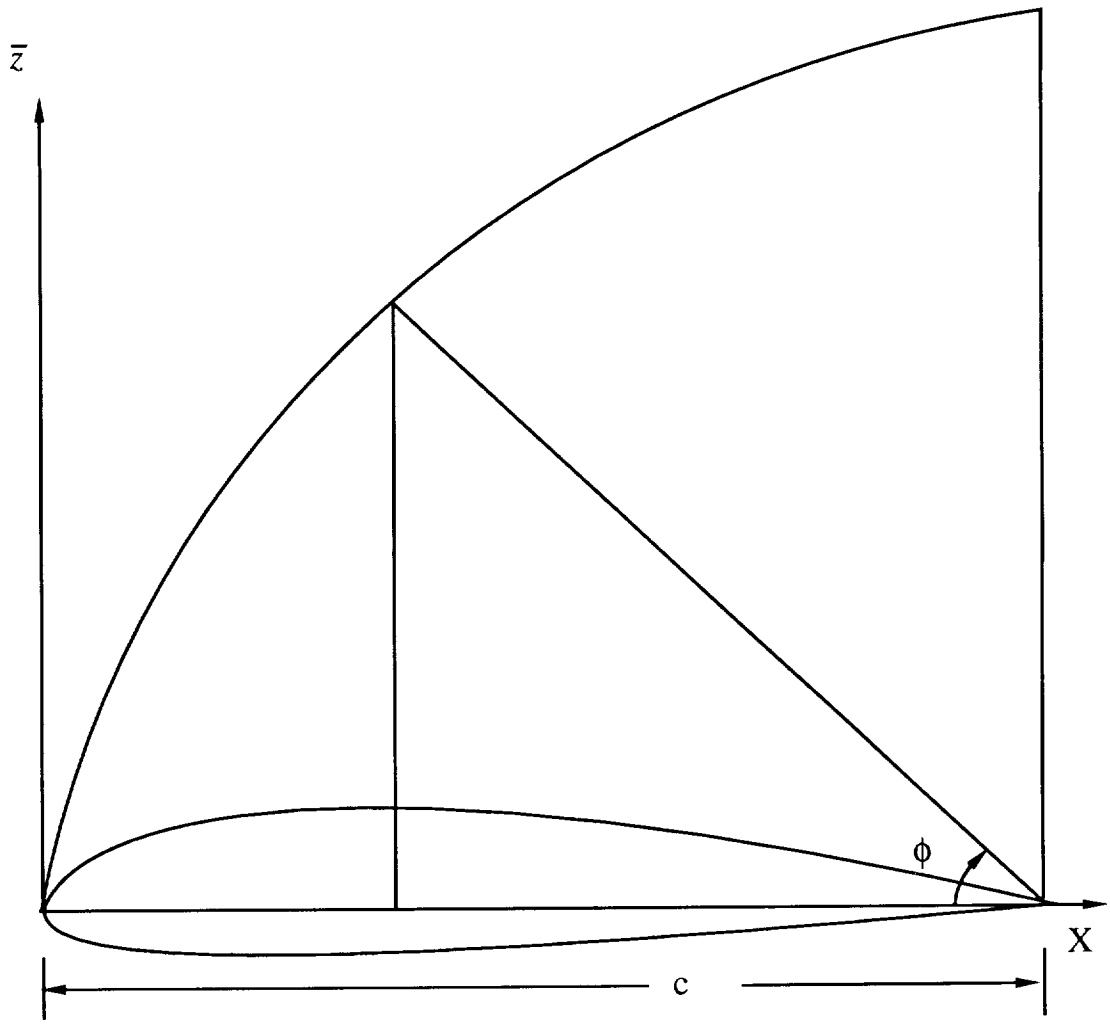

Figure 6. Airfoil Definition for Swept Wing Flow

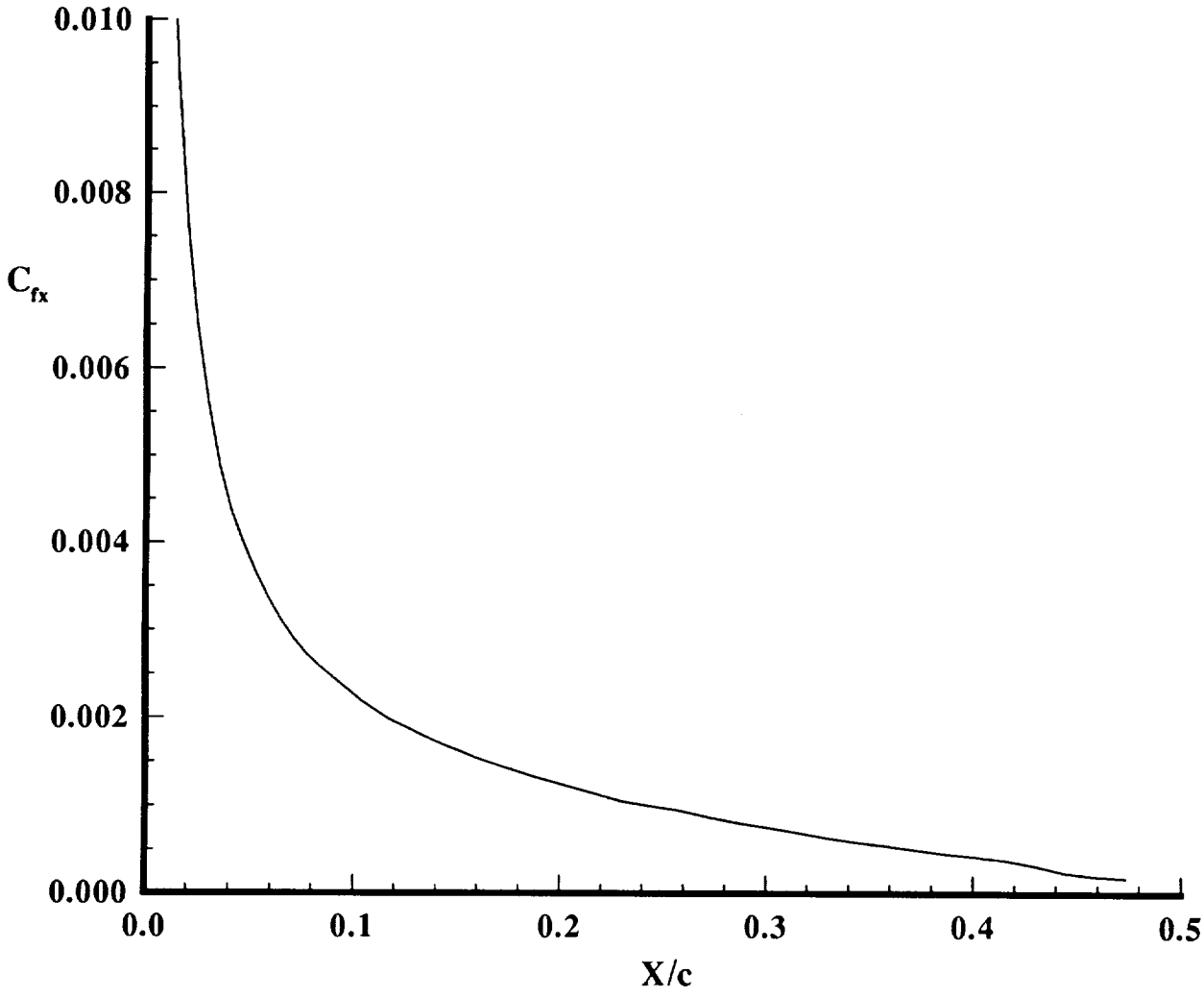

Figure 7. Skin Friction Coefficient (NACA 0012 Airfoil, $M_\infty = 0.5$, $\alpha = 0^o$)

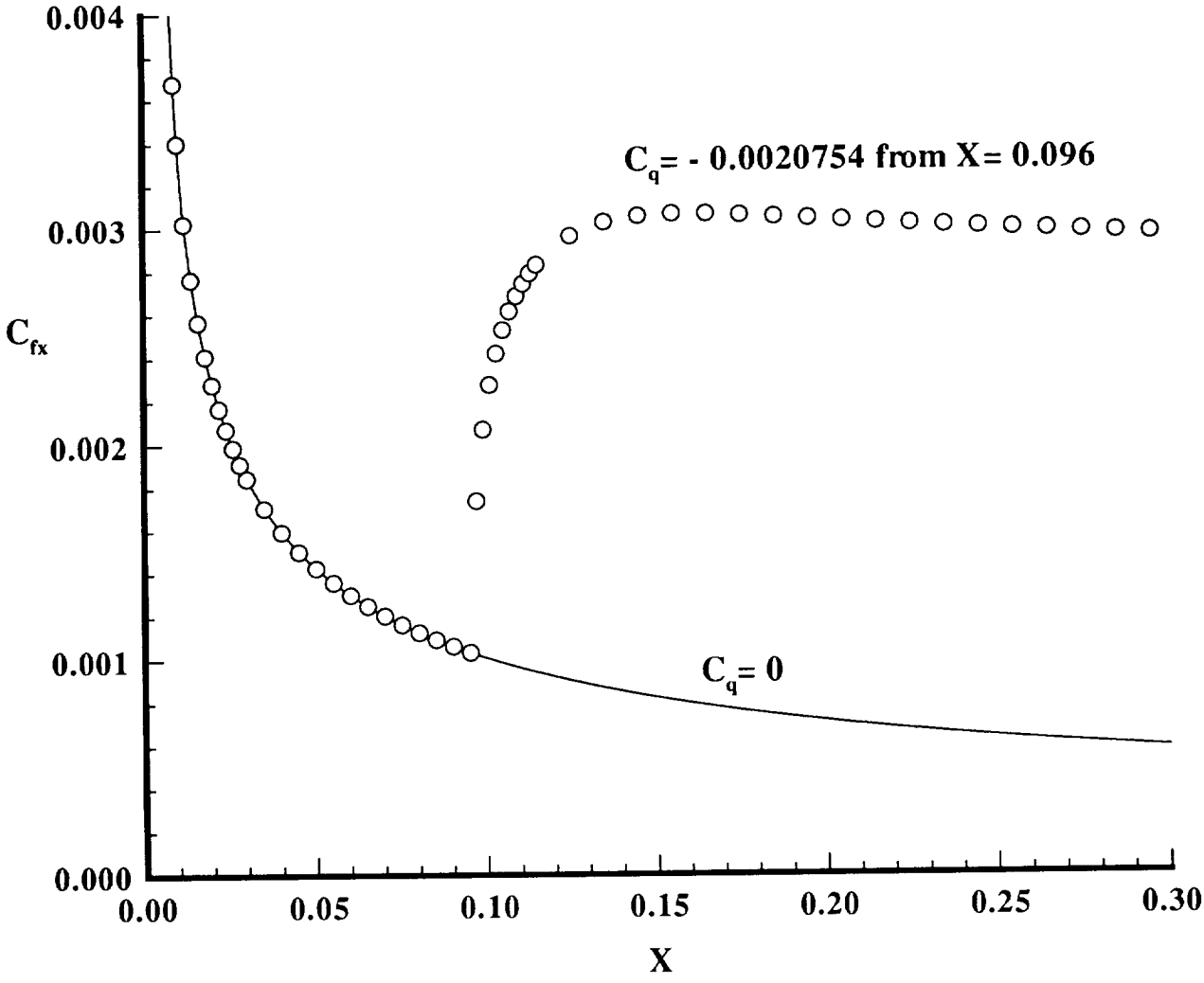

Figure 8. Skin Friction Coefficient (Hypersonic Cone, $M_\infty = 7.4$, $\alpha = 0°$)

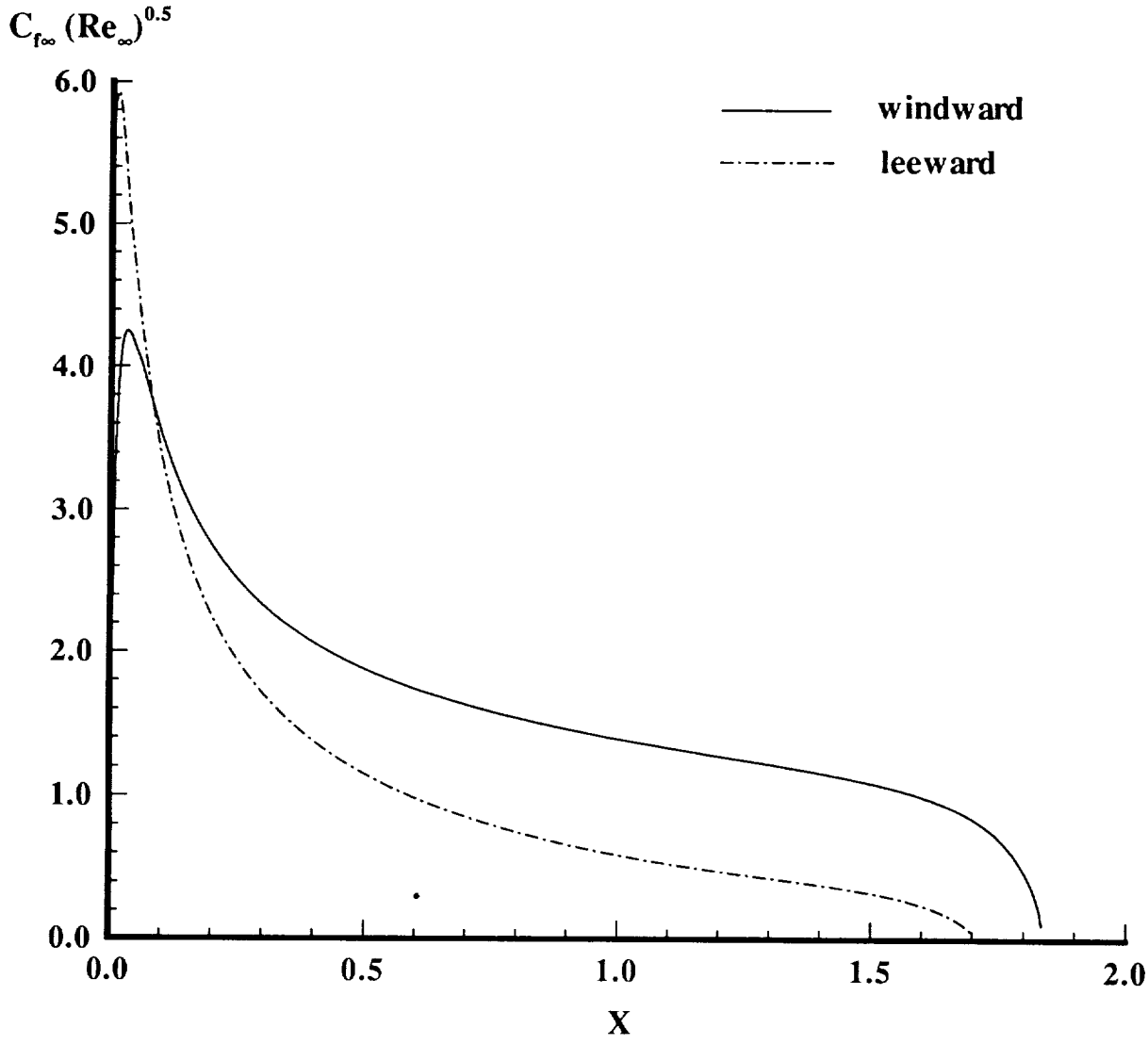

Figure 9. Skin Friction Coefficient (Ellipsoid of Revolution, $M_\infty = 0.05$, $\alpha = 6^o$)

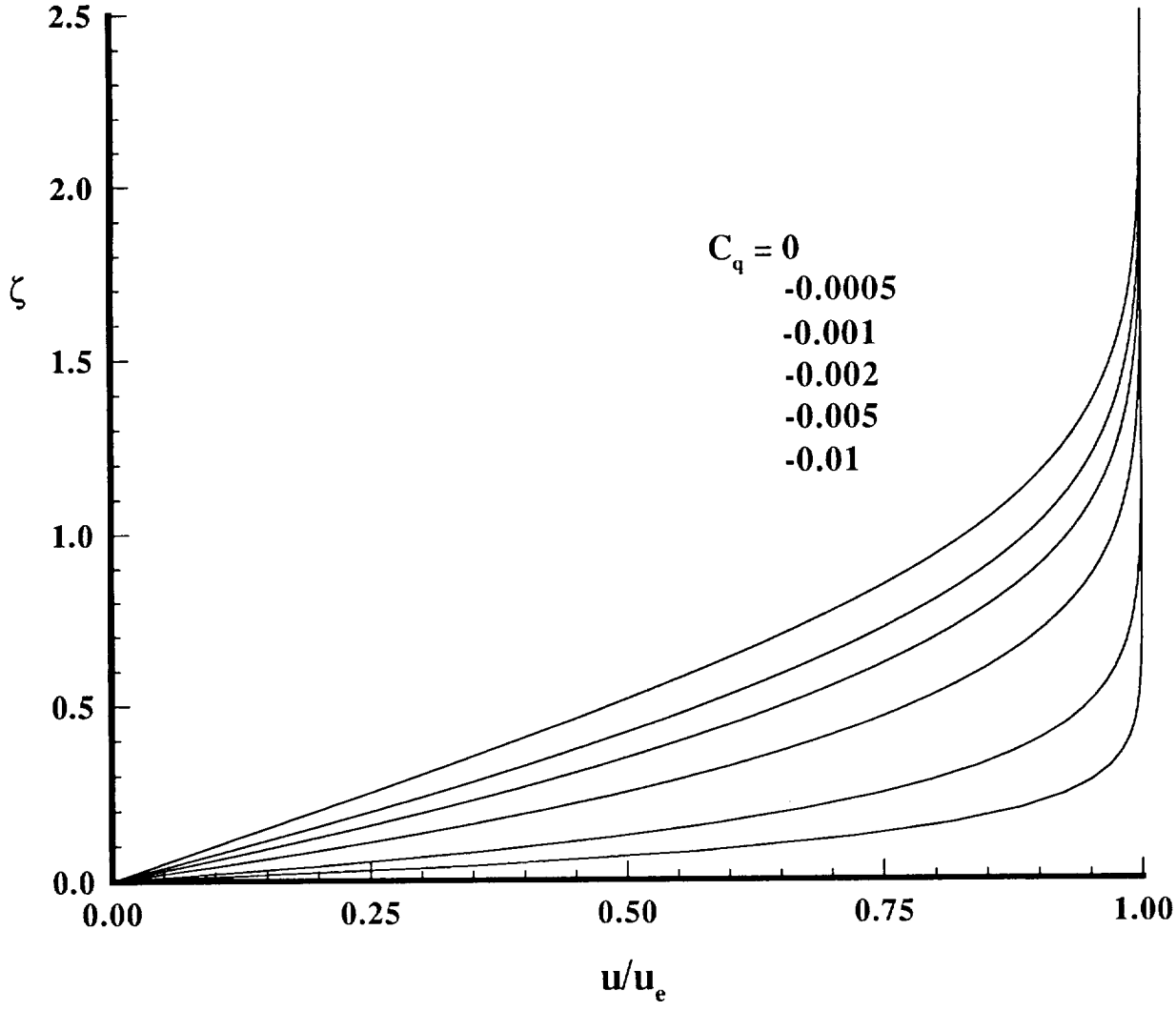

Figure 10. Velocity Profiles (Infinite Swept Cylinder, $M_\infty = 0.126675$, $\alpha = 0^o$)

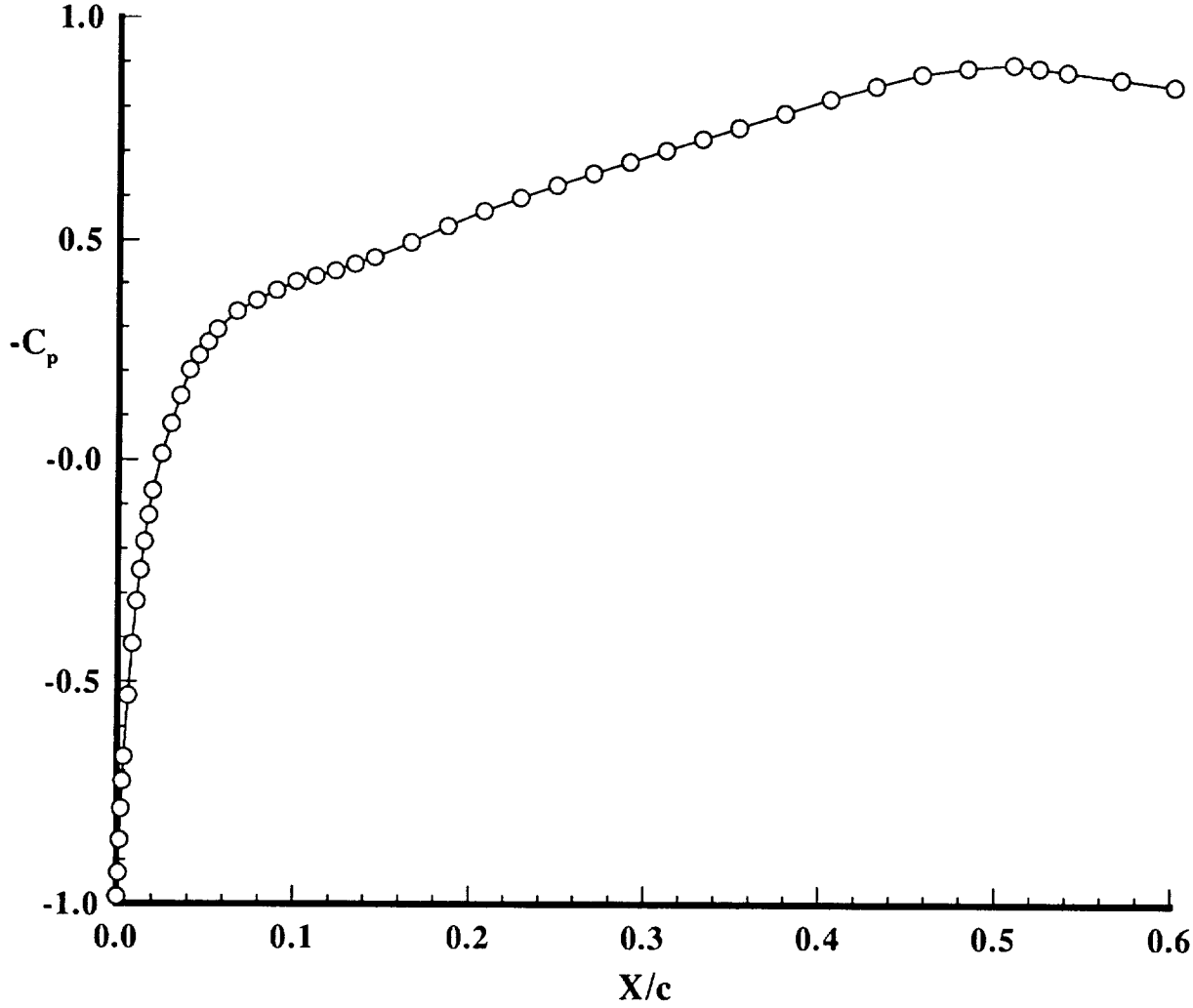

Figure 11. Pressure Distribution (Swept Wing, $M_\infty = 0.80$)

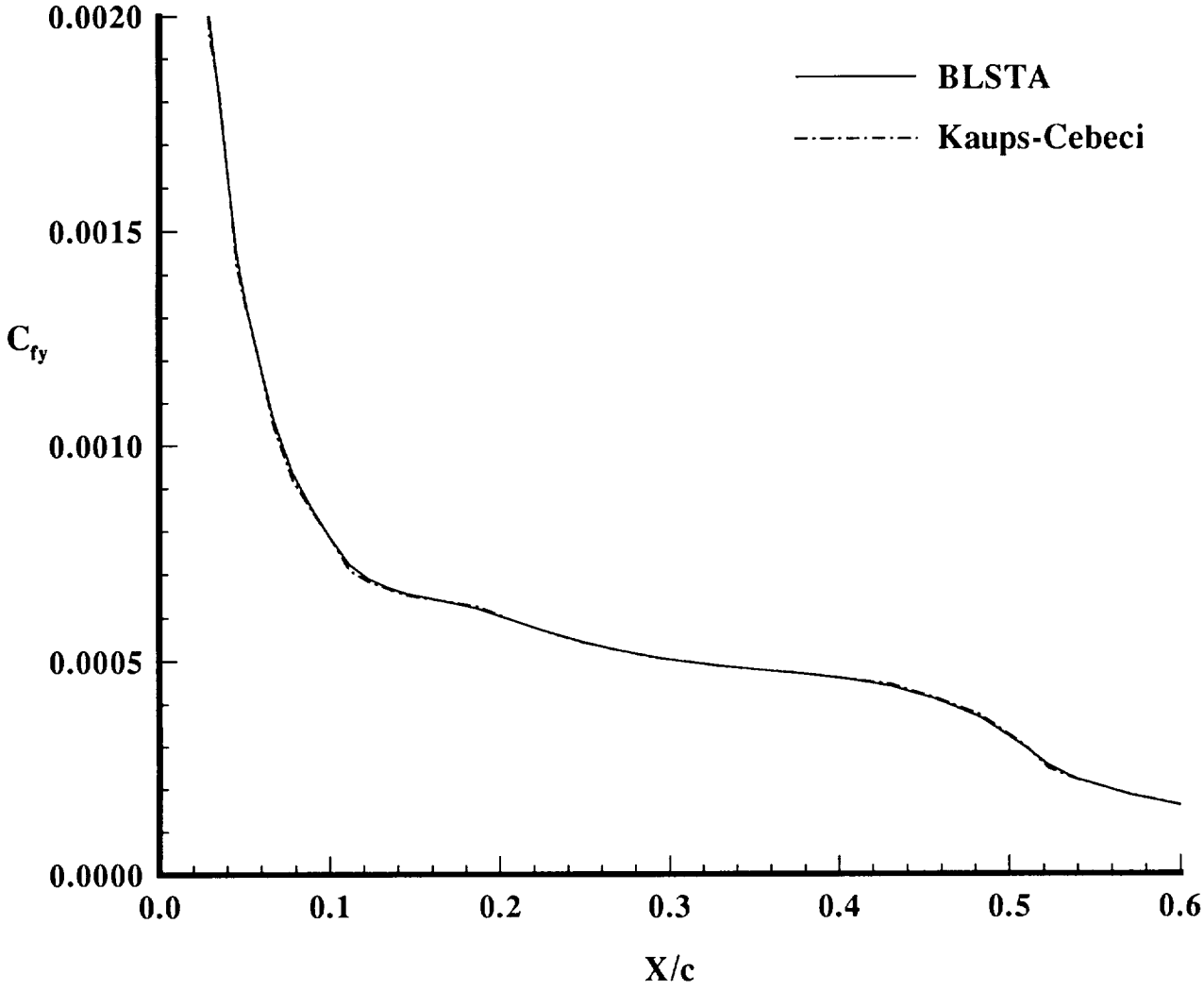

Figure 12. Skin Friction Coefficient (Swept Wing, $M_\infty = 0.80$, without suction)

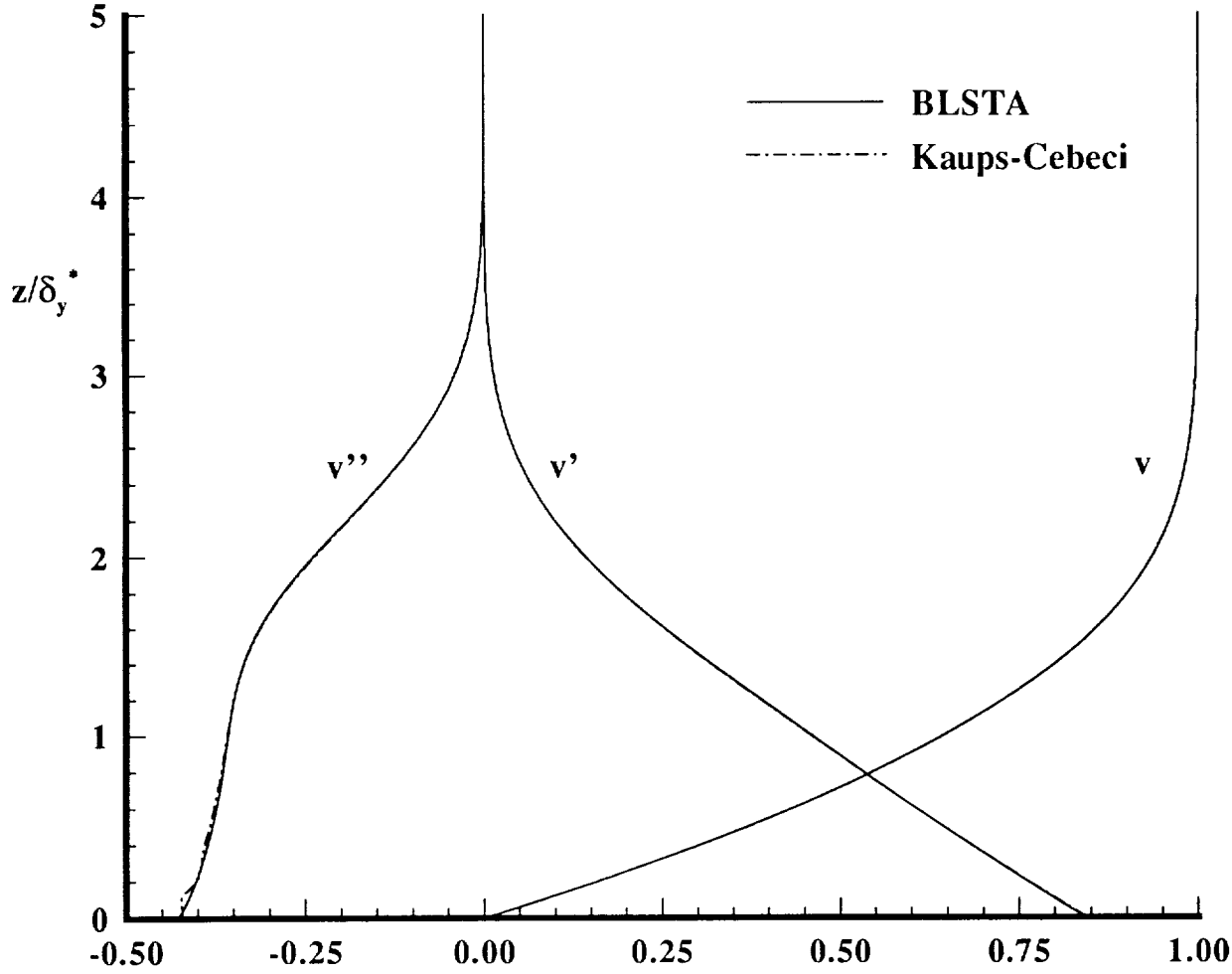

Figure 13. Velocity Profile and Its Normal Derivatives

(Swept Wing, $M_\infty = 0.80$, without suction)

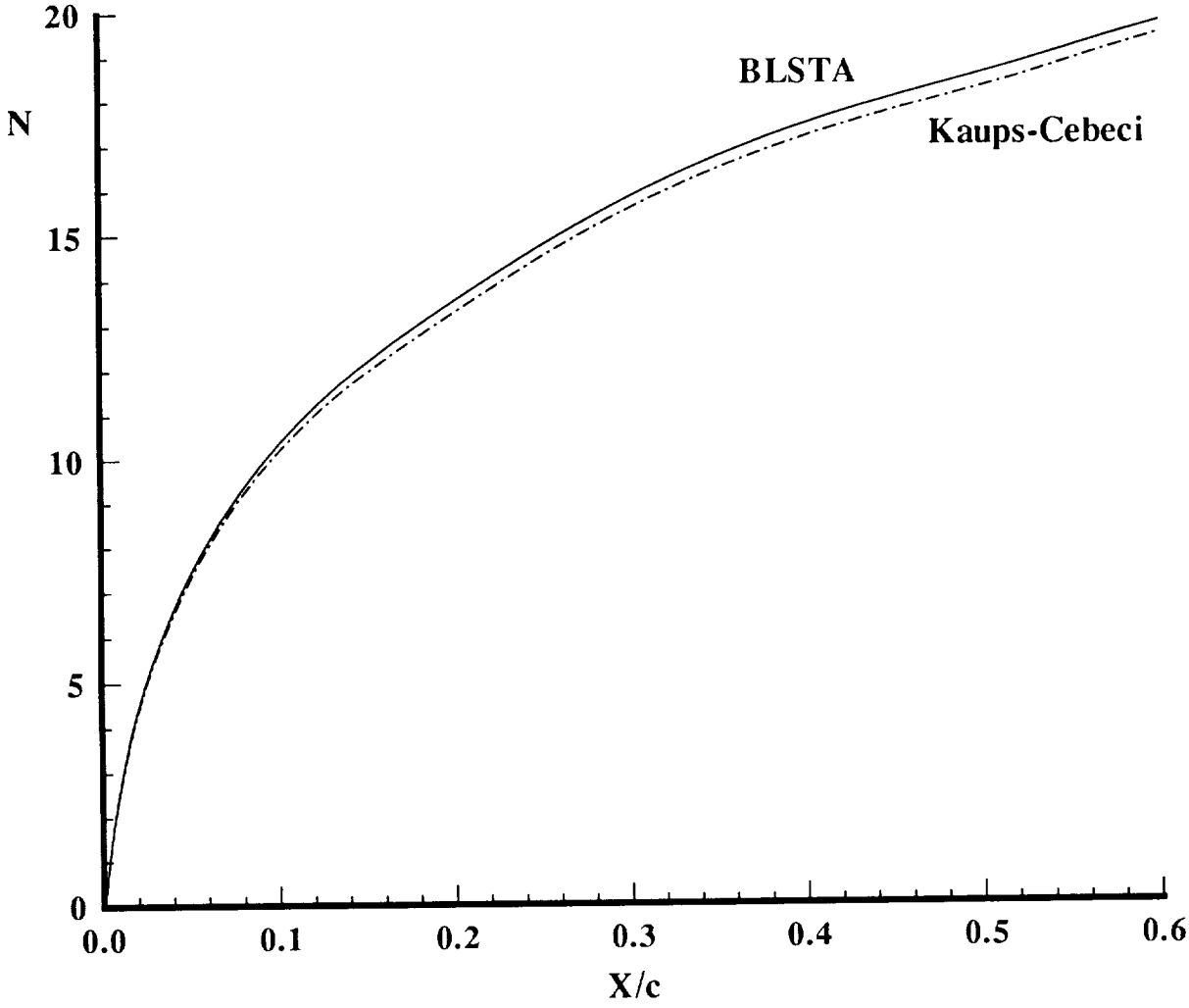

Figure 14. Comparison of Calculated N factor (Freq=3000 Hz)

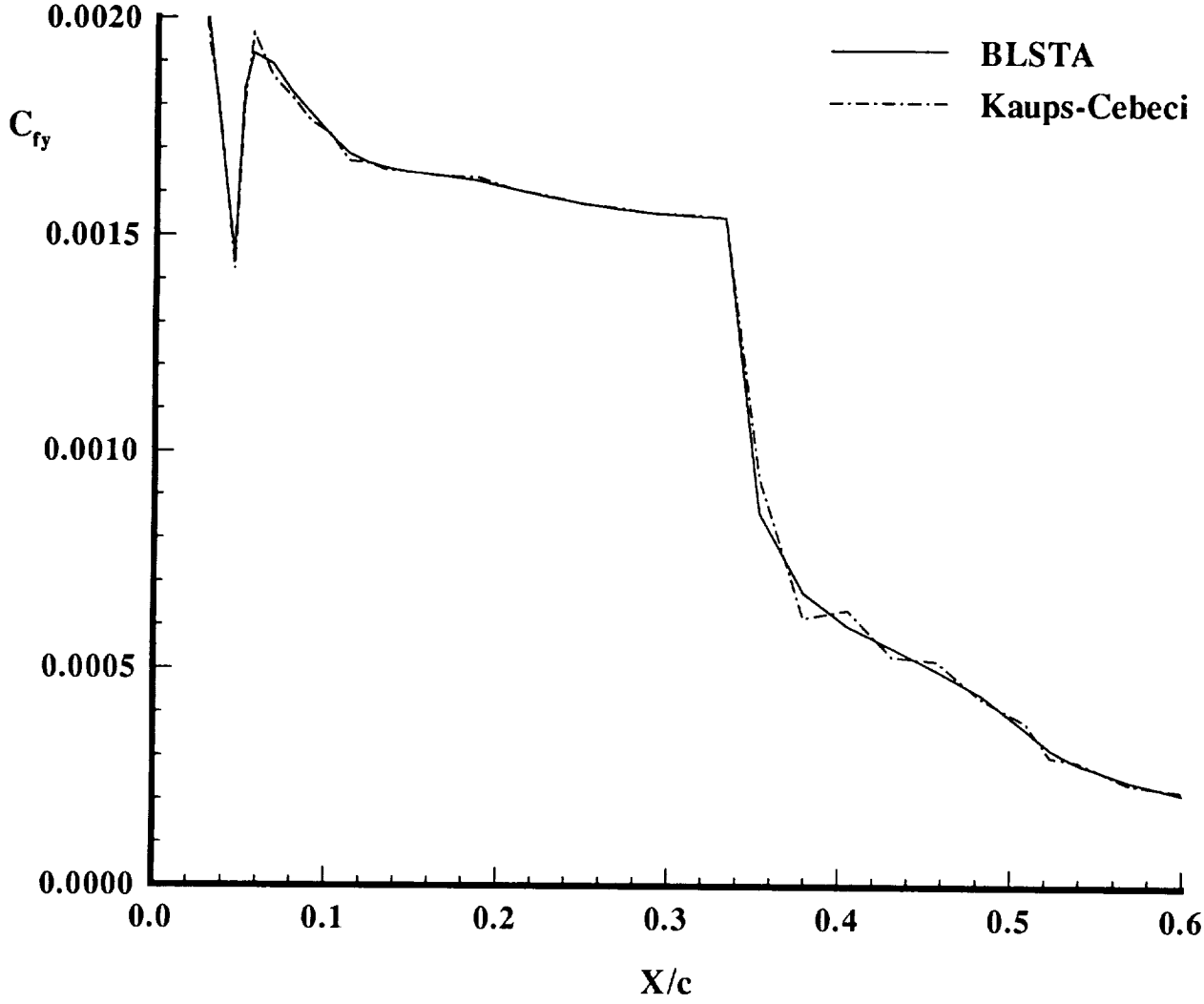

Figure 15. Skin Friction Coefficient (Swept Wing, $M_\infty = 0.80$, with suction)

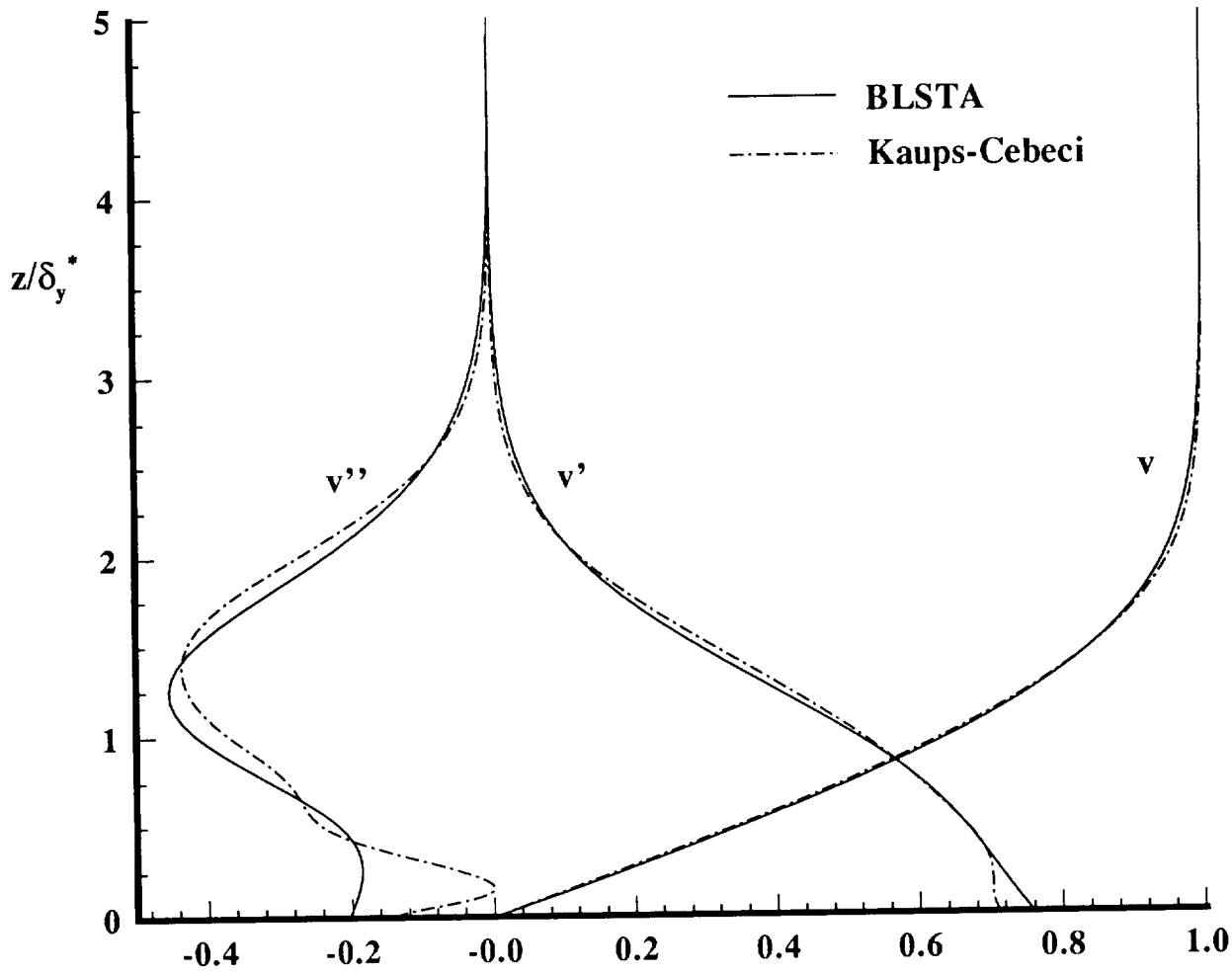

Figure 16. Velocity Profile and Its Normal Derivatives

(Swept Wing, $M_\infty = 0.80$, with suction)

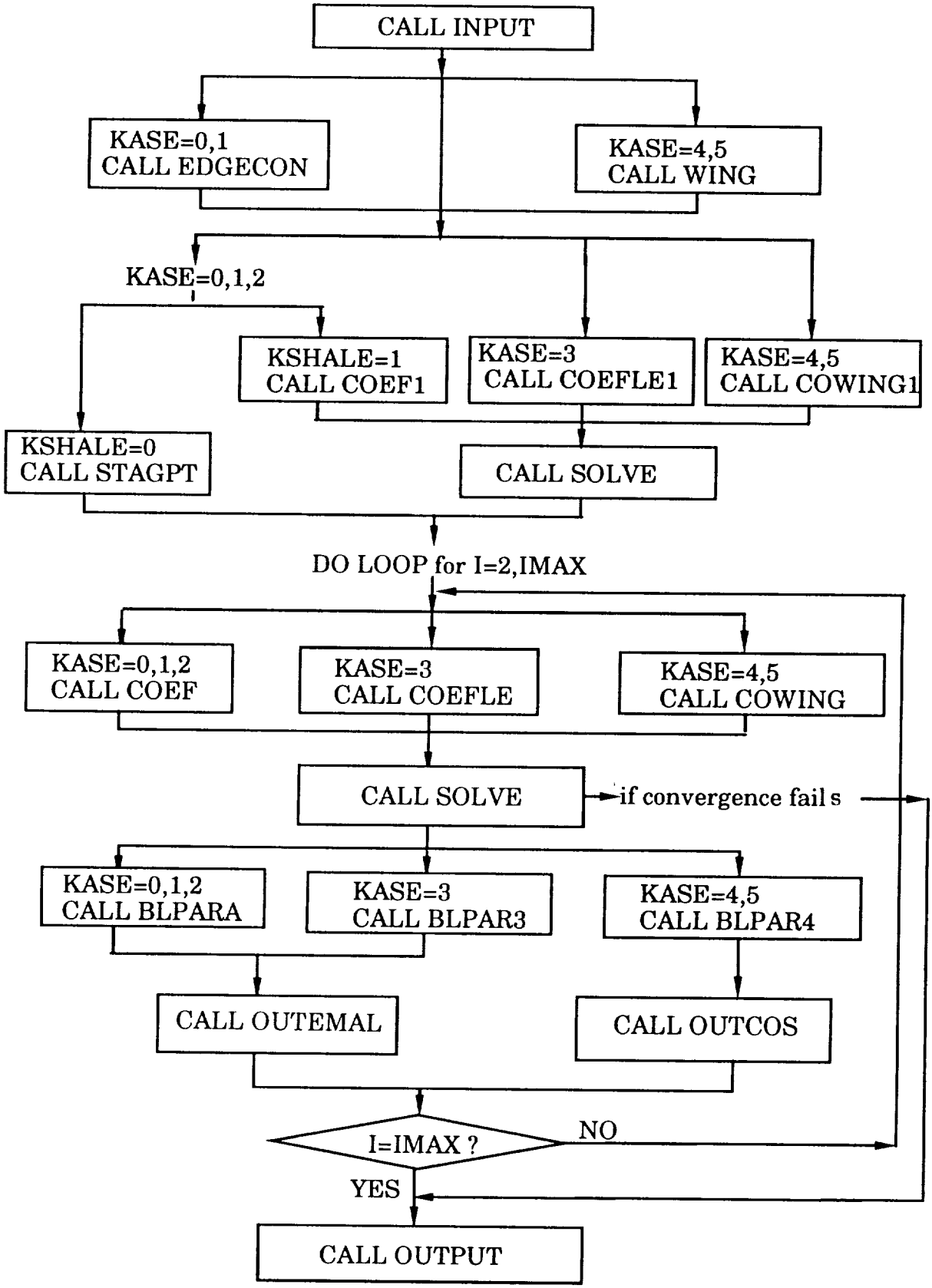

Figure 17. Flow chart of BLSTA

REPORT DOCUMENTATION PAGE

Form Approved
OMB No 0704-0188

1. AGENCY USE ONLY (Leave blank)	2. REPORT DATE	3. REPORT TYPE AND DATES COVERED
	December 1992	Contractor Report

4. TITLE AND SUBTITLE
BLSTA - A Boundary Layer Code for Stability Analysis

5. FUNDING NUMBERS
C NAS1-19299
WU 505-59-10

6. AUTHOR(S)
Yong-Sun Wie

7. PERFORMING ORGANIZATION NAME(S) AND ADDRESS(ES)
High Technology Corporation
28 Research Drive
Hampton, VA 23666

8. PERFORMING ORGANIZATION REPORT NUMBER
HTC-9204

9. SPONSORING / MONITORING AGENCY NAME(S) AND ADDRESS(ES)
National Aeronautics and Space Administration
Langley Research Center
Hampton, VA 23681

10. SPONSORING / MONITORING AGENCY REPORT NUMBER
NASA CR-4481

11. SUPPLEMENTARY NOTES
Langley Technical Monitor: Fayette S. Collier, Jr.
Final Report

12a. DISTRIBUTION / AVAILABILITY STATEMENT
Unclassified - Unlimited
Subject Category ~~43~~ 34

12b. DISTRIBUTION CODE

13. ABSTRACT *(Maximum 200 words)*

A computer program is developed to solve the compressible, laminar boundary-layer equations for two-dimensional flow, axisymmetric flow, and quasi-three-dimensional flows including the flow along the plane of symmetry, flow along the leading-edge attachament line, and swept wing flows with a conical flow approximation. The finite-difference numerical procedure used to solve the governing equations is second-order accurate. The flow over a wide range of speed, from subsonic to hypersonic speed with perfect gas assumption, can be calculated. Various wall boundary conditions, such as wall suction or blowing and hot or cold walls, can be applied.

The results indicate that this boundary-layer code gives velocity and temperature profiles which are accurate, smooth, and continuous through the first and second normal derivatives. The code presented herein can be coupled with a stability analysis code and used to predict the onset of the boundary-layer transition which enables the assessment of the laminar flow control techniques. A User's Manual is also included.

14. SUBJECT TERMS	15. NUMBER OF PAGES
laminar boundary layer, linear stability analysis, conical flow approximation	116
	16. PRICE CODE: A06

17. SECURITY CLASSIFICATION OF REPORT	18. SECURITY CLASSIFICATION OF THIS PAGE	19. SECURITY CLASSIFICATION OF ABSTRACT	20. LIMITATION OF ABSTRACT
Unclassified	Unclassified		

NSN 7540-01-280-5500

Standard Form 298 (Rev 2-89)
Prescribed by ANSI Std 239-18
298-102

NASA-Langley, 1992

National Aeronautics and
Space Administration
Code JTT
Washington, D.C.
20546-0001

Official Business

Penalty for Private Use, $300

BULK RATE
POSTAGE & FEES PAID
NASA
Permit No. G-27

POSTMASTER: If Undeliverable (Section 158 Postal Manual) Do Not Return